Integrating Building Information Modelling and Geographic Information Systems for Characterising Urban Risk and Resilience—

A proposed geospatial workflow

A thesis submitted in fulfilment of the requirements for the Degree

of

Master of Engineering in Earthquake Engineering

By

Daniel Jones

Supervised by

Dr Matthew Hughes

Department of

Civil and Natural Resources Engineering and Geological Sciences

University of Canterbury

New Zealand

2019

Frontispiece

Taiora QEII and its digital twin. Photograph sourced from Apollo Projects (2018).

Abstract

The development of Digital City technologies to manage and visualise spatial information has increasingly become a focus of the research community, and application by city authorities. Traditionally, the Geographic Information Systems (GIS) and Building Information Models (BIM) underlying Digital Cities have been used independently. However, integrating GIS and BIM into a single platform provides benefits for project and asset management, and is applicable to a range of issues. One of these benefits is the means to access and analyse large datasets describing the built environment, in order to characterise urban risk from and resilience to natural hazards.

The aim of this thesis is to further explore methodologies of integration in two distinct areas. The first, integration through connectivity of heterogeneous datasets where GIS spatial infrastructure data is merged with 3D BIM building data to create a digital twin. Secondly, integration through analysis whereby data from the digital twin are extracted and integrated with computational models. To achieve this, a workflow was developed to identify the required datasets of a digital twin, and develop a process of integrating those datasets through a combination of; semi-autonomous conversion, translation and extension of data; and semantic web and services-based processes. Through use of a designed schema, the data were streamed in a homogenous format in a web-based platform.

To demonstrate the value of this workflow with respect to urban risk and resilience, the process was applied to the Taiora: Queen Elizabeth II recreation and sports centre in eastern Christchurch, New Zealand. After integration of as-built GIS and BIM datasets, targeted data extraction was implemented, with outputs tailored for analysis in an infrastructure serviceability loss model, which assessed potable water network performance in the 22nd February 2011 Christchurch Earthquake. Using the same earthquake conditions as the serviceability loss model, performance of infrastructure assets in service at the time of the 22nd February 2011 Christchurch Earthquake was compared to new assets rebuilt at the site, post-earthquake. Due to improved potable water infrastructure resilience resulting from installation of ductile piles, a decrease of 35.5% in the probability of service loss was estimated in the serviceability loss model. To complete the workflow, the results from the external analysis were uploaded to the web-based platform.

One of the more significant outcomes from the workflow was the identification of a lack of mandated metadata standards for fittings/valves connecting a building to private laterals. Whilst visually the GIS and BIM data show the building and pipes as connected, the semantic data does not include this connectivity relationship. This has no material impact on the current serviceability loss model as it is not one of the defined parameters. However, a proposed modification to the model would utilise the metadata to further assess the physical connection robustness, and increase the number of variables for estimating probability of service loss.

This thesis has made a methodological contribution to urban resilience analysis by demonstrating how readily available up-to-date building and infrastructure data can be integrated, and with tailored extraction from a Digital City platform, be used for disaster impact analysis in an external computational engine, with results in turn imported and visualised in the Digital City platform. The workflow demonstrated that translation and integration of data would be more successful if a regional/national mandate was implemented for the submission of consent documentation in a specified standard BIM format. The results of this thesis have identified that the key to ensuring the success of an integrated tool lies in the initial workflow required to safeguard that all data can be either captured or translated in an interoperable format.

Acknowledgements

My first thanks are to my supervisor Dr Matthew Hughes who, when faced with the unexpected situation of a topic change half-way through the project (due to circumstances beyond our control), was able to quickly come up with this Plan B for which I am very grateful. Also for Dr Hughes continued support, guidance, and motivation throughout this research journey in an area relatively new to both of us. I would like to acknowledge the financial support provided by the New Zealand Centre for Earthquake Resilience (QuakeCoRE). Without the assistance from QuakeCoRE, this research would not have been possible.

I also wish to thank the many individuals and organisations that have contributed and provided invaluable knowledge and resources to aid in this research. First of all, my thanks to Xavier Bellagamba at the University of Canterbury for the use of his serviceability loss model to test my thesis. His support, assistance, and provision of his computational engine have greatly helped in demonstrating the capabilities of my research. Secondly, I would like to thank the team at NextSpace Ltd in particular, Mark Thomas, Alex Lavrinovich, and of course *Bruce*. Without their what almost felt like 24/7 support, the use of *Bruce*, and the many tweaks and updates we went through to get *Bruce* to do what I needed for my research, this thesis would not have been as successful so I thank you for that. Next, I would like to show my appreciation to Christchurch City Council and Dave Bain for their assistance and provision of the QEII BIM data for the case study. I hope that this research will provide you with some outcomes that benefit you also, as it certainly has for me.

To my friends, I apologise for all the absences due to the many days and nights locked away in solitary confinement whilst working away at this thesis. In reality, you were probably all very grateful for the peace and quiet. But thank you for your support over the last two years and helping me retain some sanity.

Steph, without your love, support, and patience during this process, particularly the late nights and difficult times, I would still be writing this thesis for years to come. The fact that you've been there for me during this thesis, whilst we've been living apart for the last year is testimony to your strength of character, and knowing you're here for me has made this whole thing a lot easier.

Finally, to my family, my sister Lauren and her husband Pete, my Grandad Mick, and in particular my parents Kevin and Tracey, thank you for your eternal support and encouragement throughout my life, it means everything to me. Mum and Dad, you have always encouraged me to strive for greatness and without your love and the incredible upbringing I had, I wouldn't be the man I am today and nowhere near as successful. As a final sign-off, I would like to dedicate this thesis to my Nan, Barbara. She was the best. When I started this thesis two years ago, she was so proud and supportive and despite being on opposite sides of the world, half a day apart, she was always there. My only wish is that you could have been here to see the finished product. This is for you. I love you all.

Table of Contents

List of Figures

List of Tables

List of Units of Measure

g	Acceleration due to gravity
M_w	Moment Magnitude
kV	Kilovolt
km	Kilometre
Φ	diameter
Ma	Million years
a^{-1}	Per year

List of Acronyms

AC	Asbestos Cement
AIA	American Institute of Architects
BB	Brick Barrel
BIM	Building Information Model
CBD	Central Business District
CCC	Christchurch City Council
CES	Canterbury Earthquake Sequence
CI	Cast Iron
CLS	Concrete-Lined Steel
COLLADA	Collaborative Design Activity
CONC	Concrete
EW	Earthenware
GI	Galvanised Iron
GIS	Geographical Information System(s)
GSDRC	Governance and Social Development Resource Centre
GXP	Grid Exit Point
HDPE	High-density Polyethylene
ICSU	International Council for Science
IFC	Industry Foundation Classes
IPWEA	Institute of Public Works Engineering Australia
IRDR	Integrated Research on Disaster Risk
ISSC	International Social Science Council
LINZ	Land Information New Zealand

MCDEM	Ministry of Civil Defence and Emergency Management
MDPE80	Medium-density Polyethylene 80
MPVC	Modified Polyvinyl Chloride
NAMS	National Asset Management Steering Group
NELC	National Engineering Lifelines Committee
NZGD	New Zealand Geotechnical Database
NZLC	New Zealand Lifelines Council
ODRC	Optimised Depreciation Replacement Cost
PGA	Peak Ground Acceleration
PGV	Peak Ground Velocity
PILCA	Paper Insulated Lead-Covered, Armoured
PVC	Polyvinyl Chloride
QA	Quality Assurance
RC	Reinforced Concrete
RCRR	Reinforced Concrete Rubber-Ring jointed
SCIRT	Stronger Christchurch Infrastructure Rebuild Team
SRS	Spiral-welded/ Riveted Steel
UI	User interface
UNISDR	United Nations Office for Disaster Risk Reduction
UPVC	Unplasticised Polyvinyl Chloride
URM	Unreinforced Masonry
WFS	Web Feature Service
XLPE	Cross-laminated polyethylene

Chapter 1
—Introduction and Objectives

Contents

1.1. Background and Research Significance

The occurrence of natural hazards and their impact on urban populations has existed since ancient times, from the Minoan eruption in Santorini in 1645 BC (Barclay, 2010), to the moment magnitude (M_w) 6.9 earthquake in Indonesia in August 2018 (United States Geological Survey [USGS], 2018). With ongoing expansion of cities and urban areas, along with increasing complexity of the built environment, the means with which to identify, monitor, and recover from these natural hazards also needs to expand.

The *Sendai Framework for Disaster Risk Reduction 2015–2030* (United Nations Office for Disaster Risk Reduction [UNISDR], 2015) recognises that the increasing demand on infrastructure, through urbanisation and population growth, brings with it an increase in exposure and vulnerability during a disaster. While there have been some achievements in building resilience and reducing loss and damage, perseverance and persistence is required to succeed in the substantial reduction of disaster risk. Also noted is the requirement for strong commitment and involvement of political leadership at all levels, and that responsibility should be shared with other stakeholders, including the private sector. In order to achieve its goals, seven global targets were established and this thesis focusses on the following three:

- *Substantially reduce the number of affected people globally by 2030, aiming to lower the average global Figure per 100,000 in the decade 2020-2090 compared to the period 2005-2015.*
- *Reduce direct disaster economic loss in relation to global gross domestic product (GDP) by 2030.*
- *Substantially reduce disaster damage to critical infrastructure and disruption of basic services, among them health and educational facilities, including through developing their resilience by 2030.*

Bruneau *et al.* (2003) described disaster resilience as a function of the 4 Rs: Robustness and Redundancy of infrastructure in its ability to limit damage, and Rapidity and Resourcefulness in returning the affected area to its pre-disaster condition. The New Zealand Lifelines Infrastructure Vulnerability Assessment report: Stage 1 (New Zealand Lifelines Council [NZLC], 2017) defined resilience as "the state of being able to avoid utility supply outages, or maintain or quickly restore service delivery, when events occur". Also presented in NZLC (2017) was the recognition of cohesiveness of a system whereby interdependencies between other lifelines and critical infrastructure are mapped, catalogued and analysed appropriately, as shown in Figure 1-1 and Figure 1-2.

The degree to which the utilities listed to the right are dependent on the utilities listed below	Roads	Rail	Sea transport	Air transport	Water supply	Wastewater	Storm water	Electricity	Gas	Fuel	Broadcasting	VHF radio	Telecoms	**Total Dependency**
Electricity	1	2	3	3	3	3	2		2	2	3	3	3	**30**
Road		3	3	3	2	2	2	2	2	3	2	2	2	**28**
Fuel	2	3	3	3	2	2	2	2	2		2	2	2	**27**
Telecoms	2	2	2	2	2	2	2	2	2	2	2	3		**25**
Water supply	1	1	1	2		3	1	1	1	1	1	1	2	**16**
VHF radio	2	2	2	2	1	1	1	1	1	1	1		1	**16**
Storm water	2	1	1	2	1	1		1	1	1	1	1	1	**14**
Wastewater	1	1	1	2	1		1	1	1	1	1	1	1	**13**
Rail	1		1	1	1	1	1	1	1	1	1	1	1	**12**
Sea transport	1	1		1	1	1	1	1	1	1	1	1	1	**12**
Air transport	1	1	1		1	1	1	1	1	1	1	1	1	**12**
Gas	1	1	1	1	1	1	1	1		1	1	1	1	**12**
Broadcasting	1	1	1	1	1	1	1	1	1	1		1	1	**12**

Figure 1-1: Business as usual infrastructure interdependency matrix (NZLC 2017)

The degree to which the utilities listed to the right are dependent on the utilities listed below	Roads	Rail	Sea transport	Air transport	Water supply	Wastewater	Storm water	Electricity	Gas	Fuel	Broadcasting	VHF radio	Telecoms	**Total Dependency**
Fuel	3	3	3	3	3	3	3	3	3		3	3	3	**36**
Roads		3	3	3	3	3	3	3	3	3	2	2	3	**34**
Telecoms	3	2	2	2	3	3	3	3	3	2	2	3		**31**
Electricity	1	2	3	3	3	3	2		2	2	3	3	3	**30**
VHF radio	2	2	3	3	2	2	2	2	2	2	2		2	**26**
Broadcasting	2	2	2	2	2	2	2	2	2	2		2	2	**24**
Air transport	2	1	1		2	2	2	2	2	2	2	2	2	**22**
Water supply	1	1	1	2		3	1	1	1	1	1	1	2	**16**
Storm water	2	1	1	2	1	1		1	1	1	1	1	1	**14**
Wastewater	1	1	1	2	1		1	1	1	1	1	1	1	**13**
Rail	1		1	1	1	1	1	1	1	1	1	1	1	**12**
Sea transport	1	1		1	1	1	1	1	1	1	1	1	1	**12**
Gas	1	1	1	1	1	1	1	1		1	1	1	1	**12**

Figure 1-2: During/post-disaster interdependency matrix (NZLC 2017)

A comparison of the above two tables highlight how interdependencies become more apparent, as well as highlighting critical infrastructures increasing importance, post disaster. Also interpreted from the tables is that risk to a city is not simply an aggregate of each building's risk, but that the urban system as a whole, such as roads and other infrastructure lifelines, and the urban spatial pattern, plays an important role in the city's vulnerability. Historically, the recording, managing, and modelling of urban infrastructure has been conducted across independent databases, primarily due to policy and technology limitations between the various stakeholders (Li *et al.*, 2019; Song and Li, 2017). However, in the area of disaster research, organisations such as the International Social Science Council (ISSC), International Council for Science (ICSU), and UNISDR recognise the importance of developing trans-disciplinary, multi-sectorial alliances for in-depth disaster risk reduction studies, and aim to overcome the challenges associated with heterogeneous databases through the Integrated Research on Disaster Risk (IRDR) research programme (IRDR, 2013).

Of these heterogeneous databases, smart technologies such as Geographic Information Systems (GIS), and Building Information Modelling (BIM)-based systems, which contain building and infrastructure spatial and attribute data, are examples of more commonly used tools for managing large spatial datasets and accurately characterising an urban system. Whilst the likes of GIS have a long history and are essential in the management of data and assessment of risk, BIM has only been in development since the 1990s (Liu *et al.*, 2017) and has predominantly been used for engineering design and asset management. However, whilst BIM continues to evolve in its conventional uses of engineering and asset management (BIM Acceleration Committee, 2016; Kassem *et al.*, 2015), it is recognised that data contained within the models are an equally important resource in the assessment of resilience of the built environment.

The integration of BIM and GIS is an even newer research topic, and despite most of the literature highlighting this integration's potential use as an asset management tool (Boyes *et al.*, 2017; Zhang *et al.*, 2009), commonalities and complementary attributes of the systems also lend themselves to becoming a crucial application in the characterisation of urban resilience and vulnerability. By having access to up-to-date, accurate quantitative citywide data, showing a fully integrated model of the lifelines (horizontal infrastructure) and the critical sites (vertical infrastructure) they service, provides the ability to assess the 4 Rs and in turn demonstrate the progress/success of the Sendai targets set by UNISDR (2015).

A key example of the impact of a natural hazard on a modern city was the 2010-2011 Canterbury Earthquake Sequence (CES), which caused extensive damage to Christchurch City's natural and built environments. It is estimated that insurance claims across the sequence were in the order of magnitude of NZ$40 billion, making it the fifth largest insurance event in the world since 1953 (Deloitte Access Economics, 2015). The main series of earthquakes, which spanned approximately 15 months between September 2010 and December 2011, caused widespread ground deformation as a result of seismically-induced liquefaction (Hughes *et al.*, 2015; Quigley *et al.*, 2016). The manifestations of liquefaction during this period caused significant damage to vertical and horizontal infrastructure. The comprehensive data gathered during the Canterbury Earthquake Sequence (CES), characterising impacts on the built environment, have provided valuable lessons in disaster impact and urban resilience.

Learnings from the CES have also contributed to significant development in modelling seismicity and impacts to infrastructure lifelines in New Zealand, along with spurring development of computational platforms with which to do so. Examples include: the 3D modelling of physics-based ground motion response, utilising site-specific data from 16 strong motion stations in Christchurch (de la Torre and Bradley, 2018); the exposure, impact, and recovery model of interdependent critical infrastructure in an Alpine Fault M_w 8.0 (AF8) event (Zorn *et al.*, 2018); and the characterisation of vertical and horizontal ground deformation for comparison with the performance of the city's potable and wastewater networks (Bellagamba *et al.*, 2018b; Liu, 2016; O'Rourke *et al.*, 2014).

Despite GIS and BIM data integration being in its infancy, recent developments in Christchurch and New Zealand present the opportunity to research more evolved tools. An example of this is the work by Christchurch City Council (CCC) who, following the CES and the ongoing rebuild of Christchurch, saw the opportunity provided by integrated BIM and GIS technologies as a means to better record, monitor and collate vertical and horizontal infrastructure data. In a collaborative project with NextSpace Ltd., a geospatially-referenced platform (codenamed *Bruce*) that provides a single-source viewer of highly detailed BIM data provided by designers as part of the consenting process, and their own assets such as the 3 Waters network is being developed. This thesis research is improving data sharing and visualisation protocols in the *Bruce* project, and extending its capabilities by integrating the earthquake modelling outputs of Bellagamba *et al.* (2018b).

1.2. Conceptual Frameworks

Two conceptual frameworks are used for the basis of this thesis: risk, and resilience. Table 1 provides an overview of contrasting approaches to risk and resilience concerning infrastructure, demonstrating how the assessment of risk considers likelihood and consequence of known, quantifiable hazards; and resilience assessment considers unpredictable events with low-probability, high consequence. Whilst the treatment classification of risk and resilience are the same in that they both use transfer of responsibility, removal, mitigation (improvement), or do nothing approaches, how these strategies are implemented differ between the two, as shown in Table 2 from Institute of Public Works Engineering Australia [IPWEA] *et al.* (2015). Further details on each of the frameworks are presented in Sections 1.2.1 and 1.2.2, with discussion on how aspects of each can be integrated through use of a geospatial workflow in Section 1.2.3.

Table 1: Comparison of risk and resilience (from IPWEA,2015)

Risk	Resilience
Considers degree of certainty related to the hazard likelihood and range of potential consequences. If there is significant uncertainty, a "resilience approach" should also be used.	Consideration of over-design events. Identification of consequences and management procedures following the occurrence of an event.
Consideration of multiple interdependencies related to a piece of infrastructure and methods of efficient reduction or management should be considered. Review and planning of potential failure possibilities/modes across interdependencies should also be carried out.	Considers the cost/benefit analysis of managed failure due to an unspecified cause (e.g. by providing redundant systems, safe-failure approaches, given the criticality of a specific system or asset.
Focus on prioritising risk reduction for those assessed as being high.	Focus on measuring attributes of resilient systems.

Table 2: Comparison of risk and resilience treatments (from Ettouney, 2016)

Category	Risk	Resilience
Transfer	Yes (e.g. via insurance)	Indirectly as part of improving redundancy which is a function of mitigation.
Mitigate	Through reduction in one or more of: • Threat • Vulnerability • Consequence	Through improvement of one or more of: • Robustness • Resourcefulness • Redundancy • Recovery
Ignore	Yes	Yes
Remove	Yes	May not be fully removed, as operations will always continue. Therefore, removal could be considered a mitigation method.

1.2.1. Risk Management

The Risk Management Framework (New Zealand Standards, 2009) provides a methodological approach to handle complex processes associated with risk assessment and eventually risk reduction. Through identification, analysis, evaluation, and treatment, as shown in Figure 1-3, the Framework is used here as one of the conceptual bases of this study.

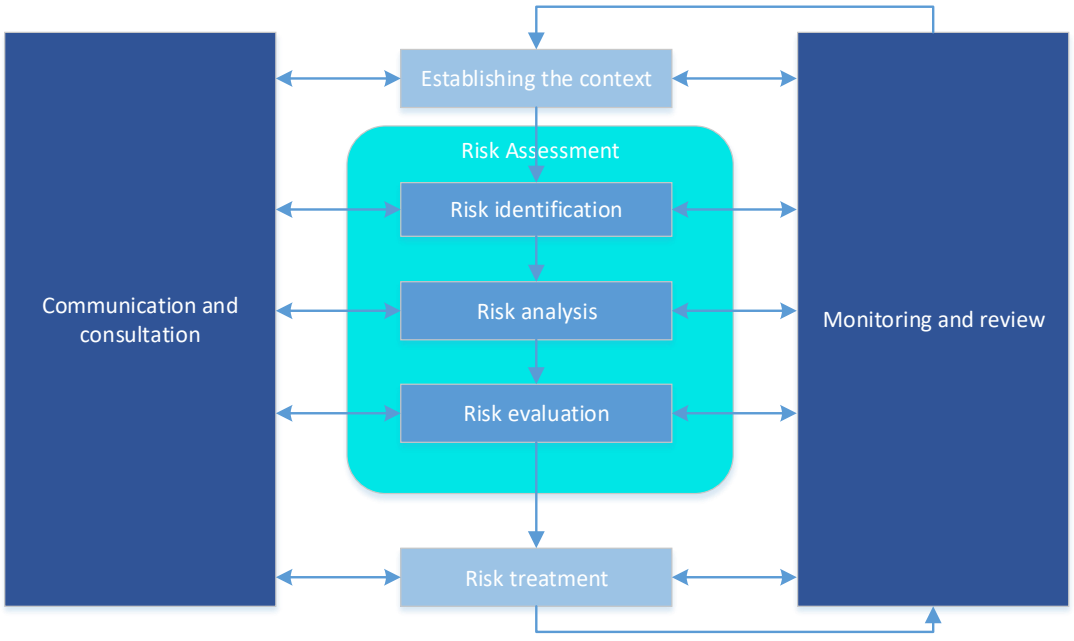

Figure 1-3: Risk Management Framework (New Zealand Standards, 2009)

Disaster Risk is expressed by the National Disaster Resilience Strategy (Ministry of Civil Defence and Emergency Management [MCDEM], 2018) in the following equation:

$$Risk = Hazard \times Exposure \times Vulnerability \times Capacity$$

whereby the equation parameters are defined as:

i. Risk (Disaster Risk): *The potential loss of life, injury, or destroyed or damaged assets, which could occur to a system, society or community in a specific period, determined as a function of hazard, expose, vulnerability and capacity.*
ii. Hazard: *A process, phenomenon, or human activity that may cause loss of life, injury or other health impacts, property damage, social and economic disruption, or environmental degradation.*
iii. Exposure: *People, infrastructure, buildings, the economy, and other assets that are exposed to a hazard.*
iv. Vulnerability: *The conditions determined by physical, social, economic, and environmental factors or processes that increase the susceptibility of an individual, a community, assets, or systems to the impacts of hazards.*
v. Capacity: *The combination of all the strengths, attributes, and resources available within an organisation, community, or society to manage and reduce disaster risks and strengthen resilience.*

The research presented in this thesis focusses on the means of undertaking citywide seismic risk assessment through digital engineering techniques (predominantly BIM and GIS technologies) and encompasses the entire process of risk assessment within the Risk Management Framework.

1.2.2. Resilience Management

Disaster resilience is determined by the capability of individuals, communities, public and private organisations, and is informed by past disasters to reduce risks from future ones, at international, regional, national and local levels, without compromising long-term prospects for development (Combaz, 2014; UNISDR, 2005).

Generally, within the literature, disaster resilience is defined as either a function of four or five Rs. Ettouney (2016) and Bruneau *et al.* (2003) refer to 4 Rs, when describing physical and social system resilience, as follows:

1) Robustness: *Ability to withstand a given level of stress or demand without suffering degradation or loss of function.*
2) Redundancy: *Extent to which elements, systems or other units of analysis are substitutable i.e. capable of satisfying functional requirements in event of disruption, degradation, or loss of functionality.*
3) Resourcefulness: *capacity to identify problems, establish priorities, and mobilise resources (human and material i.e. monetary, physical, technological, and informational) to meet established priorities and achieve goals, when conditions exist that threaten to cause disruption.*
4) Rapidity: *capacity to meet priorities and achieve goals in a timely manner to contain losses and avoid future disruption.*

Linkov (2015) categorises resilience as a function of 5 Rs, whereby rapidity is subcategorised into response and recovery but the remaining three definitions remain the same. Ettouney and Alampalli (2016) expand on these definitions by incorporating a *Time-Function* scale whereby *Time* has an origin beginning with the occurrence of a hazard, and *Function* is a subjective estimate of operational efficiency of the asset, or community of assets. The interrelationships between the 4 Rs and the *Time-Function* variables in the context of resilience are illustrated in Figure 1-4.

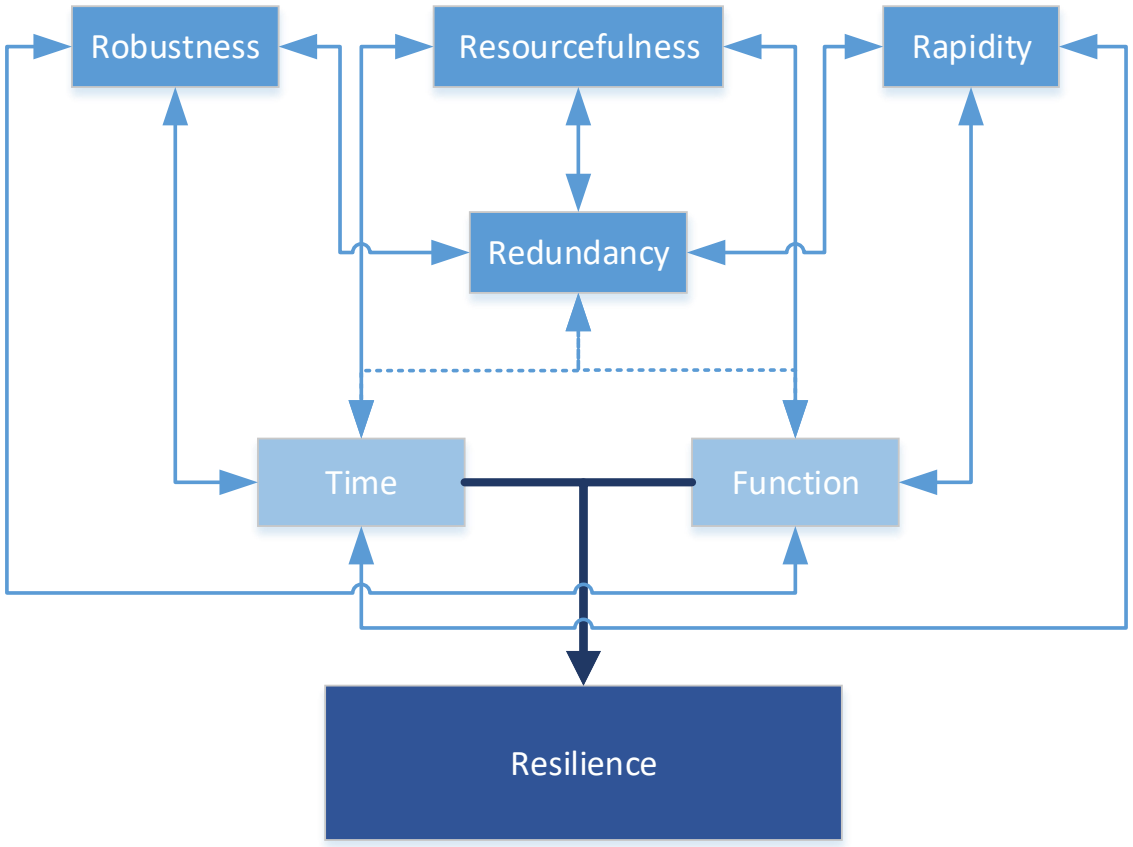

Figure 1-4: Interrelationships between 4 Rs and Time-Function scale (from Ettouney and Alampalli, 2016)

Resilience management (Figure 1-5) has historically been defined as the ability to return to the status quo after a disturbance event (Hassenzahl, n.d.). However, resilience management cannot be based solely on the capability to recover from the types of disasters previously faced (learning, or resourcefulness in the context of the 4 Rs), but requires capacity be built to avoid damage and/or to recover from likely future disasters (anticipation/rapidity). In order to manage resilience, the risks must be understood so that adequate preparation can be undertaken through modelling and measurement acquisition (sensing/redundancy), for both expected and unexpected events (adaptation/robustness). To that end, it is critical that risks are identified, assessed, communicated about, and planned for.

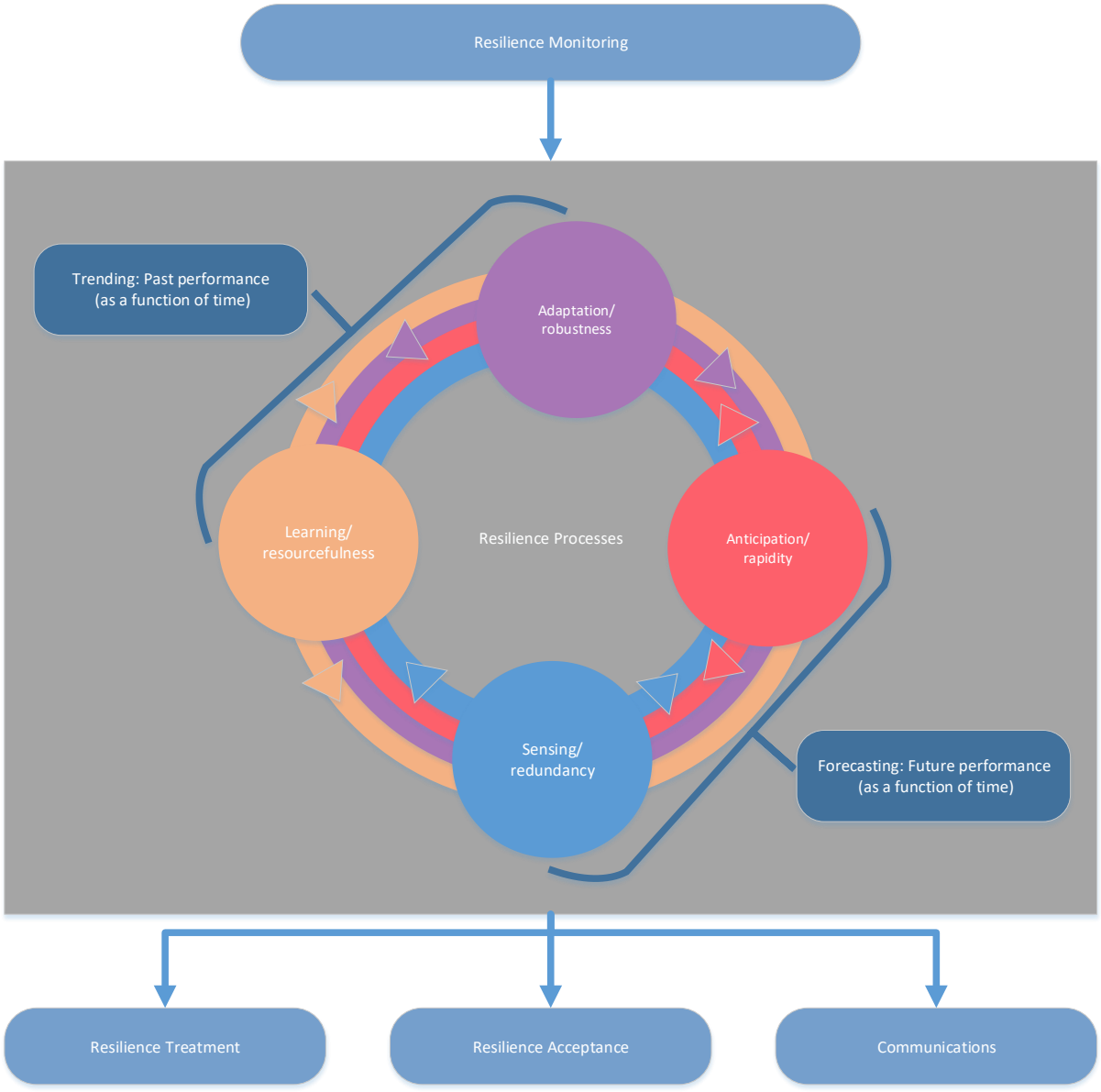

Figure 1-5: Resilience management (modified from Ettouney, 2016 and Linkov, 2015). Note:- the arrows in the figure do not necessarily represent a particular sequence between linked processes.

1.2.3. Integrating Risk and Resilience through Digital Engineering

As discussed in Sections 1.2.1 and 1.2.2, risk and resilience are not completely independent. Their frameworks are generally comparable (Figure 1-7), with the Risk Management Framework showing a more bidirectional workflow than the resilience management framework. Linkov *et al.* (2014) illustrated that risk assessment forms one part of resilience, at the point immediately following an event, prior to the recovery (or rapidity in the context of the 4 Rs) phase, as shown in Figure 1-6, the definition of *Capacity* by MCDEM (2018) directly references resilience.

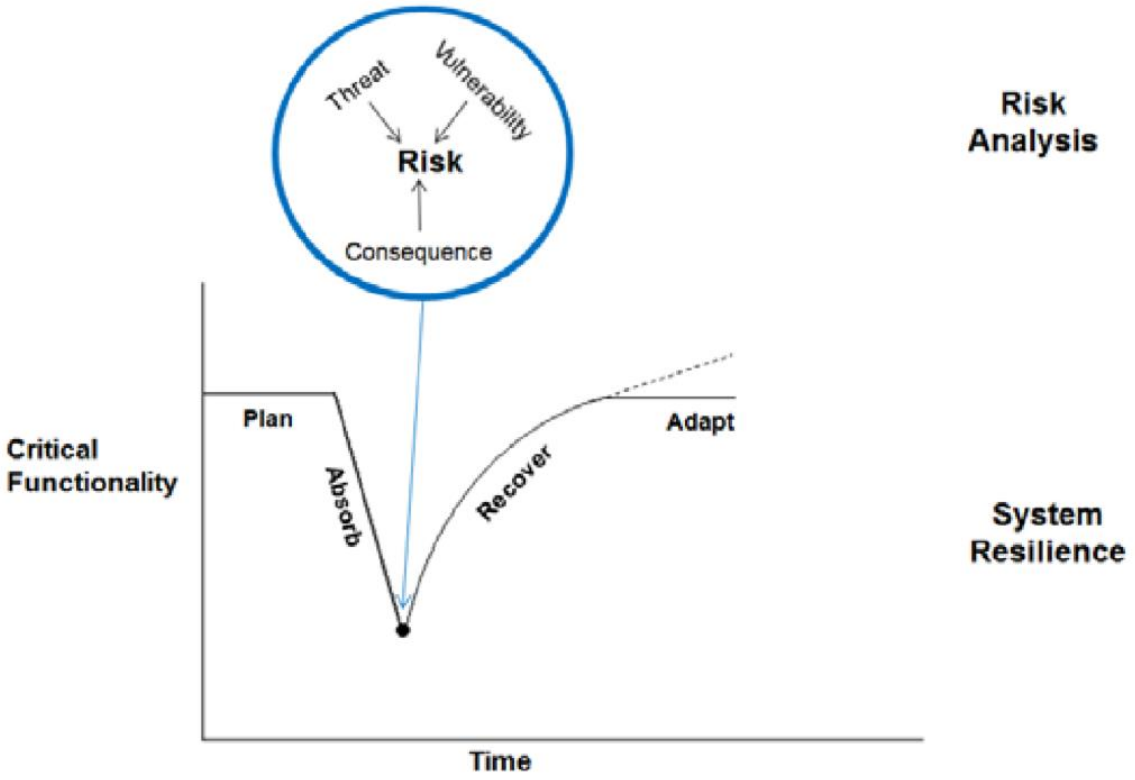

Figure 1-6: Resilience Management Framework with risk analysis as a central component (from Linkov et al., 2014)

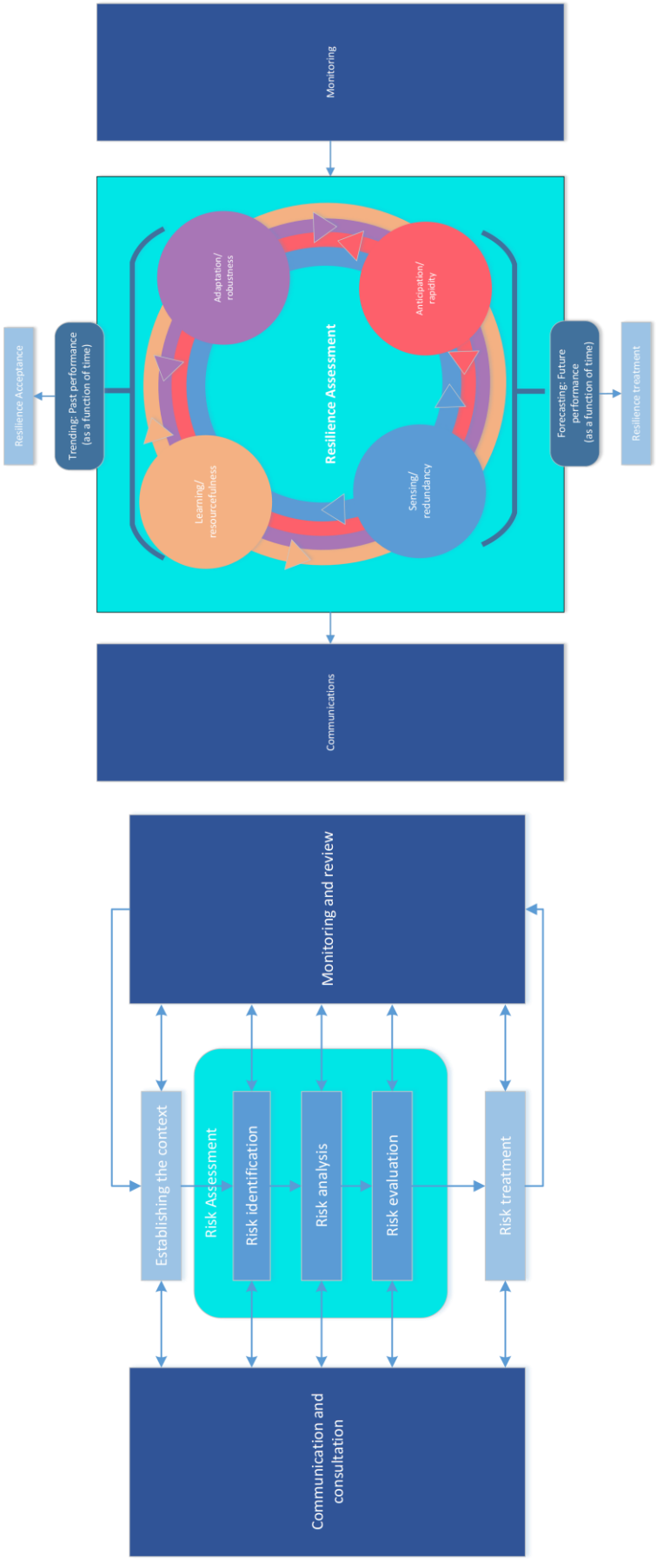

Figure 1-7:Comparison of the similarities between the Risk Management Framework and Resilience Management Framework

Similar relationships between risk and resilience can be seen when assessing the components of each framework, as presented in Figure 1-8. In the context of risk management, Suter (2011) noted how resilience replaces/complements the concept of protection, previously defined as the goal of risk management activities. Resilience also forms part of risk management whereby it is required to mitigate the residual risks remaining from those unidentified or underestimated, and therefore not covered by preventative measures adopted as part of the Risk Management Framework. Lastly, referring back to some of the contrasting dynamics between the two frameworks, resilience presents an alternative to the traditional method of risk management by way of dealing with risks in a complex environment. In particular, with socio-economic systems that are confronted with highly complex non-linear and dynamic risks through which, their resilience should be enhanced by increasing adaptive capacities.

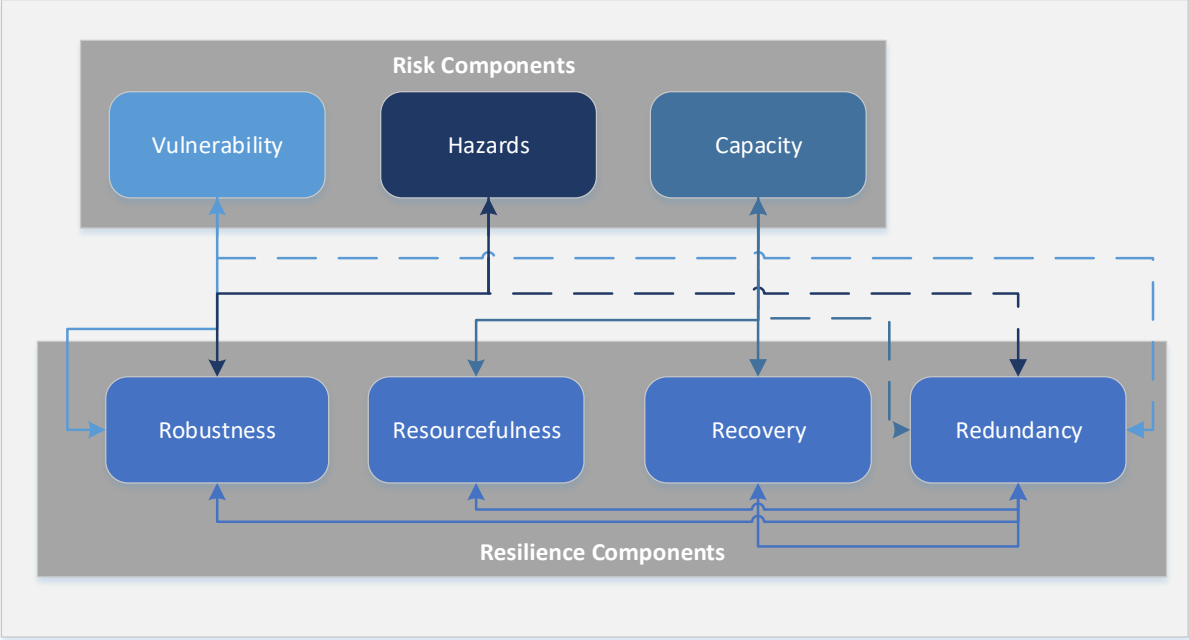

Figure 1-8: Relationships between risk and resilience components (modified from Ettouney and Alampalli, 2016). Dashed lines represent unidirectional relationship.

The interrelationship between risk and resilience is further demonstrated by way of the graphics in Figure 1-9 whereby the *Time-Function* scale from Ettouney and Alampalli (2016) is considered. The graphs show how traditional risk management, with the absence of resilience, (graphs *c* and *d*) result in a lengthy recovery period relative to the degree of risk. However, where resilience management is considered (graphs *a* and *b*), there is an additional emphasis on decreasing the recovery time and facilitating adaptation.

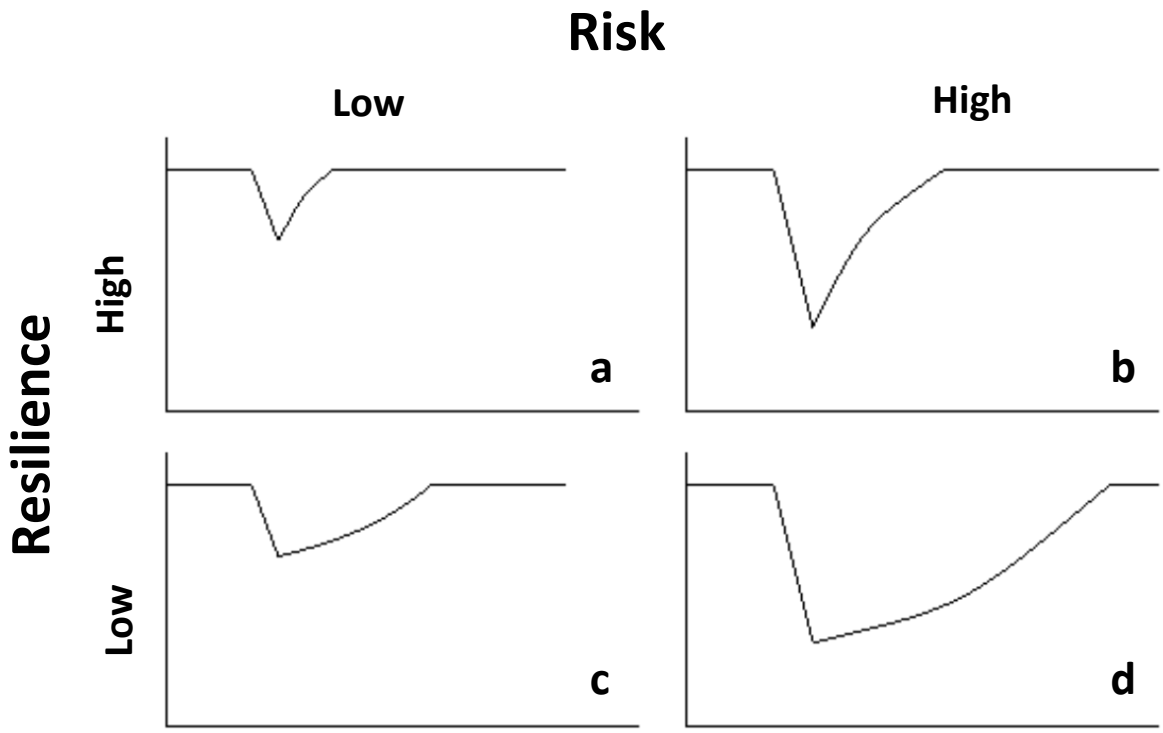

Figure 1-9: Graphical representation of risk versus resilience (from Linkov et al., 2014) .

In the context of the research presented in this thesis, the purpose is to develop a workflow to aid in a citywide seismic risk assessment through digital engineering techniques (predominantly BIM and GIS technologies) and provide the means for integrating the risk and resilience management frameworks.

As shown in Figure 1-7, there are three predominant processes within risk and resilience management: context establishment/resilience acceptance, assessment, and treatment. These are supplemented by communication and consultation, and monitoring and review. The context establishment/resilience acceptance component of this research is presented in Sections 1.1, 1.2, and 1.3. Assessment is required as part of the second process in risk and resilience management. Risk assessment includes identification, analysis, and evaluation of risk, and considers the extent and vulnerability of the exposed assets. Resilience assessment reviews past performance under similar hazardous events through learning and adaptation, and forecasts future performance through anticipation and sensing (Figure 1-5).

Risk identification from the perspective of this study requires recognition of potential seismic hazards within a defined area. Additionally, the exposure (e.g. buildings and horizontal infrastructure) at risk from the hazard also need to be catalogued. This process is achieved through a literature review of: existing seismic modelling of the CES (Section 2.3.3), reviewing the performance of building and infrastructure during the CES (Sections 2.3.3.3 and 2.3.3.4), and integration methodologies of digital building and infrastructure data (Section 2.2.4).

The analysis conducted here is via the integration of vertical and horizontal infrastructure data into a geospatial platform to allow identification of risk of service loss. Data extracted from the *Bruce* platform was analysed using the Bellagamba *et al.* (2018b) serviceability loss model that is based on quantitative analysis using probabilistic modelling utilising potable water network performance data during the CES.

Risk evaluation assesses risks and establishes methods to minimise hazard impact and therefore reduce the risk. Levels of risk as defined by Layfield and Great Britain. Dept. of Energy (1987) can be either acceptable, tolerable, or intolerable and are essential in the assessment of risk treatment. Evaluation assists in the development and amendment of strategic planning and decision making as it allows for the prioritisation of resources in the reduction of intolerable risks. Modelling also provides the means of evaluating alternative scenarios and designs of buildings and infrastructure, and the impacts from a seismic event.

The "trending" component of resilience assessment weaves itself through the risk assessment described above. In the context of this thesis, the damage observations gathered throughout the CES of both land and the built environment enabled the wider infrastructure community (engineers, policy makers, private insurers, contractors) to learn about the performance of land and infrastructure when subjected to shaking and permanent ground deformation. These observations and subsequent risk analyses informed new Ministry of Business Innovation and Employment (MBIE) Guidelines, a set of requirements for building foundations designed for earthquake events comparable to, and of greater magnitude, than that experienced during the CES (MBIE, 2012). The development of these guidelines is also an example of resourcefulness in the context of the 4 Rs. The observations made for the case study site in Chapter 4 also provided the ability to adapt and design a new, more robust sports facility that should perform better than its predecessor, a hypothesis explored as part of the analytical component of this thesis.

The final phase in the Risk Management Framework is risk treatment, which identifies the means to lessen vulnerability of the exposure, reduce the hazard, or both. Mitigation strategies can also be applied to aid in the reduction of risk such as engineered options (e.g. infrastructure strengthening) or through non-engineered solutions (e.g. asset relocation, modifying land-use, and monitoring). To determine the impact of risk reduction requires forecasting of future performance, the second half of the resilience assessment component of the resilience framework.

For this study, the focus is on engineered solutions whereby a comparison is made between: a pre-CES building and its servicing infrastructure and their performance during the 22nd February 2011 Christchurch Earthquake; and the new building and infrastructure built at the same site following the CES. This demonstrates the sensing component of the resilience framework by modelling expected performance of an asset before an event occurring (redundancy in accordance with the 4 Rs). This thesis demonstrates one scenario (an event of equal magnitude to the 22nd February 2011 Christchurch Earthquake). However, the benefit to the geospatial workflow and the serviceability loss model is that reiterative simulations could be run for a variety of scenarios. From these results, asset owners could undertake a cost-benefit analysis of concept improvement works to determine the degree of risk is acceptable, tolerable, or intolerable (Layfield and Great Britain. Dept. of Energy, 1987), and determine the capacity of the asset (or response and recovery in the context of the 5 Rs).

The supplementary component of monitoring and reviewing provides the means to calibrate and update models as new data become available. This is one of the fundamental principles of this thesis, whereby the proposed workflow allows for the continual uploading of both new building and infrastructure data, or where external analysis is conducted and its outputs fed back into the integrated *Bruce* platform (also demonstrating learning and resourcefulness in the resilience framework).

Communication and consultation through the integrated *Bruce* platform allows stakeholders to identify requirements of risk management organisations and communities. The intent of the platform is to provide a single-source database that all lifeline and asset owners, and local authorities, can contribute to and assess risk at a citywide level through external modelling. This allows for the provision of risk reduction options through determining the current resilience of the built environment.

1.3. Thesis Outline

1.3.1. Project Objective

The objective of this research is to demonstrate a workflow of integrating geospatially (GIS) and non-geospatially referenced (BIM) data into a unified, geospatial, web-based platform, and to highlight its capabilities as a research tool.

Whilst Smart Cities and Digital Twins are continually being researched as a means of asset management (Section 2.2.5.4), the CES and ongoing work associated with an AF8 event (MCDEM, 2019) have highlighted the importance of having easily accessible and accurate data for preparatory analysis and risk modelling, prior to an event. To that end, the following research aims have been developed to identify the workflow required to obtain *easily accessible* data for urban resilience analysis:

- Categorise the current uses of BIM and GIS.
- Identify the current difficulties with integrating BIM and GIS data.
- Discuss how integrated data benefits urban resilience analysis of the built environment.
- Identify the roles/users best placed for managing and co-ordinating citywide datasets as well as providing access to, for a variety of stakeholders.
- Demonstrate the seamless extraction of up-to-date BIM and GIS infrastructure data stored and managed within Bruce.
- Present a demonstration of the geospatial workflow in an earthquake analysis of infrastructure lifeline performance.

To achieve these aims, a literature review focussing on BIM and GIS was conducted to identify current methodologies of integration and their associated challenges. GIS data of the 3 Waters infrastructure and as-built BIM Data for the case study site were provided by CCC and with the assistance of NextSpace Ltd and their current version of *Bruce*; a workflow was developed to integrate GIS and BIM data. The workflow functionality is extended by demonstrating how typical data held within the integrated tool are used in the serviceability loss model developed by Bellagamba *et al.* (2018b). Finally, a review of future needs and applications outside of those included in this thesis is discussed.

1.3.2. Thesis Structure

This study is organised into four main chapters. Chapter 2 provides the results of the literature review, which identified previous studies on the uses and integration techniques associated with GIS and BIM, including existing applications for hazard analysis. An overview of the geological and seismic conditions of Christchurch, as well as a summary on the performance of the vertical and horizontal infrastructure during the CES, is also presented.

Chapter 3 presents the developed geospatial workflow, utilising two tools. First, a web-based BIM-GIS integration platform (codenamed *Bruce*) under development by NextSpace Limited, for collecting building and infrastructure data. Second, a serviceability loss model developed by Bellagamba *et al.* (2018b), which was used to model performance of the potable water network during the 22nd February 2011 Christchurch Earthquake. The chapter also highlights the workflow to collate relevant building and infrastructure data from the NextSpace model, and the method for inputting these data into the loss model.

Chapter 4 demonstrates the application of the workflow by means of a case study. Vertical and horizontal infrastructure data provided by CCC for the Taiora: QEII recreation and sports centre were uploaded and integrated into *Bruce.* A tailored metadata extraction was then completed to demonstrate the extension of the workflow. The extraction was tailored to the requirements of the serviceability loss model so that a comparison could be undertaken between the performance of the pre-CES QEII building and associated infrastructure (from Bellagamba *et al.*, 2018b) with the new Taiora: QEII infrastructure, using the ground deformation data from the 22nd February 2011 Christchurch Earthquake. The conclusion of this section presents the various outputs and results of the case study.

Finally, Chapter 5 discusses recommendations for the further development of the *Bruce* tool, such as the addition of other lifeline networks, and the generation of alternative modelled seismic events (such as AF8, MCDEM, 2019) to assess the performance of the infrastructure systems in areas of liquefiable soils. It will also identify the benefits of other outputs for stakeholders such as MCDEM for hazard analysis and response planning, for asset managers and stakeholders such as other infrastructure lifeline providers and local/national government.

Chapter 2
—Literature Review

Contents

2.1. Introduction

This research collates building data managed by CCC, characterises the spatial distribution and causative mechanisms of damage to horizontal infrastructure, and then applies the learnings to case study site. Damage to infrastructure lifelines networks during the CES is well documented in the literature, as is the development of GIS databases for the use of horizontal infrastructure risk analysis and modelling of various seismic hazard scenarios. Studies have been undertaken to identify relationships between the infrastructure networks, their geographical environment, and the resulting impacts from natural hazard events, along with management and restoration of those networks with the goal of improving physical asset and community resilience.

However, there is a gap in research linking BIM and GIS data for horizontal and vertical infrastructure systems, and their integrated use in risk and resilience analysis appears to be a relatively a new field. Most current studies focus on methods of integration, rather than their uses in analysis and modelling, particularly for natural hazards. This section reviews the key published works documenting the uses of BIM and GIS, previous attempts at integrating the two, the applications of the integration, and existing examples of digital cities both internationally and within New Zealand. The second half of this chapter describes impacts of the CES on Christchurch City's built environment, as a background to the case study analysis described in Chapter 4.

2.2. Geographic Information Systems (GIS) and Building Information Modelling (BIM)

2.2.1. GIS

GIS have a long history. One of the first examples of "GIS" dates back to 1854 with John Snow's mapping of Cholera outbreaks in London, whereby he identified the trend of outbreaks occurring along water lines (and subsequently becoming the birth of spatial analysis) (GISGeography, 2018). With the rapid improvement in technology in recent times, GIS are essential in the management of large spatial datasets, accurate characterisation of urban systems, and risk assessment. They are designed for capturing, storing, analysing, managing, and displaying detailed geospatial information (such as topography and building and infrastructure attribute data) using a particular geographic reference system (Amirebrahimi *et al.*, 2015; Esri, 2018; Fazal, 2008; Fosu *et al.*, 2015; GISGeography, 2019b). The transference of geospatial data and interoperability between systems are organised using the Geographic Markup Language (GML), an Open Geospatial Consortium (OGC) standard data model for defining data types and describing geographic features.

Applications using GIS include remote sensing, land surveying, and geography; however, some sources claim anywhere between 28 and 1000 uses ("67 Important GIS Applications and Uses", 2015; GISGeography, 2019a; Landis, n.d."Major areas of GIS application" (n.d.) has grouped these uses into five main fields as shown in Table 3. Despite this thesis focussing on uses in asset/facilities management and environment and natural resources management, all fields in Table 3 are discussed throughout this research, as they are all key criteria in the development of a "digital twin" (discussed in detail in Section 2.2.5.4).

Table 3: Classification of main GIS uses (from "Major areas of GIS application", n.d.)

Field	Application
Facilities and Asset management	• Buried utility location • Facility maintenance planning • Telecommunication network services • Planning and monitoring of energy consumption
Environment and natural resources management	• Agricultural land planning, forest management • Water resource management • Environmental impact analysis • Disaster management and risk mitigation • Waste facility site location analysis
Street network	• Traffic management • Emergency response • Transport planning
Planning and engineering	• Urban planning • Regional planning • Infrastructure feasibility studies
Land information system	• Cadastre administration • Taxation • Land use zoning • Land acquisition

Natural hazards are characterised by their intensity, location, and return period. The occurrence of a disaster from a natural hazard is governed by many factors, and the spatial information associated with these factors is crucial to risk assessment and resilience management (Section 1.2.1). Therefore, the analysis of natural hazard impacts greatly benefits from GIS, as it assesses the intersection of hazards and associated risks. This is achieved through use of geographical datasets such as topography, land use, infrastructure, and human/cultural, which aid in the assessment of hazard intensity, exposure and vulnerability of things and people, and therefore potential disaster risks. Biophysical datasets (e.g. landslide, flood, sea-level rise, earthquake, fire) gathered through predictive modelling or historic records help characterise hazards and evaluate degree of risk imposed on assets (Gunes and Kovel, 2000; Tarolli and Cavalli, 2013; Vatseva *et al.*, 2013). Attributes of asset datasets such as population age, transport links (i.e. road access, alternative route options, location of emergency services), building age, and utility age and topology, can be analysed to understand vulnerability to a disaster (Johnson, 2000; Van Westen, 2013).

GIS also offers the ability to carry out risk analysis utilising the datasets. By overlaying or intersecting the geographical and biophysical layers of information identified above, it provides the means to estimate the degree of risk, pinpointing areas that may be at high risk of exposure to extreme conditions, such as densely populated regions or old and fragile lifelines. Specific examples of this type of analysis include; the multi-hazard (flooding, landslides and earthquake) risk assessment of Costa Rica (Van Westen *et al.*, 2002) and seismic risk analyses by Cubellis and Carlino (2004); Nath (2005); Selçuk and Yücemen (2000). Flood analysis by Schulte and Coors (2009) used CityGML (discussed further in Section 2.2.3) to model water bodies in flood analysis; however, the water bodies were only 3D visualisations and did not include other vector-based metadata (such as velocity and temporal dynamics). These limitations extend into the representation of 3D buildings in CityGML and their lack of metadata, preventing CityGML's effective use for hazard analysis. Further discussion on the use and comparisons of CityGML with BIM are presented in Section 2.2.3.

Post-disaster, the response and recovery phases of risk management can also utilise GIS technologies, and the lessons captured during these phases aid in the trending component of resilience management as per Figure 1-5. Remote sensing using visible and near-infrared channels and GIS can quickly estimate the extent of a flood, delineate landslides, and in some cases identify damaged buildings and roads if high-resolution images are available (Tarolli and Cavalli, 2013; Vatseva *et al.*, 2013; Zerger, 2002). Light Detection and Ranging (LiDAR) techniques can be used to measure ground deformation after an earthquake, such as was conducted in Christchurch following the Canterbury Earthquake Sequence (CES) (Hughes *et al.,* 2015; see Section 2.3.3.2). Emergency and first responders rely on GIS and Geographic Projection Systems (GPS) to efficiently reach affected locations, monitor disruptions to the road networks and find alternative routes, and utilise census data in the determination of population densities that are likely to be the most adversely affected (Gunes and Kovel, 2000; Johnson, 2000; Rich and Davis, 2010). Using lessons learned from disasters can guide land use planning to restrict development in certain places (i.e. the Residential Red Zone in Christchurch, discussed in Section 2.3.3.4), or engineering civil works to withstand greater natural forces, such as those recommended by MBIE (2012) following the CES. Catalogues of historic events provide crucial information, especially when they are incorporated into a GIS, as they characterise spatial and temporal aspects of disasters.

Asset management (AM) requires not only having visibility of asset location, but also knowing its performance. Given that all assets have a geospatial location, mapping provides the most effective method of cataloguing; however, this only offers a simple geographical inventory. The combination of geospatial location with other datasets in a GIS offers the ability for deeper analysis as shown in Figure 2-1. However, according to Hurley (2018), 80% of asset managers do not effectively use GIS, and so have incomplete visibility of the AM components in Figure 2-1.

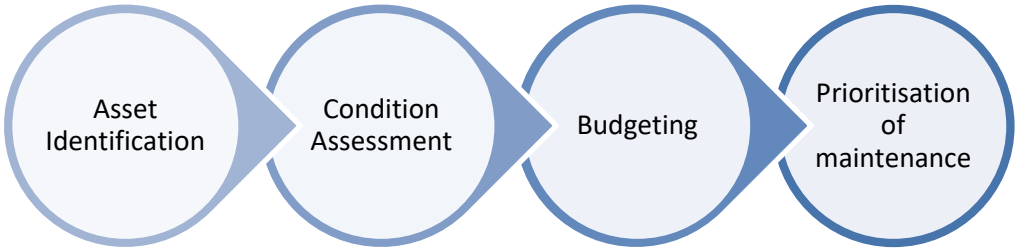

Figure 2-1: Asset Management components

Al-Kasisbeh and Abudayyeh (2018) demonstrated the implementation of GIS in AM using the Western Michigan University (WMU), USA, as a case study. By undertaking a data collection and conversion exercise of the WMU campus assets (e.g. buildings, pavements, utilities) in ArcGIS server manager, risk management and condition assessment approaches were developed for defining strategies for operations and capital maintenance. By implementing the condition index and risk assessment methodologies, prioritisation maps for wastewater manholes and mains were produced, as shown in Figure 2-2.

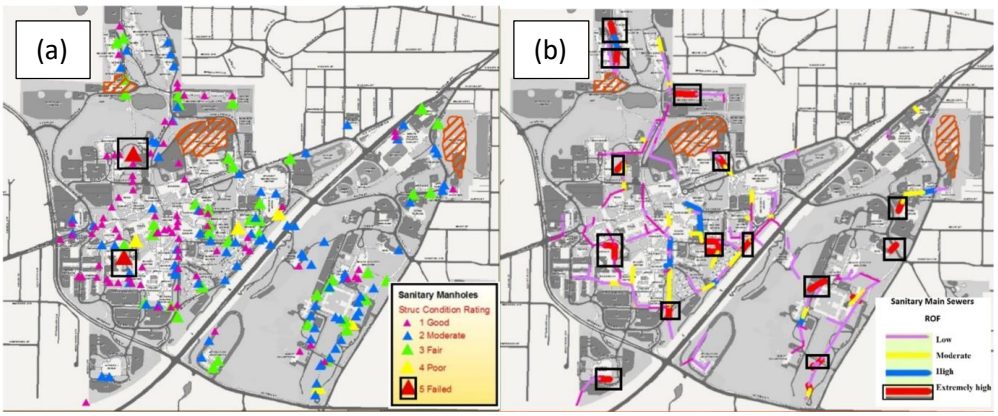

Figure 2-2: Condition and risk assessments of wastewater assets in GIS (from Al-Kasisbeh and Abudayyeh, 2018)

Schultz (2012) further developed the AM and GIS integration research by Al-Kasisbeh and Abudayyeh (2018), by providing a method for mapping existing AM databases to a developed GIS database for the Otay Water District (OWD), USA. Mapping was achieved using relational database management system (RDBMS) Sequential Query Language (SQL) statements. Results from mapping allowed grouping of vertical assets in the asset management system (such as pipes, values, and engines) to their associated pump station, and assigned these as point features in the GIS model. The integrated databases allowed risk and resilience metrics to be developed, similar to the analysis by Al-Kasisbeh and Abudayyeh (2018). However, in the case of the OWD, the two assessment criteria to test the GIS model were criticality/consequence of failure, i.e. combination of vulnerability and robustness, while also considering redundancy (from Section 1.2), and probability of failure (based on condition and age of asset).

Where Al-Kasisbeh and Abudayyeh (2018) and Schultz (2012) predominantly focussed on the integration and assessment of single-sector infrastructure, Bhamidipati *et al.* (2016) noted that hazards are not selective of the assets they impact, and so they investigated the means to develop an interconnected infrastructure model. Interconnectedness differs from interdependency, whereby the former is defined as a physical linking of systems but with unidirectional relationships. Interdependency is symbiotic in nature with bidirectional relationships i.e. how the relationships in a city's digital twin would operate (Section 2.2.5.4). However, Bhamidipati *et al.* (2016) presented examples of interconnected relationships that would still benefit from such analysis of a GIS-based AM system, such as modelling electrical distribution networks providing power to water distribution and pumping stations (cross-sector), and network infrastructure flow patterns transitioning from high to low capacity (single-sector). Also in contrast to Al-Kasisbeh and Abudayyeh (2018) and Schultz (2012), who both dealt with vulnerability, reliability, and robustness, Bhamidipati *et al.* (2016) proposed a GIS-based AM system, prioritising the requirements of an asset manager (i.e. maintenance and replacement assessment) through the use of GIS and Agent-based Modelling Architecture (GAMA) (Grignard *et al.*, 2013).

The adopted layering approach of each asset in Bhamidipati *et al.* (2016) meant that as each layer increases in data, individual asset layers could be improved further without affecting other connected asset layers. Similarly, individual layers can be weighted based on their importance relative to other layers. A small area of North Rotterdam in The Netherlands was tested against a flood event scenario in three separate experiments of varying degrees of interconnectedness. The results highlighted the additional impacts caused to the road assets when factoring in other interconnected assets such as sewer and electricity. This presents a significant analytical tool for asset managers, enabling them to become more aware of vulnerabilities from the condition of other connected assets. Having an integrated platform that all asset managers can access and provide input to (such as a citywide digital twin discussed in Section 2.2.5.4) enables greater collaboration, and is essential in the budgeting and prioritisation of maintenance works components (Figure 2-1).

The above asset management examples demonstrate that with the use of GIS, organisations are able to:

- Identify preventive maintenance requirements (forecasting through the resilience framework in Section 1.2.2),
- Estimate asset lifecycle more accurately,
- Adopt a preparedness approach to faulting of assets (anticipation component of Figure 1-5) (Al-Kasisbeh and Abudayyeh, 2018; Schultz, 2012),
- Determine vulnerability caused by faulting (such as number of affected customers through loss of service) (Schultz, 2012),
- Impacts caused by disruption from interconnected assets (Bhamidipati *et al.*, 2016; Schultz, 2012).

2.2.2. BIM

Unlike GIS, which has had a long evolution, BIM has only been in development since the 1990s (Liu *et al.*, 2017) and has predominantly been used for engineering design and asset management. During the lifecycle of a building project, stakeholders such as Architects, Engineers, Construction, and Operations and Facility Management (AECOFM) all have varying degrees of involvement and input, so a system was needed to improve the effectiveness in exchange of information; hence the development of BIM. BIM provides the means of recording geometric and semantic building information in a highly detailed model, and is a tool for capturing a project workflow. Its means as a tool for integration, interoperability, and process automation for construction projects further demonstrates its usefulness within industry. BuildingSMART (n.d.-b) defines BIM as "a digital representation of physical and functional characteristics of a facility. A building information model is a shared knowledge resource for information about a facility, forming a reliable basis for decisions during its life-cycle; defined as existing from earliest conception to demolition." BIM is an intelligent 3D model-based process that gives AECOFM professionals the insight and tools to more efficiently plan, design, construct, and manage buildings and infrastructure (Autodesk, 2018).

The cost and schedule aspects of a BIM are not only beneficial during the design and construction phase, but also upon project completion during the facilities/operations and maintenance (FM/OM) phase (Kurwi *et al.*, 2017). Studies have shown that traditional paper-based methods and a lack of interoperable model-based applications contribute to total life-cycle FM/OM costs being three times higher than construction costs, and accounts for two-thirds of the total cost (Yalcinkaya and Singh, 2014). Current non-digital handover practices from construction to FM/OM phase often result in the delivery of incomplete, out-of-date, and unstructured data, and is a costly and time-consuming process (Patacas et al., 2015). Equally, common organisation and maintenance of FM data are dispersed through several information systems, arrive from different sources, are created and manipulated numerous times through the asset life-cycle, and are unsynchronised between systems, often resulting in error-prone processes. BIM provides a centralised database for information transferral between the design, construct, and FM/OM phases (Becerik-Gerber *et al.*, 2011).

During the FM/OM phase, BIM enables asset managers to proactively track the facility/asset, hand information from one contractor to another, and schedule maintenance and review maintenance history. However, upon review of literature, BIM use in FM/OM is in its infancy. For example, Kivits and Furneaux (2013) list 13 projects that had adopted BIM in at least one phase of the infrastructure life-cycle, and of those 13, only four made reference to facilities or asset management, the remainder were used predominantly during the design phase. Similarly, Pocock *et al.* (2014) recognised that current industry perception is that BIM and AM are isolated practices, and so provided recommendations identifying the key benefits to integrating the two such as:

- Government and engineering professional bodies taking a "whole life-whole system-whole industry" approach in the further development of BIM and AM standards,
- Raise awareness of the need to develop BIM and AM in organisations in an integrated way through established channels and promote training programmes and professional qualifications to develop the required competencies,
- Develop and embed enterprise-wide information systems and processes combining BIM and AM in compliance with emerging BIM and AM standards to ensure consistent application across all planning, projects, and FM/OM functions,
- Develop appropriate client requirements for BIM and AM and communicate these to the supply chain,
- Take a phased approach to extending BIM for existing assets prioritised by asset criticality.

Research has been undertaken to develop systems to overcome the disparity between BIM and FM/OM information and integrate them in a unified database including knowledge-based BIM systems and cloud environments (Jiao *et al.*, 2013; Wang and Xie, 2002; Zou *et al.*, 2017). Yalcinkaya and Singh (2014) recognised that even with the integration of BIM and FM as a virtual database application, for operational success BIM cannot collect and transfer facility data on its own. Therefore, the use of other smart technologies such as radio frequency identification (RFID) and other wireless sensors (Ko, 2009; Shen *et al.*, 2012) contribute to the creation of a digital twin (section2.2.5.4), providing the means to track and monitor assets and the building environment.

Regarding the use of BIM for risk management, Zou *et al.* (2017) provided a table from their own literature review, in which the significant majority of cases were grouped into four categories; project management, design, construction (including health and safety), and FM/OM. The table also presented examples of the benefits under two themes: "Research", and "Practice". Of particular note is a lack of citation for a "Practice" example for the FM/OM category, further cementing the notion that the use of BIM in this phase of project life-cycle is in early development. There was only one example of BIM use for performance analysis of a bridge design; no other examples of risk assessment of natural hazards were identified. Table 4 presents a modified version of Zou *et al.* (2017), supplemented with other literature; it incorporates identified examples of BIM use in natural hazard risk assessment.

It is clear from the literature that the focus of BIM research and development has been biased toward evolution and standardisation in the engineering and design aspects of the project life-cycle. Pocock *et al.* (2014) and Kivits and Furneaux (2013) recognised the potential of BIM as an FM/OM tool, but acknowledged this application is still in its infancy and there are few case studies of its adoption in the industry. Equally, this literature review has identified few cases where BIM has been used in disaster and hazard management. However, a commonly-identified theme was that BIM's potential significantly increases when linked with other existing tools and systems, such as sensor technology in the FM/OM phase of a project life-cycle (Jiao *et al.*, 2013; Wang and Xie, 2002; Zou *et al.*, 2017), and with GIS in the design and FM/OM phase (discussed in detail in Section 2.2.4.).

Table 4: Examples of BIM for risk management (modified from Zou et al., 2017)

Category	Functionality	Benefit for risk management
Project management	Interoperability	Reducing information loss of data exchange
	Collaboration and communication facilitation	Facilitating early risk identification and risk communication
	4D Construction scheduling/planning	Facilitating early risk identification and risk communication
	5D Cost estimation or cash flow modelling	Planning, controlling and managing budget and cost reasonably
Design	3D Visualisation	Facilitating early risk identification and risk communication
	Clash detection	Automation of detecting physical conflicts in model
	Urban planning and design	Integrating planning and design of urban space and AEC projects; facilitating land-use planning, design and management
	Space management	Improving the consideration of space distribution and management in design
	Code compliance	Use of automatic rule checking technologies to ensure design complies with building costs and regulatory authorities (Eastman *et al.*, 2009)
Hazard Assessment	Structural analysis	Improving structural safety
	Detailed internal room layout	Disaster risk management (flow paths of mud/lava, identification of social conditions for exposure and vulnerability components of risk assessment) (Kemec *et al.*, 2012)
	Damage assessment	Damage estimation to assist in cost estimating and scheduling for post-disaster rehabilitation (Alirezaei *et al.*, 2016; Charalambos *et al.*, 2014) Seismic risk mitigation (Welch *et al.*, 2014)
Construction	Construction progress tracking	Improvement management level for quality, safety, time, and budget
	Safety management	Reducing personnel safety hazards
	Risk scenario planning	Reducing personnel safety hazards
	Quality control	Improving construction quality
FM/OM	FM/OM	Improving management level and reducing risks

2.2.3. Comparison of GIS and BIM

Although the examples presented in Section 2.2.1 demonstrate applications of pure GIS in asset and facilities management, many of the examples have direct linkages with BIM, in either a direct translation of BIM to GIS (vertical assets captured in Al-Kasisbeh and Abudayyeh, 2018), or complementary dynamics between GIS and BIM systems (interconnected infrastructure in Bhamidipati *et al.*, 2016). Although the main functionality of both BIM and GIS is to create digital representations of the real world, they were developed as solutions for different problems in different domains. Where GIS is used generally at a macro-level in the real world (e.g. terrain, river, land parcels, "outdoor" data), BIM is in a relatively micro-level of detail e.g. buildings and "indoor" data. Table 5 summarises the key features of both GIS and BIM, highlighting areas of comparability and areas of conflict; further discussion regarding each of the features is below. Liu *et al.* (2017) recognised macro-scale areas of overlap between BIM and GIS, as shown in Figure 2-3.

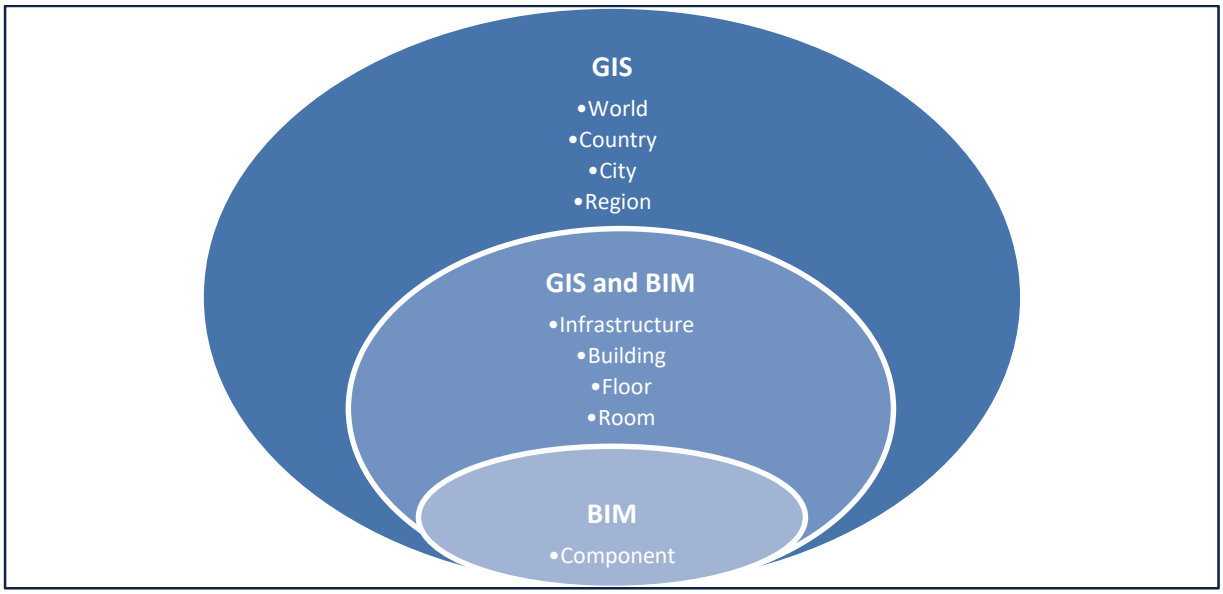

Figure 2-3: Overlap between fields of GIS and BIM (after Liu et al., 2017)

Table 5: Comparison of key BIM and GIS features

Feature	BIM	GIS
Standard	Industry Foundation Classes (IFC) described by one of six Level of Development (LOD) categories (AIA, 2019; BIMForum, 2018): • LOD100 –*non-geometric representations and any information derived from these models should be considered approximate.* • LOD200 – *Elements are generic placeholders with some distinguishing features of the elements they represent, or are volumetric space placeholders. Similar to LOD100, information from this LOD should also be considered an estimate.* • LOD300 – *Quantity, size, shape, location, and orientation can be measured directly from the model. The project origin is also defined and elements are accurately scaled and located from this origin.* • LOD350 – *same as LOD300 but with the addition of interfaces with other building systems. Numerical data as designed can be measured directly from the model and parts necessary for coordination with nearby or attached elements are modelled such as supports and connections.* • LOD400 – *Model is sufficient for fabrication of the represented elements.* • LOD500 – *Field verified model.*	City Geographic Markup Language (CityGML) specified as Extensible Markup Language (XML) described by one of five Level of Detail categories (Liu *et al.*, 2017): • LOD0 – Region and landscape. • LOD1 – City and region. • LOD2 – City, city district, and project. • LOD3 – City district, exterior architectural model and landmark. • LOD4 – Landmark and interior architectural model.
Resolution	3D, generally non-georeferenced (pre-introduction of IFC4 – see Section 2.2.4). Spatial data relative to origin of object.	Georeferenced, large-scale, predominantly two-and-a-half-dimension city-wide level.
Scale	Individual building/infrastructure/asset.	Heterogeneous geospatial information for example buildings, transport, vegetation and water bodies. Currently no representation for utilities/horizontal infrastructure.
Concept	Single database or group of databases that can be linked together, thereby, easing accessing and sharing information in an effective way through the whole lifecycle of the building (Autodesk, 2018; Isikdag *et al.*, 2008).	Manage large spatial datasets, accurate profiling of an urban system, and assessment of risk. Designed for capturing, storing, analysing, managing, and displaying detailed geospatial information.
Accuracy	Optimised for the modelling of new, well defined objects.	Reconstruction of existing objects often only sparse and incomplete information available.

i. Standard: Generally for buildings, Industry Foundation Class (IFC) is the predominant standard for BIM developed by the AIA/buildingSMART whose goal is to specify a common language for technology to improve communication, delivery time, cost, and quality throughout the whole project life-cycle (Isikdag and Zlatanova, 2009). Each "class" represents a range of elements that have common characteristics as shown by the class "*IfcBuildingElements"* in Figure 2-4. The six BIM Level of Development (LOD) categories shown in Table 5 are taken from the AIA protocol form (AIA, 2019), as it is likely the best-known and most commonly-used worldwide (Renehan, 2016). Renehan (2016) presented a summary of other LOD schemas used internationally, including the Open Geospatial Consortium (OGC) – international, the developers of CityGML. The intent of CityGML is to represent large- and small-scale regions of both terrain and 3D objects in simultaneous levels of detail. It defines classes and relationships for topographic objects in cities and regional models with respect to their geometry, topology, appearance, and semantic properties. Objects in CityGML are not limited to built structures, but also include elevation, vegetation, water bodies, and "city furniture" e.g. street lights, public telephone boxes, benches ("Citygml wiki", 2017).

ii. Resolution: BIM and GIS have similar specifications for degree of resolution from their corresponding standards. An increase in BIM resolution provides a higher degree of accuracy of building elements and the associated dimensional data for a single building i.e. it is not until LOD300 whereby a model is no longer considered an estimate. GIS, however, transitions from macro- to micro-scale of the built and natural environment with an increase in resolution. Visual representations of buildings at LOD4 and LOD300 (or higher) are generally comparable, as shown in Figure 2-5. However, IFC contains more numerical data on measurable quantities and relationships between elements, particularly in the model of building interiors. There are other common dissimilarities and mismatches between IFC and CityGML, such as CityGML representing a wall as a surface for each room separately, whilst IFC treats a wall as a volume object shared between rooms and the exterior shell (Figure 2-6). As a result, the conversion and integration of one to the other is not easy (discussed further in Section 2.2.4).

iii. Scale: Both GIS and BIM provide heterogeneous models, with the former usually separated into architectural, structural, and Mechanical/Electrical/Plumbing (MEP) models, the latter representing buildings, transport, vegetation and water bodies. However, the key difference identified in Table 5 is that BIM represents a single building and its associated infrastructure, whereas GIS can cover much larger areas representing many objects. Therefore, GIS with its broader built environment view and means of geovisualisation-based decision making and geospatial modelling, is essential for data management in modern construction (Song and Li, 2017). As discussed in Table 5, CityGML has no means of representing utilities in the same manner that BIM does. However, a range of Application Domain Extensions (ADEs) have been developed to improve CityGML's functionality such as "CityGML UtilityNetworkADE" (Hijazi *et al.*, 2011), a topic further discussed in Section 2.2.5.1.

iv. Concept: Generally, GIS and BIM attempt to overcome the same issue in their goal to be a centralised database, or group of linked databases, that can capture, store, manage and disseminate information whilst providing a visual output. A current detrimental similarity between GIS and BIM is their incomplete ability to transition through a whole project life-cycle (Sections 2.2.1 and 2.2.2), particularly in the FM/OM phase, where the integration of sensor technology with both GIS and BIM is a relatively new field of research. The key differences however, as explained previously, is that BIM operates at a micro-scale compared to the larger spatial datasets that GIS can manage. Also, based on the available literature presented in Section 2.2.1, GIS appears to be more advanced in its ability and use in risk assessment for natural hazards (Cubellis and Carlino, 2004; Nath, 2005; Schulte and Coors, 2009; Selçuk and Yücemen, 2000), and consequential risk caused by failure of assets in the same or interconnected topological networks (Al-Kasisbeh and Abudayyeh, 2018; Bhamidipati *et al.*, 2016; Schultz, 2012).

v. Accuracy: The mismatch between BIM and GIS (pre-construction versus as-built) is another challenge, which needs to be overcome. Fosu *et al.* (2015) acknowledged this challenge, particularly where older buildings with non-existent or less accurate building plan information are present. However, as is discussed in Section 2.2.5.1, Yang *et al.* (2012), Centofanti *et al.* (2011), SanJosé-Alonso *et al.* (2009), and Dore and Murphy (2012) have presented methods to retrospectively capture digital information for heritage buildings. For new buildings developed in BIM, the implementation of an LOD500 model would provide an as-built version and close the gap between GIS and BIM representations of buildings. However, along with few demonstrable cases of LOD500 models in the literature, there is no mandated Quality Assurance (QA) process in place, particularly in New Zealand, to validate a LOD500 model with its real world counterpart. This challenge also affects the transition of data during the project life-cycle to the FM/OM phase and reduces the accuracy of a digital twin (Section 2.2.5.4).

The above shows many of the existing characteristics of GIS and BIM are comparable and interoperable. Whilst it has been recognised that there have been developments in improving GIS and BIM separately, in their functionality for use in the whole project life-cycle, there are still several gaps, particularly between the design and construction phases, and construction and FM/OM phases. The research by Bhamidipati *et al.* (2016), in the development of interconnected and interdependent relationships, is a key basis for integrating GIS and BIM technologies by increasing the number of semantic properties between building and utilities. The following sections further explore methods of integrating GIS and BIM that form the basis of this thesis.

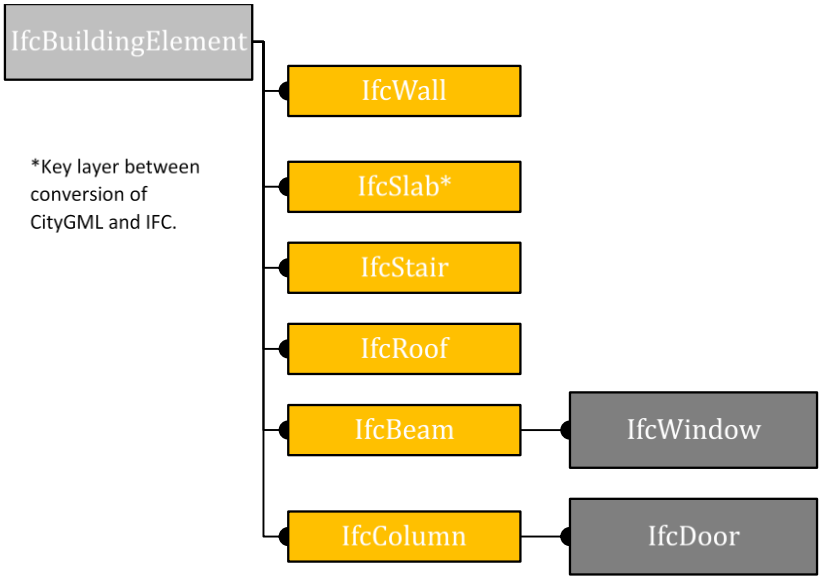

Figure 2-4: Excerpt of IfcBuildingElement schema (from BuildingSMART, n.d.-a)

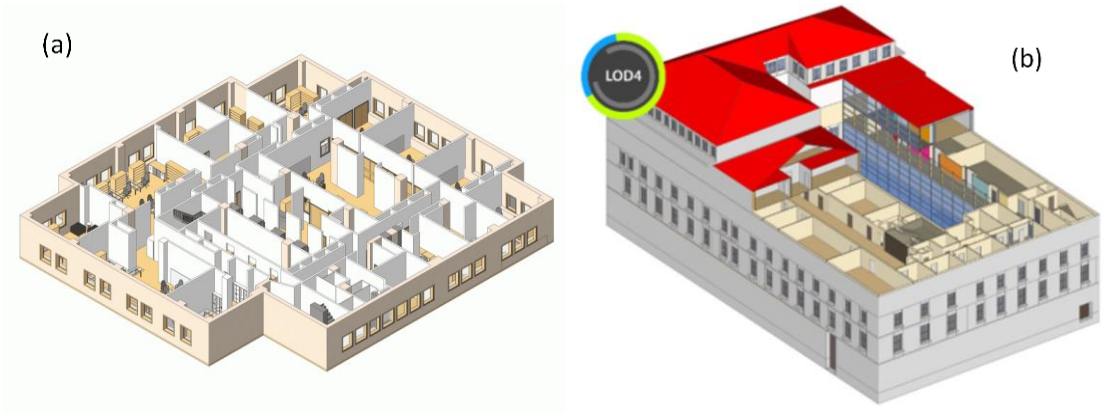

Figure 2-5: Interior room layout comparison of LOD400 (a) and LOD4 (b) from "Marvelous Design Revit House Plans..." (2018) and "About Level of Details" (2016), respectively

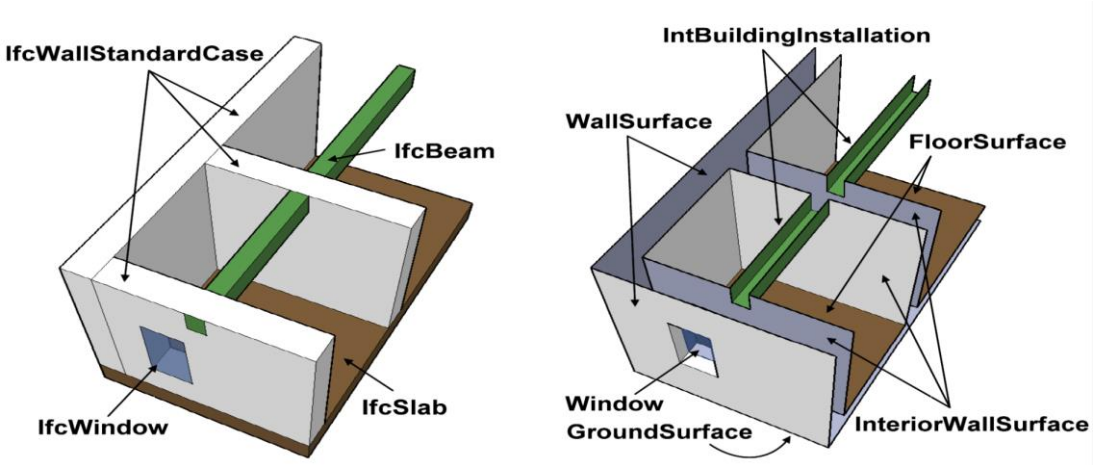

Figure 2-6: IFC and CityGML comparison of room elements (from de Laat and Van Berlo, 2011)

2.2.4. Methods of GIS and BIM Integration

As demonstrated in the previous Sections, there is a substantial amount of research in the fields of GIS and BIM independently of one another, each with their own strengths and weaknesses. The complementary nature of information provided by GIS and BIM highlights the usefulness of their potential integration, bridging the gap between the macro-scale environment and detailed building data at micro-scale, offering a large quantity of information from GIS to detailed information in BIM. Furthermore, the use of an integrated GIS and BIM system for urban management tasks and processes throughout a project life-cycle provide high efficiency through knowledge capture and continuous analysis of work, resulting in increased productivity in the AECOFM industry. Integrating BIM with GIS is not a novel idea (Fosu *et al.*, 2015) and with the continuing evolution of GIS and BIM in their conventional uses of engineering and asset management (BIM Acceleration Committee, 2016; Kassem *et al.*, 2015), the data contained within the models are an equally important resource in the assessment of resilience of the built environment (Section 2.2.5).

When combining GIS and BIM, Liu *et al.* (2017) used the term "Effectiveness, Extensibility, Effort, and Flexibility" (EEEF) to describe the method of selecting parameters of interest. They recognised that success of an integrated system hinges on openness and collaboration, which can be achieved by (i) being demand driven through, (e.g. the Smart City development, Ma and Ren, 2017), discussed further in Section 2.2.5.4), (ii) frequent communication, and (iii) government initiatives.

Existing integration methods have been categorised into three main groups (Amirebrahimi *et al.*, 2015; Fosu *et al.*, 2015; Liu *et al.*, 2017):

1) *Data level* (New standards and models, and conversion, translation and extension of existing standards) – e.g. Standard for interoperability between GIS and BIM for land and infrastructure (Aien *et al.*, 2015), or creation of Unified Building Models (UBMs) (de Laat and Van Berlo, 2011; El-Mekawy *et al.*, 2012a, 2012b).

2) *Process level* (semantic web technologies and service-based methods) – e.g. use of a reference ontology to take a global view of domains through extending and specialising existing ontologies (Amirebrahimi *et al.*, 2015), and open web viewers that convert BIM and GIS data for web visualisation (Hagedorn and Döllner, 2007; Lapierre and Cote, 2007).

3) *Application level* – existing GIS or BIM tools are either modified or rebuilt to include the functionality of the other. Data are extracted for a specific use, saved locally, and manipulated manually.

The *Process* and *Application* levels generally result in the least data loss and provide the means to derive elements and objects from either format. Table 6 summarises the main integration methods, the benefits and drawbacks to each, and scores them based on the EEEF criteria. Examples of each of the three categories are presented in subsequent sections. The development of CityGML by the OGC closes the gap between the two languages of BIM and GIS, which represents a significant step towards the use of GIS data in a BIM platform. Similarly, IndoorGML complements the existing IFC and CityGML LOD4 standards. This system supports BIM data with potential to support geospatial information.

Table 6: Comparison of integration solutions by "EEEF" criteria (Liu et al., 2017).

	Key Benefits	Key Drawbacks	Integration Method	After Liu *et al.* (2017)			
				Effectiveness	Extensibility	Effort	Flexibility
Data Level	• Potential to overcome integration problem both fundamentally and revolutionarily. • Risk of drawbacks can be reduced through application-oriented, focused and less ambitious model development. • UBM acts as an intermediate to relate GIS andBIM. • UBM able to be revised for different applications.	• Generally, can only provide solution to one particular view (e.g. building, infrastructure and indoor space). • No single standard can cover all aspects in a region. • Time and cost consuming process. • Information loss unavoidable due to differences between class type and LOD in original and object schema. • Ambitious and can be complex.	New standards and models	C	C	C	C
	• Geometry and semantics should stay relatively consistent during translation. • Semi-automatic Convert/translate/extend considered a good compromise of all methods. • Good for translating large volumes of data in batches. • ETL provides bidirectional conversion. • Schema mapping in ETL is flexible. • Enables data sharing rather than converting existing standards or developing new ones.	• Minor Information loss commonly occurs during conversion • ETL process (Section 2.2.4.3) requires operator to be highly knowledgeable in GIS and BIM semantics for schema mapping (risk of human error). • Quick response ETL still unachieved at practical level i.e. cannot implement on-demand and real-time data conversion. • Schema mapping process is time consuming and costly (but less so than new standard methods). • Normally no geospatial coordinate reference in IFC (unless using IFC4). • ETL from one study would require revision for use in another.	Manual conversion, translation and extension of existing standards	M	H	H	M
			Semi-automatic conversion, translation and extension of existing standards	M	M	M	M

(continued)

	Key Benefits	Key Drawbacks	Integration Method	After Liu *et al.* (2017)			
				Effectiveness	Extensibility	Effort	Flexibility
Process Level	• Generalised integration solution. • No change in data format or structures. • Provides machine accessible semantics to annotations using schema-ontologies. • Acts as a means of sharing data, rather than converting existing standards or creating new ones. • Natural ability to integrate from different sources. • Enable bidirectional conversion.	• Requires extensive human intervention – low productivity at early stage. • Costly method at an early stage. • Semantic web technology isolated and independent ontologies exacerbate challenges for scientists and engineers of different domains.	Semantic web technologies	H	H	H	M
	• Good integration results. • Enables data sharing rather than converting existing standards or developing new ones. • Effective semantic and geometric conversion. • Less information loss.	• Requires extensive human intervention – low productivity at early stage. • Specialised problem solving. • Expensive and specialised solution requited when problems occur such as low efficient mapping process due to non-optimised programming code.	Services-based methods	H	L	H	L
Application Level	• Generally, requires least effort when compared to Data and Process levels as source data, object data, service, and ontology are neither changed nor developed. • Low cost and relatively good integration result.	• Costly and inflexible. • Cannot easily be adopted by others. • Developed to solve a particular problem and is not generalised.	Application focused methods	C	L	L	L

Note: C= “Case by Case”, L= ”Low”, M= ”Medium”, H= ”High”

2.2.4.1. Data level

The OGC and buildingSMART International proposed a new standard of IFC interoperability with CityGML named InfraGML, a successor to LandXML. The new specification will look specifically at Computer Aided Design (CAD)-GIS-BIM integration, defining the requirements for bridging the data models and workflows between the AECOFM and geospatial communities. InfraGML covers area of land development and civil engineering infrastructure facilities, with potential to include transport networks, terrain, land parcels, drainage, wastewater and water distribution systems in the future (Aien *et al.*, 2015).

One of the semi-automatic ways to convert/translate GIS and BIM data are through the Extract Transform Load (ETL) process. Homogenous data are extracted from the source system and loaded by transformation into an appropriate format and structure to a data warehouse. To improve efficiency, geometry is also processed by ETL before being represented in the integrated system (Kang and Hong, 2013). The process often begins with geometry conversion, followed by Global ID allocation used to automate semantic translation. Translation is achieved through schema mapping to a data format the destination can recognise (Kang and Hong, 2015; Rafiee *et al.*, 2014).

2.2.4.2. Process level

Deng *et al.* (2016) used an instance-based method that compares instances from the IFC and CityGML schema and generated mapping rules between the two, based on inspection of entities representing the same components in the same model. A reference ontology (Semantic City Model ADE) was developed to act as the intermediary between the IFC and CityGML schema structures and capture all the relevant information of the two during the schema mapping process. There were several limitations with the study, which included the consideration of buildings only, and other 3D objects such as roads, bridges, and tunnels were not modelled. In addition, the framework, reference ontology, and translator were only applicable for IFC and CityGML, and finally, Boundary Representation (BRep), Swept Solid, and Constructive Solid Geometry (CSG) were the only geometry transformations considered.

Four challenges in data integration were identified that Deng *et al.* (2016) proposed to overcome by:

i. Transformation of geometric representations. IFC supports use of BRep, Swept Solid, and CSG, whereas CityGML only supports BRep. The use of a translator paired with the Semantic City Model ADE successfully demonstrated the bidirectional conversion of common building components such as walls, doors, windows, roof, slabs, and floors, (Figure 2-7), whilst retaining the IFC semantic information in the CityGML conversion.

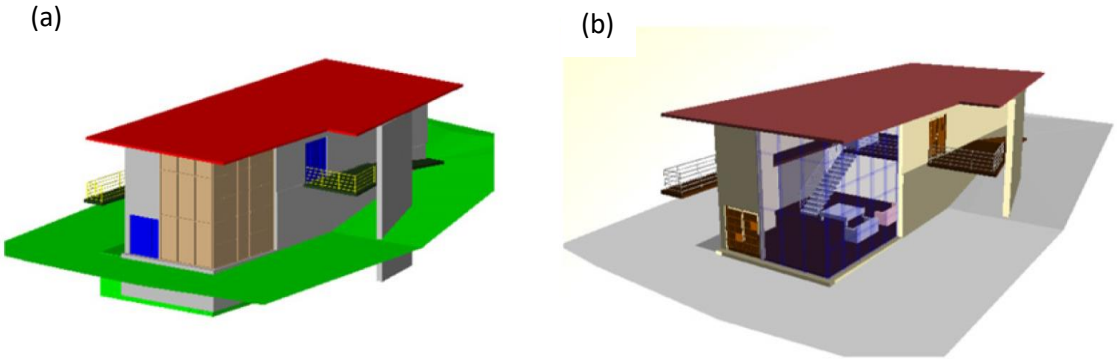

Figure 2-7: Comparison of IFC and CityGML geometric representations where (a) is the BIM model in IFC and (b) is the CityGML model generated (from Deng et al., 2016)

ii. Transformation of local placement system (IFC) to world coordinate system (CityGML). Functions were developed for IFC Swept Solid to CityGML BRep and IFC BRep to CityGML BRep. The former is the most commonly seen geometric transformation based on a function given coordinates "A" and "B" and sweeping vector "V" from the sweeping planning and sweeping line, a new IFC BRep surface is generated which can be transformed to CityGML BRep directly. The latter extracts the coordinates of IFC BRep from the parser and translates to CityGML through the following function:

$$\begin{bmatrix} C_X \\ C_Y \\ C_Z \end{bmatrix} = \begin{bmatrix} I_X \\ I_Y \\ I_Z \end{bmatrix} \times M + \Delta \qquad (2)$$

where:

C represents the CityGML coordinate system

I is the IFC local placement system

M is the coordinate system transformation matrix

Δ is the origin difference

iii. Harmonisation of LODs (both levels of detail – CityGML, and levels of development - IFC) between IFC and CityGML. Currently, there are no complete transformation frameworks between LODs in CityGML. The developed translator was able to downscale higher LODs to lower versions whilst retaining the semantic information associated with the higher LOD, even if components were deleted in the visual output (i.e. interior walls). The harmonisation of LODs is fully customisable allowing simplification of models to reduce file size. The results of the study demonstrated that the translation of high to low LOD was successfully generated with no loss of information or incorrect geometry.

iv. Data loss during the integration process, many entities in IFC, particularly relating to; owners, construction processes, cost information, and FM/OM, do not have corresponding CityGML entities. Likewise, CityGML contains information relating to cartography, which has no IFC equivalent. The developed reference ontology from the study by Deng *et al.* (2016) was able to capture all information from both CityGML and IFC, by using Semantic City Model ADE, was also able to store IFC semantic information, and translated as a data table in CityGML. Similarly, component relationships and structural property information from IFC can also be stored in CityGML.

An example of an Open Web Service for GIS and BIM integration is presented in Lapierre and Cote (2007). The process demonstrated that Web Feature Services (WFS) could feasibly merge CAD, GIS and BIM formats by creating linkages between source data (Figure 2-8). During the development of the process, the current version of IFC did not include the elements “IfcGeographicElement” and “IfcGeographicElementType” (as IFC4, BuildingSMART, n.d.-a, had not been released), so Lapierre and Cote (2007) undertook a manual process of object coordinate to coordinate systems conversion. The progression of IFC4 included further steps towards interoperability with GIS. However, it demonstrated one of the biggest challenges where isolated ontologies within a domain are being developed, leading to other constraints of heterogeneous data fusion.

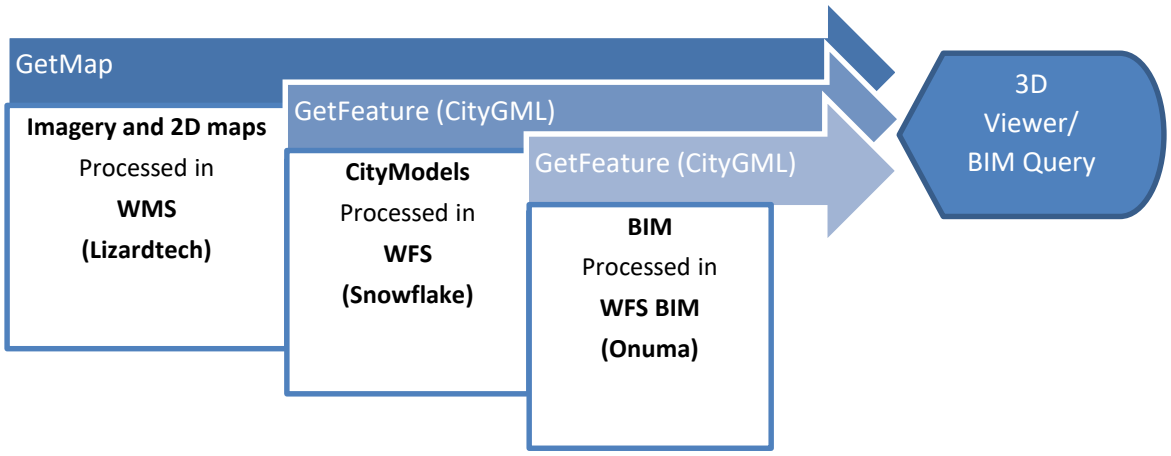

Figure 2-8: Analysis process of building information over a broad geographic area (Lapierre and Cote, 2007)

Lapierre and Cote (2007) integrated IFC objects, such as rooms, in the Open Web Service for use in temporary medical response facility selection and recognised that this scenario would normally involve collaborators from different specialties and organisations, and require the most up-to-date information in the shortest possible timeframe. Whilst the integration methodology chose a simple room view application of IFC objects (Figure 2-9), it demonstrated the applicability to other aspects of a building such as utility-building connections (discussed in detail as part of the case study in Chapter 4 and Chapter 5).

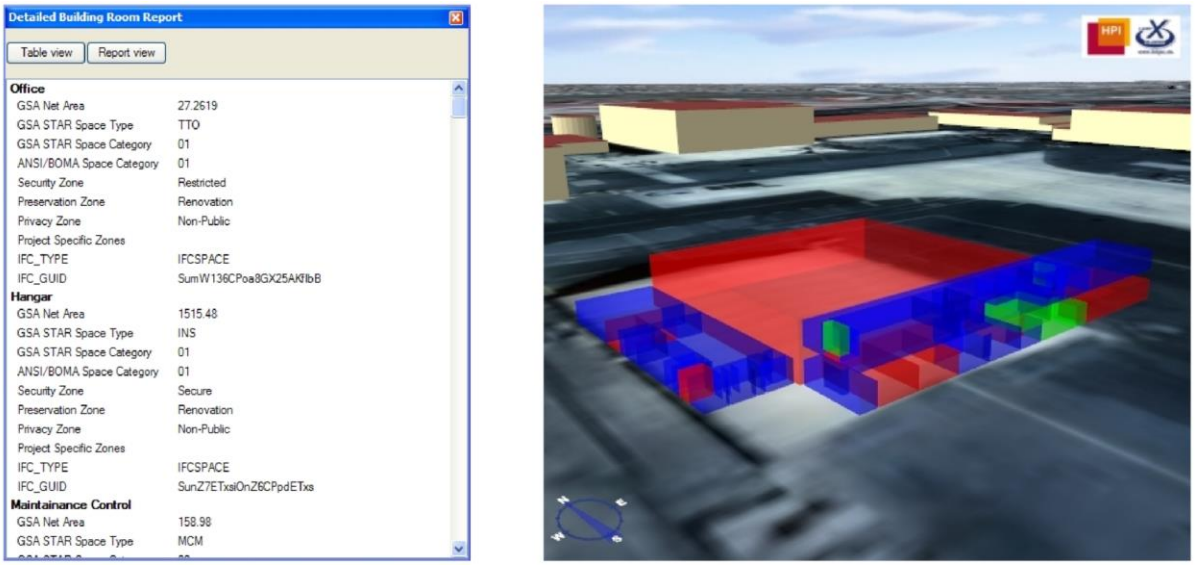

Figure 2-9: Textual building room report (left) and visual building assessment (right) (Lapierre and Cote, 2007)

2.2.4.3. Application level

Niu *et al.* (2015) presented a simplistic integration method where they developed a process of extracting the useful information out of a BIM model, simplified, and stored as a .gbXML file (Green Building XML). The .gbXML file is then converted to Keyhole Markup Language file extensions (.kml) and Collaborative Design Activity (COLLADA) and presented in Google Earth as shown in Figure 2-10. Whilst not a costly method in terms of time and labour, as presented in Table 6, application-based integration methods are designed to solve one problem and normally cannot be adopted by others. In the case of Niu *et al.* (2015), the tool was designed to assess building energy consumption.

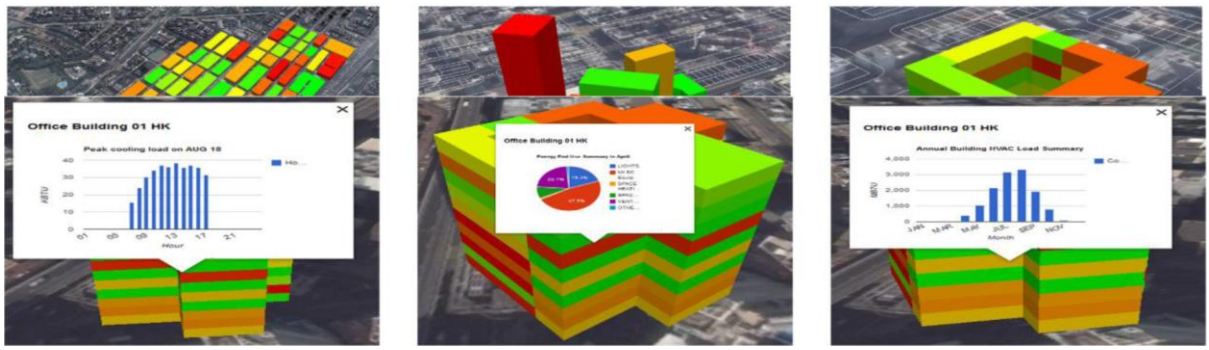

Figure 2-10: Google earth representation of 3D models showing daily peak cooling load (left), energy end use (centre), and annual HVAC electricity (right) (Niu et al., 2015)

2.2.5. Applications of Integrated GIS and BIM

The integration of GIS and BIM is a relatively modern research topic, and despite many publications highlighting its potential use as an FM/OM tool (Mignard and Nicolle, 2014; Zhang *et al.*, 2009), the commonalities and complementary attributes of the systems also lend themselves to becoming a crucial application in the characterisation of urban risk, resilience and vulnerability. By having access to up-to-date, accurate quantitative city-wide data, showing a fully integrated model of the infrastructure lifelines and the critical sites they service, the integrated tool would provide the ability to assess the 4 Rs (Section 1.2.2) and in turn demonstrate the progress/success of the Sendai targets set by UNISDR (2015) (Section 1.1). The applications of an integrated tool are discussed in detail in the subsequent sections.

Fosu *et al.* (2015), present their own literature review of future needs, and note that recent research has been trying to combine GIS and BIM data for various purposes such as utility visualisation, climate adaptation, and natural hazard damage analysis. Whilst extensive research has been undertaken within BIM and GIS, independently, the nature of their respective datasets is complementary to one another, demonstrating a need for further research in their integration (de Laat and Van Berlo, 2011). Kurwi *et al.* (2017) provided a table of applications of an integrated BIM and GIS system, an excerpt of which is presented in Table 7.

Table 7: Applications of GIS and BIM integration (modified from Kurwi et al., 2017)

Project Stage	Application	Reference
Planning and design	Select the site and manage fire response	Isikdag *et al.* (2008)
	Easiest collaboration between planning	Niu *et al.* (2015)
Construction	Managing construction supply chain, green design, construction and sustainable sequences	Irizarry *et al.* (2013)
Operation and Facility management	Emphasise the material delivered by enabling tracking the status of the supply chain.	Irizarry *et al.* (2013)
	Flood damage assessment	Amirebrahimi *et al.* (2015)
	Detect and map the information for pipe networks	Liu and Issa (2012)
	Managing the processes of maintenance and repair of facility management	Karan and Irizarry (2014)

Other applications for integrated GIS and BIM include the following, which are discussed in the remainder of this section:

- *Asset management,*
- *Heritage Management*,
- *Urban Environment Analysis,*
- *Performance of the Built Environment to Hazards,*
- *Location-based services and navigation in applications such as emergency response*.

The combination of BIM and GIS allows for effective management of heterogeneous information from different sources and can provide essential support for decision-making (i.e. resilience planning).

2.2.5.1. Vertical and Horizontal Infrastructure Connectivity

Whilst the previous section presented methods integrating BIM into a GIS platform, there are very few examples where horizontal infrastructure and utilities are geospatially referenced within a BIM model, and even fewer linking buildings to their associated utilities in a GIS platform. The concept of integration itself is not new. Aien *et al.* (2015) presented a 3D conceptual data model (3DCDM) integrating legal (e.g. land use zoning, cadastral boundaries) and physical objects, which included utility networks. The lack of utility networks in a 3D digital built environment are further reinforced in Liu *et al.* (2017) who recognised having utilities network BIM data combined with InfraGML (Section 2.2.4.1) will improve GIS management and network analysis.

Hijazi *et al.* (2011) acknowledged that 3D models have neglected utility networks in built environments. To overcome this, they presented a method to integrate interior building utilities (Figure 2-11, highlighted red area) into a city model by means of semantics mapping using UtilityNetworkADE in CityGML and the IFC entity *IfcRelAssignsToGroup.*

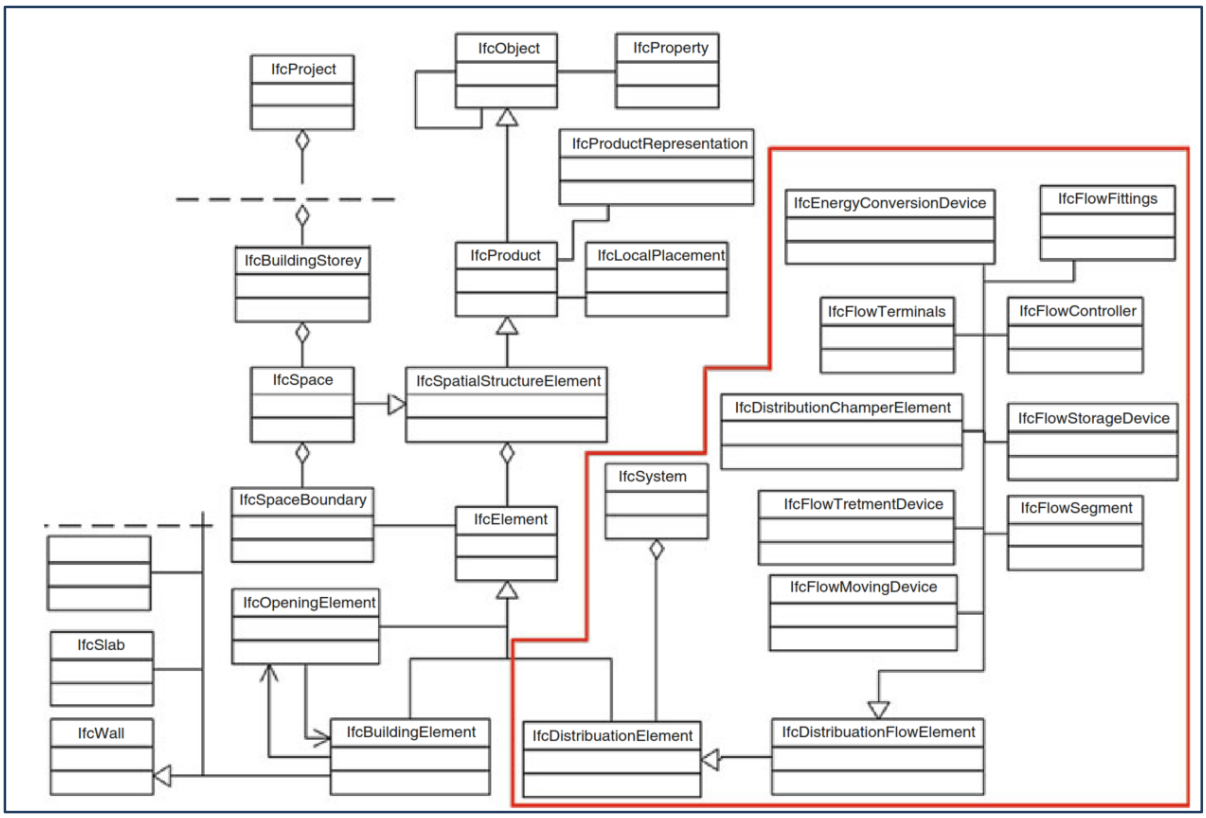

Figure 2-11: IFC schema representing the interior utility hierarchy chart (red area) (Hijazi et al., 2011)

A secondary benefit to the research by Hijazi *et al.* (2011) is that their model allowed integration of multiple utility networks within a city, and enabled one element to be used in more than one system e.g. a water heater (electricity network) connected to the hot and cold water systems (potable water network), providing a truer reflection of the "real world" environment. The resulting semantic mapping integrated IFC and CityGML schema without loss of data, and grouped the main concepts of utility networks at an abstract data level regardless of type, as shown in Figure 2-12. Figure 2-13 presents the graph structure generated in UtilityNetworkADE by transforming IFC entities and creating logical and physical port connectivity links, without physical connectivity geometry.

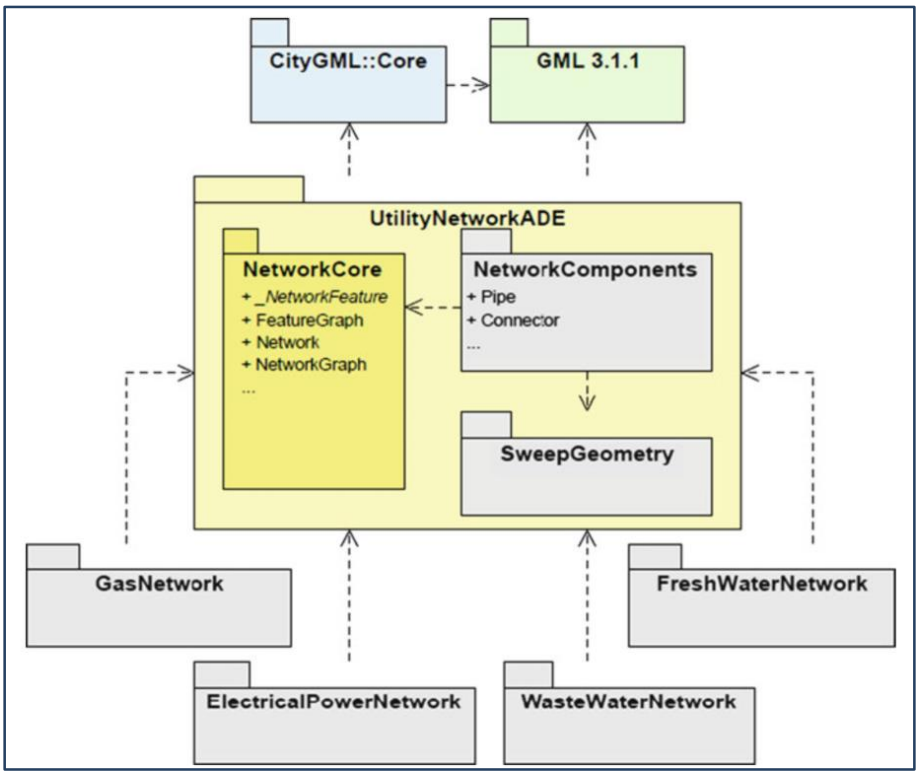

Figure 2-12: UtilityNetworkADE and its relation to CityGML (Hijazi et al., 2011)

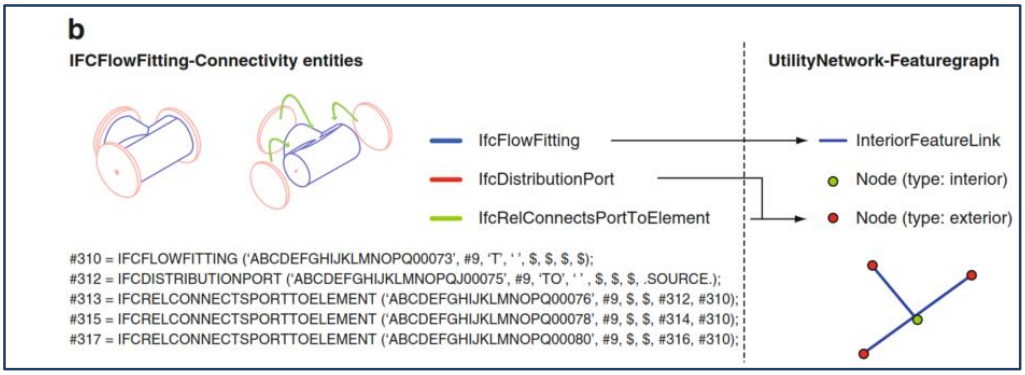

Figure 2-13: Comparison of three port models between IfcFlowFitting and the corresponding model using FeatureGraph in UtilityNetworkADE (Hijazi et al., 2011)

Expanding on the work by Hijazi *et al.* (2011), Liu and Issa (2012) presented a four-step process for producing a 3D visualisation of a building interconnected with its street-level utilities, through conversion and integration of BIM and GIS data as per the following:

1. Collect the BIM Revit model (in .adsk format) and GIS dataset for the utilities from the corresponding departments.
2. Clean up the GIS .shp files in ArcMap and ArcCatalog, confirm corresponding attribute fields.
3. Ensure .adsk and .shp files share the same coordinate system and then import into Civil3D.
4. Depending on the type of data, clean up utility information to ensure only one line is present to represent one pipe.

Once the C3D file had been created, manual review was recommended to query the model regarding location and elevation of each pipe and structure. Figure 2-14 demonstrates this review process and the resulting visualisation of connection between interior and exterior pipes.

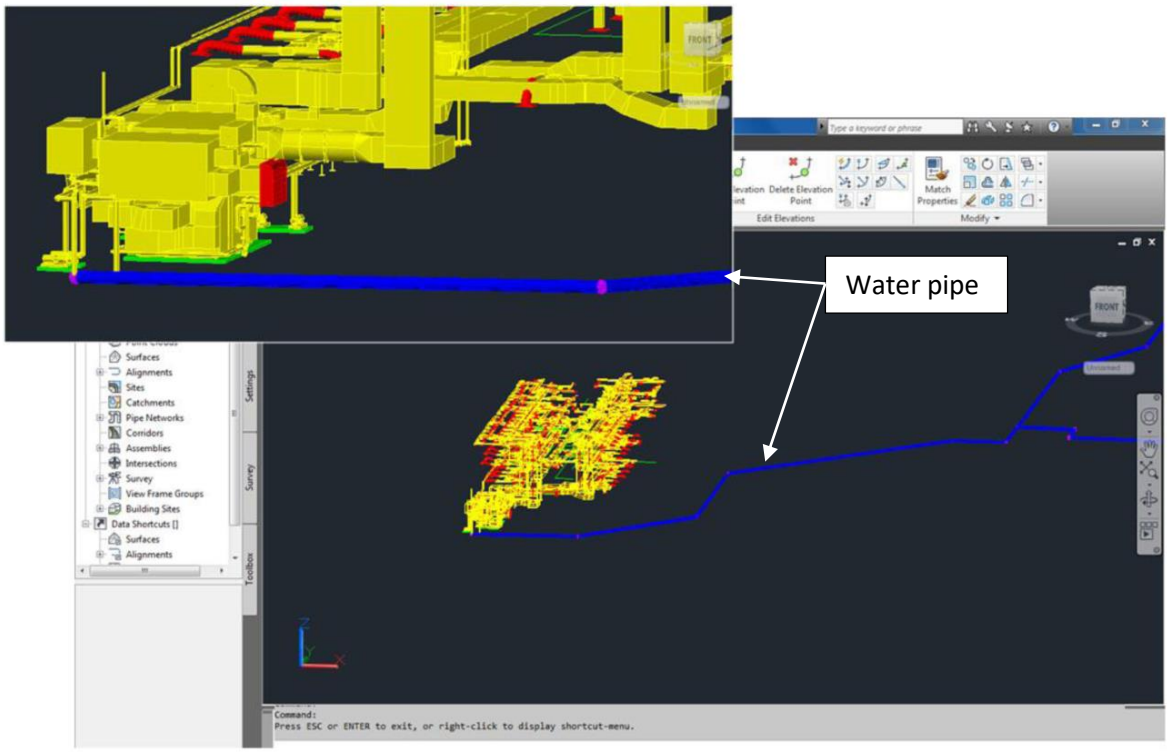

Figure 2-14: Visualisation of integrated building and utility connection in Civil3D (Liu and Issa, 2012)

Whilst Liu and Issa (2012) demonstrates the means to integrate horizontal and vertical infrastructure, the method was only applied to one utility type for one building. In order to implement this for an entire city, huge amounts of data are required, as well as a method for mass integration. Limitations of this process are that it is time-consuming and requires several commercially available software packages. In addition, interrogation to ensure accuracy is a manual process. However, if local government and asset managers are going to manage the data in an integrated tool (basis of the focus of this thesis; see Chapter 3 and Chapter 4) with respect to their own assets, and how designers submit their consent applications, the submitted data could be federated to make integration easier. Alternatively, the implementation of an Artificial Intelligence (AI) QA process would identify erroneous data for further investigation (discussed further in Section 5.2.1).

2.2.5.2. Asset Management and Facilities Management

The integration of GIS and BIM for asset management is in early stages of development, predominantly due to the inconsistent provision of as-built BIM data (Section 2.2.2). However, the applications and benefits from integrating these two technologies are significant. The non-graphic information contained in a BIM (e.g. manufacturer, serial number, model number) can be migrated into an asset management system. These non-graphic data are critical for maintenance management such as preventative maintenance works orders. Visualising assets in a 3D geospatial interdependent network (Bhamidipati et al., 2016), combined with geometric and non-graphic data, can assist in supply chain management for maintenance works orders (calculating costs based on lengths and component types for example) and improve on the operation life-cycle of components within the BIM data (Irizarry *et al.*, 2013; Zhang *et al.*, 2009). Similarly, Zhang *et al.* (2009) identified the capability of GIS and BIM in modelling for uses such as heating and cooling utility costs. Other abilities included querying interactions among building assets in risk analysis for example, the consequences associated with a break in a pipeline on other buildings and assets (Al-Kasisbeh and Abudayyeh, 2018; Bhamidipati *et al.*, 2016; Schultz, 2012).

Mignard and Nicolle (2014) built a semantics-based ADE (Section 2.2.4.2) as an extension to ACTIVe3D (Vanlande *et al.*, 2008), for integrating IFC and CityGML data, termed an Urban Information Model (UIM). Mignard and Nicolle (2014) also developed an evolutive ontology as part of the ADE whereby the use of specific operators, able to log changes in data, can track the evolution of the environment, and model the whole lifecycle of the ontology. The semantic and geometric data are stored separately through the ontology. The SIGA3D viewer combined with the ADE is able to operate bidirectional queries, in that geometric queries using the semantic data can produce 3D views, and vice versa (semantic queries using the 3D data can obtain the additional information from the 3D objects). Whilst Mignard and Nicolle (2014) concluded that the UIM is able to integrate CityGML and IFC data into a platform and present them visually in SIGA3D, what is not clear from the research is the interconnectedness between the elements. Using Figure 2-15 as an example, it is not clear if the representation of trees can be used to assess shadows cast on buildings.

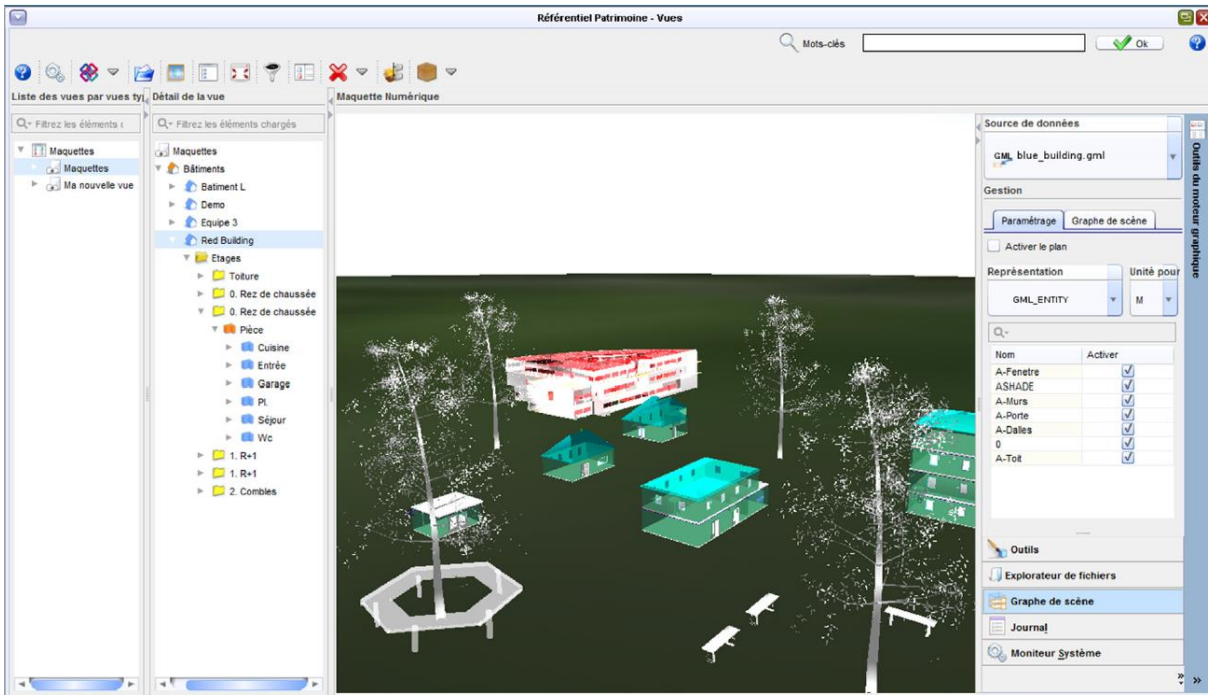

Figure 2-15: 3D visualisation of integrated CityGML and IFC data in SIGA3D (from Mignard and Nicolle, 2014)

Centofanti *et al.* (2011) presented a simplistic methodology of developing 3D building models in software such as AutoCAD and integrating them into a GIS environment. The results demonstrated basic interrogation functions of dimension data that can be calculated in the Esri ArcSuite of software (ArcScene and ArcGIS). Other basic semantic information was mapped to components in an attribute schedule. This functionality was expanded in further research by creating retrospective BIM models, generated through laser scanning and photogrammetric surveying (Dore and Murphy, 2012). However, the semantic data associated with these models had to be manually entered (except for geometry and geospatial coordinate reference data, which was obtained through laser scanning). Equally, for complex models containing architectural type features such as columns, these also had to be manually drawn and mapped to the scanned models. The developed BIM models were converted to CityGML in Google SketchUp through use of a plugin.

While Dore and Murphy (2012) and Centofanti *et al.* (2011) focussed on building exteriors with limited interior information, InteliBuild (2016) used laser scanning and point cloud technology to develop as-built models of building interiors. The scans were able to produce geometrically accurate 3D models and 2D plans, which could aid asset managers with renovation concept design, rent calculation based on floor area, and provide a basic model for facility management. Similar to Dore and Murphy (2012) and Centofanti *et al.* (2011), InteliBuild (2016) also contains geometry but lacks the detailed semantic information of a traditionally designed BIM model. However, where these technologies are able to add value, particularly in the development of digital twins (Section 2.2.5.4), is the ability to carry out laser and point cloud scanning during the various stages of construction. This would provide the ability to generate as-built BIM models for new builds, an issue identified as part of the integration of GIS and BIM (Section 2.2.3). Figure 2-16 presents some of the outputs from Dore and Murphy (2012)showing the degree of information contained in the system.

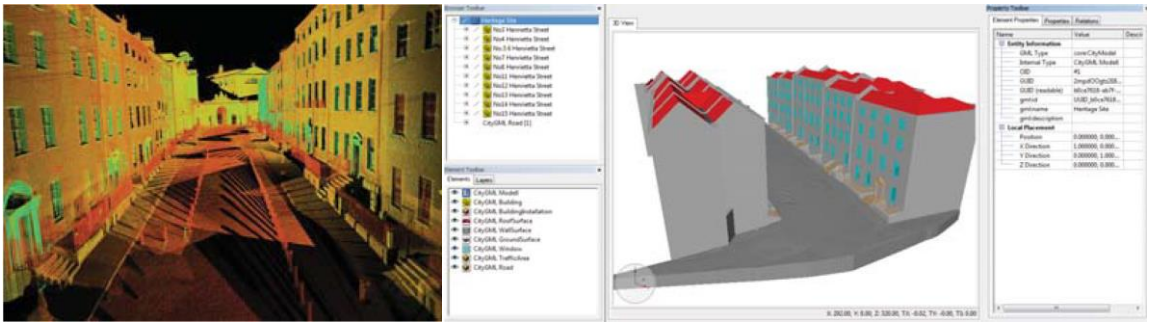

Figure 2-16: Laser scan and CityGML output of retrospective BIM model (from Dore and Murphy, 2012)

2.2.5.3. Hazard Response (Predictive and Reactive)

The semantic mapping system proposed by Hijazi *et al.* (2011) (Section 2.2.5.1) presents a means of identifying the various connections between buildings and utilities. In the context of risk analysis, Hijazi *et al.* (2011) noted that urban applications such as emergency response are looking for integration of interior and exterior utilities and the means of modelling areas of service loss. Similarly, Hijazi *et al.* (2011) used the example of large-scale facility maintenance operations undertaken due to planned (preventive) and "by failure" scenarios, each presenting scenarios of service outage for which facility managers would want to plan. The integration of interior and exterior utilities would provide the ability to analyse impacts on interconnected assets from loss of service, including loss caused by a natural hazard such as a seismic event, and such as is presented in this thesis as part of the case study and future works (Section 4.2.3 and Section 5.4.1., respectively).

With respect to hazard management and emergency response, Fosu *et al.* (2015) noted how future research could investigate the means to incorporate intelligent building systems and sensors into integrated GIS and BIM tools to simulate real-time response, and to conduct emergency drills after a disaster, integrating traffic conditions to calculate optimal paths. Equally, sensors could be used to alert the emergency services for those buildings that have been severely impacted by a disaster. These types of sensor technology for monitoring buildings represents progress in the development of digital twins/digital cities (discussed in Section 2.2.5.4) some of which are being implemented in New Zealand (CCC, n.d.; LINZ, 2017; New Zealand Government, 2018). Other current technologies such as GIS and GPS allow MCDEM operations centres to provide guidance to first responders in navigating to a target building following a natural hazard occurrence. However, with the introduction of detailed building information and layout including layout of water and electricity supplies, this can improve effective decision making during the planning of emergency response, such as identifying where fire hydrants are located, or electricity shut-off switches. Similarly, the development of IndoorGML as an application for indoor navigation and a data source for building interior topology provides an extension to first responder navigation (Fosu et al., 2015) by identifying safe routes into a building (Shayeganfar *et al.*, 2008; Tashakkori *et al.*, 2015).

Grasso and Maugeri (2003, 2009) presented an intelligent system for the assessment of vulnerability using building, infrastructure, seismic, and geological data in a GIS model of Catania, Italy, as a means of undertaking seismic risk analysis. Initially, Grasso and Maugeri (2003) demonstrated the means of creating a highly detailed GIS system integrating 15 databases, which comprised; 5,000 public and private buildings, the city's road network, geological data comprising 910 boreholes, and hazard models such as predicted ground motion and liquefaction susceptibility. Following this, Grasso and Maugeri (2009) used the GIS system to undertake seismic risk analysis of Catania. Grasso and Maugeri (2009) also acknowledged that seismic risk of a city is not simply an aggregate of the risk to each building, but that the whole urban system, such as road infrastructure, lifelines, and urban framework play an important role in the vulnerability of a city (reinforcing the sentiments and research by Bhamidipati *et al.* (2016) in Section 2.2.1). The highly detailed analytical procedure by Grasso and Maugeri (2009) incorporated a range of analyses for various aspects of a city including; bearing capacity analysis of foundations (using Eurocode EC8 and the nearest available geotechnical data from the 910 boreholes) and response and definition of flexural and torsional modal shapes of ancient buildings (using available building models as shown in Figure 2-17). Lifeline and urban system vulnerability assessment was also undertaken by Grasso and Maugeri (2009), with the lifeline vulnerability focussing on lateral ground movement response caused by slope instability, rather than liquefaction-induced settlement and lateral spreading. However, the discrete element method used to assess lifelines did allow for evaluation of stresses and deformation along the networks. In addition, the calculation of displacement, lateral deflection, and bending moment of the networks was not achievable with that method.

Both Bhamidipati *et al.* (2016) and Grasso and Maugeri (2009) concluded that an "intelligent Data Bank" of various land and building attribute data can be used as a means of large-scale vulnerability evaluation. Bhamidipati *et al.* (2016) and Grasso and Maugeri (2009) also proposed that local risk analysis of individual buildings could be connected into a more global analysis of a city by means of a GIS system. This thesis aims to demonstrate the citywide analysis proposed by Grasso and Maugeri (2003, 2009) through integration of GIS and BIM datasets into a 3D GIS-based semantic tool. The tool will include data that provides semantic information for private laterals (such as those included in IfcFlowFitting as discussed by Hijazi *et al.*, 2011, in Section 2.2.5.1) as an information source for assessing consequential damage within an interconnected network (building on the research by Bhamidipati *et al.*, 2016).

Whilst the proposed workflow in this thesis does not assess site-specific geotechnical data in the same way that Grasso and Maugeri (2003, 2009) did, the serviceability loss model (Bellagamba *et al.*, 2018b, in Section 3.2) used as the computational engine in this thesis, does utilise a geotechnical parameter (CRR), a liquefaction based parameter specific to soil profiles in Christchurch.

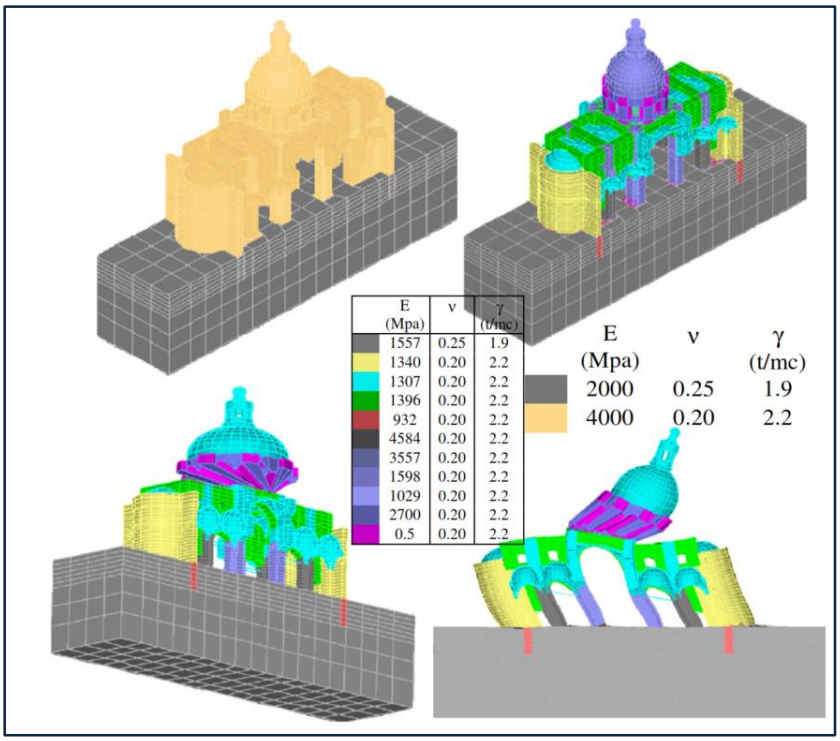

Figure 2-17: Dynamic numerical model of San Nicola alla Rena Church in Catania (Grasso and Maugeri, 2009)

Several studies have attempted to model seismically induced building damage on multiple buildings in a single simulation (Barbat *et al.*, 2010; Xiong *et al.*, 2015; Xu *et al.*, 2014). Xu *et al.* (2014) used a predominantly 3D GIS-based analysis (without BIM data) combined with nonlinear Time History Analysis (THA) and multi-storey concentrated-mass shear (MCS) modelling, to produce a simplified block building model which assessed performance using the HAZUS five states of damage (Figure 2-18a). Conversely, Barbat *et al.* (2010) and Xiong *et al.* (2015) used a combination of known building attribute data and high-fidelity building models generated in 3D-GIS (Figure 2-18b). Xiong *et al.* (2015) acknowledged that at the time of the study, there was a lack of 3D-GIS data due to confidentiality issues, and where data were available, the formats were either 3D polygonal or solid models, both lacking detailed geometry such as floor plan layout (something that would readily be available in an as-built BIM model).

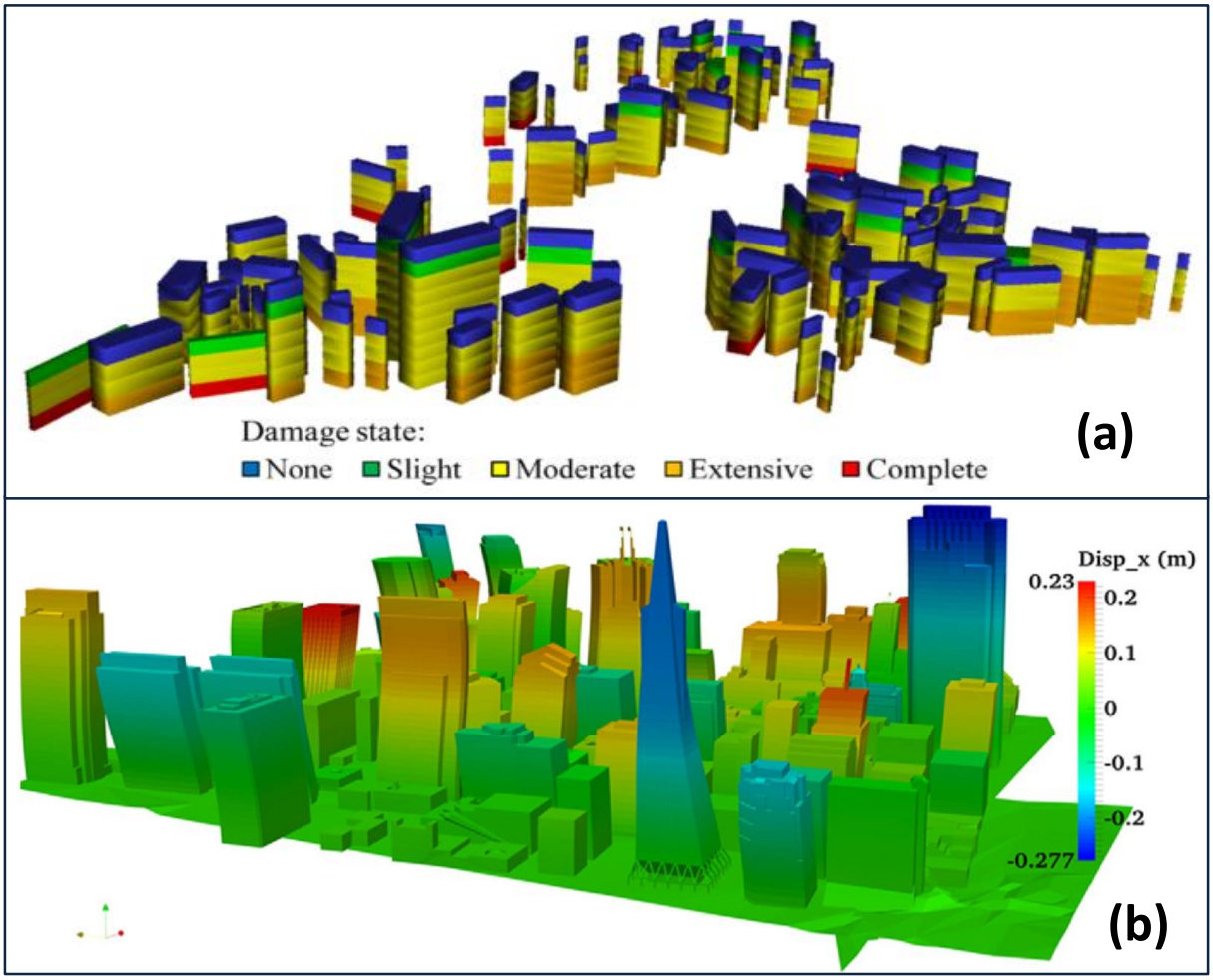

Figure 2-18: Seismic analysis of an urban area w*here (a) shows the HAZUS five damage state analysis (Xu et al., 2014) and (b) presents the high-fidelity 3D-GIS visualisation (Xiong et al., 2015)*

Along with Barbat *et al.* (2010) and Xiong *et al.* (2015), Franchin and Cavalieri (2013) considered social aspects in their respective seismic hazard analyses whereby a series of fragility functions were derived using factors such as number of injured people, population density, emergency response availability, and damage to lifelines. Both Franchin and Cavalieri (2013) and Barbat *et al.* (2010) utilised probabilistic and deterministic scenarios, implementing a Monte Carlo-based simulation. The simplified study area from Franchin and Cavalieri (2013) showing the integrated systems, along with graphical representations of results, are presented in Figure 2-19 (*a* and *b*).

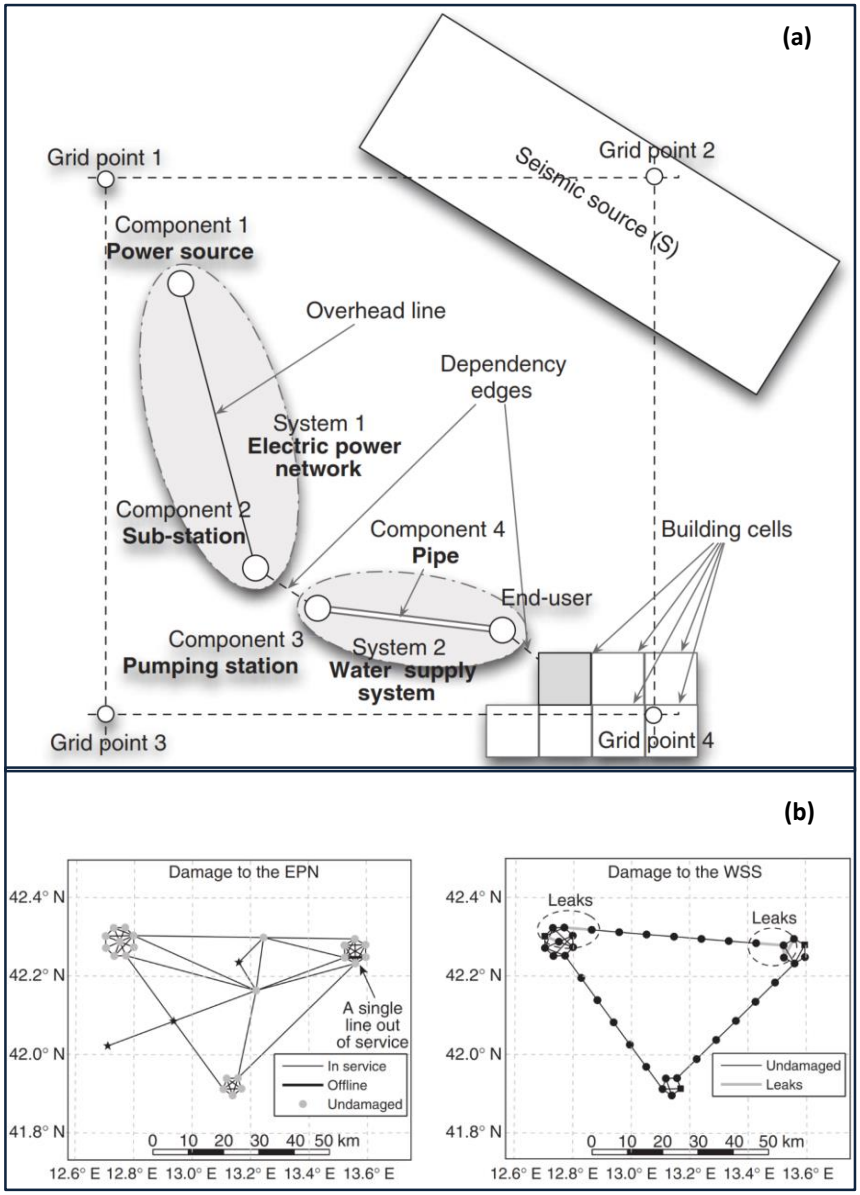

Figure 2-19: Vulnerability analysis of interconnected civil infrastructure where *(a) sectional representation of connected infrastructure and (b) results of analysis where EPN= "electric power network" and WSS= "water supply systems" (Franchin and Cavalieri, 2013)*

Outside of seismic analysis, Isikdag *et al.* (2008) and Chen *et al.* (2014) presented integrated models for fire-fighting simulations and response management operations. Modelling of surface and subsurface features such as buildings and geology in an integrated framework for planning, design and risk management was conducted by Tegtmeier *et al.* (2014). The UBM by El-Mekawy *et al.* (2012b) was used in a hospital-based evacuation simulation. Through conversion of IFC and CityGML data, and vice versa (Data level process as per Section2.2.4.1), a fully georeferenced model of the hospital (including internal room layout) was implemented in ArcGIS. Routes were calculated incorporating functions that identified doors and windows as exits (one scenario also incorporated the flat roof on the adjacent building in its route calculation), to identify all possible paths that allowed all persons within the hospital to be evacuated within two minutes. The method by El-Mekawy *et al.* (2012b) has direct applicability, and can be incorporated into the workflow proposed in this thesis by allowing emergency response organisations like CDEM to model city-wide evacuation models for various natural hazard events including earthquake, tsunami, and flood events.

Flood events have been modelled in a process-level integrated model (Table 6) by Amirebrahimi *et al.* (2015). Flood analysis was conducted for a case study site in an external computational engine and the results exported as an Esri .shp file. IFC geometry data was extracted and converted to CityGML for visual representation of the building. The semantic data were mapped, post-conversion, through unique identifiers and stored in a database (*Figure 2-20*).

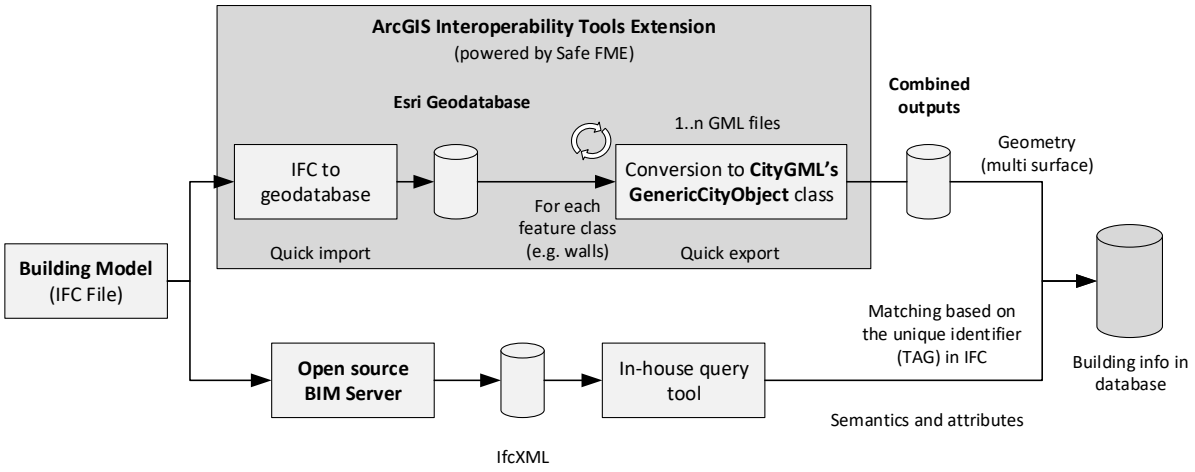

Figure 2-20: IFC to CityGML conversion from *Amirebrahimi et al. (2015)*

By combining the flood map .shp with the 3D building model, Amirebrahimi *et al.* (2015) conducted analysis to identify all walls, doors and floors that were damaged by flooding (*Figure 2-21*) and from this, estimated repair costs were calculated based on the quantities calculated from the model. Whilst the integration method followed several other examples presented in this thesis (Deng *et al.*, 2016; Hagedorn and Döllner, 2007; Lapierre and Cote, 2007), it is the aspect of estimating repair costs, which would be most applicable to the workflow in this thesis. The method could be used for other hazard analyses including seismic, and would be of use for private insurers in their estimation of exposure. Using the geospatial workflow in this thesis, if building attribute data were available for an entire city, then a forecast of citywide financial loss cost could be estimated for a modelled seismic event (such as an AF8 scenario). Similarly, cost estimation has direct applicability to asset and facilities management (Section 2.2.5.2). The scenario could be adapted to factor estimated lifespan of all building elements and so through query analysis, an asset manager could estimate annual maintenance costs of all assets.

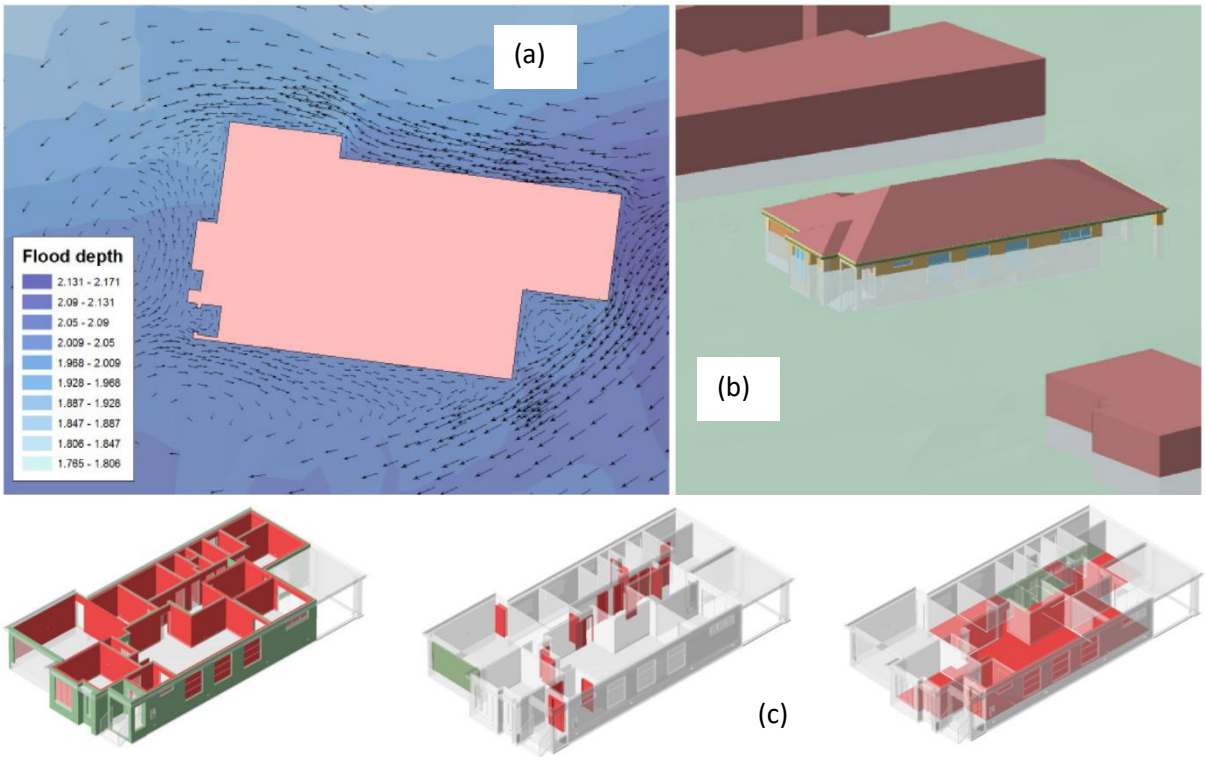

Figure 2-21: Outputs of flood analysis where (a) are the flood parameters around the house, (b) is the 3D visualisation of inundation level for house and (c) shows the damage caused by inundation to the walls, doors, and floors, respectively. Green indicates no damage to the component and red indicates full replacement is required *(from Amirebrahimi et al., 2015).*

2.2.5.4. Digital City Development

The terms "Digital City" and "Smart City" are used interchangeably, and neither is clearly defined in the literature as they can have multiple meanings depending on their context. For example, Cocchia (2014) conducted a literature review of the terminologies associated with the two and identified 11 alternative definitions of "Smart City", whereby these were grouped into three themes: technology dimension, human dimension, and institutional dimension (Nam and Pardo, 2011).

Ma and Ren (2017) provide the most comprehensive definition of "Smart City":

"Smart City is a vision to integrate multiple Information and Communication Technology (ICT) and Internet of Things (IoT) solutions in a secure fashion to manage a city's assets. In order to know what are included, what is happening in the city and how to improve the life quality of citizens, Smart City applications need mass data that are both static and dynamic, current and historical, geometrical and semantic, microscopic and macroscopic. Once collected, management and application of these data often use technologies such as Building Information Modelling (BIM) and Geographic Information Systems (GIS)."

A comparison of the above definition against an excerpt of the table from Cocchia (2014) is presented in Table 8.

Table 8: Published synonyms and definitions for Smart City (modified from Cocchia, 2014)

Concept	Definition	Reference
Virtual City	"Virtual City concentrates on *digital representations* and manifestations of cities"	Schuler (2002)
Information City	Digital environments collecting official and unofficial information from local communities and delivering it to the public via *web portals* are called information cities"	Anthopoulos and Fitsilis (2010)
Digital City	"The Digital City is as a comprehensive, *web-based representation*, or reproduction, of several aspects or functions of a specific real city open to non-experts. The Digital City has several dimensions: social, cultural, political, ideological, and also theoretical"	Couclelis (2004)
Knowledge City	"A Knowledge City is a city that aims at a knowledge-based development, by encouraging the continuous creation, sharing, evaluation, renewal, and update of knowledge. This can be achieved through the continuous interaction between its citizens themselves and at the same time between them and other cities' citizens. The citizens' knowledge-sharing culture as well as the city's appropriate design, *IT networks and infrastructures* support these interactions"	Ergazakis *et al.* (2004)

The definitions in Table 8 best describe the context for this thesis, with a focus on developing a process for collecting information from local communities and delivering via web portals a reproduction of several aspects of a city. From this, information contained within a Digital City can be used for continued creation, sharing, evaluation, renewal, and update of knowledge.

Previous models of cities under the "Digital City" umbrella include Virtual Helsinki, (Linturi *et al.*, 2000; Linturi and Simula, 2003) and Digital City Shanghai (Ding *et al.*, 2003), whose purpose were to focus on platforms for social interaction and online communication through live video. The Digital City Kyoto project (Ishida *et al.*, 1999) and e-Trikala (Anthopoulos and Tsoukalas, 2006) were conceived as research and knowledge sharing projects. Digital City Kyoto comprised 2D maps and 3D virtual spaces populated with webpages and real-time sensory data; e-Trikala was a multi-tiered architectural model providing support to citizens, offering digital public services and improvement to everyday life, whilst also acting as an e-government tool. Other cases are presented in Cocchia (2014) who provided a comprehensive list of geographies that have implemented Smart and Digital City strategies and projects based on 162 case studies as shown in Figure 2-22.

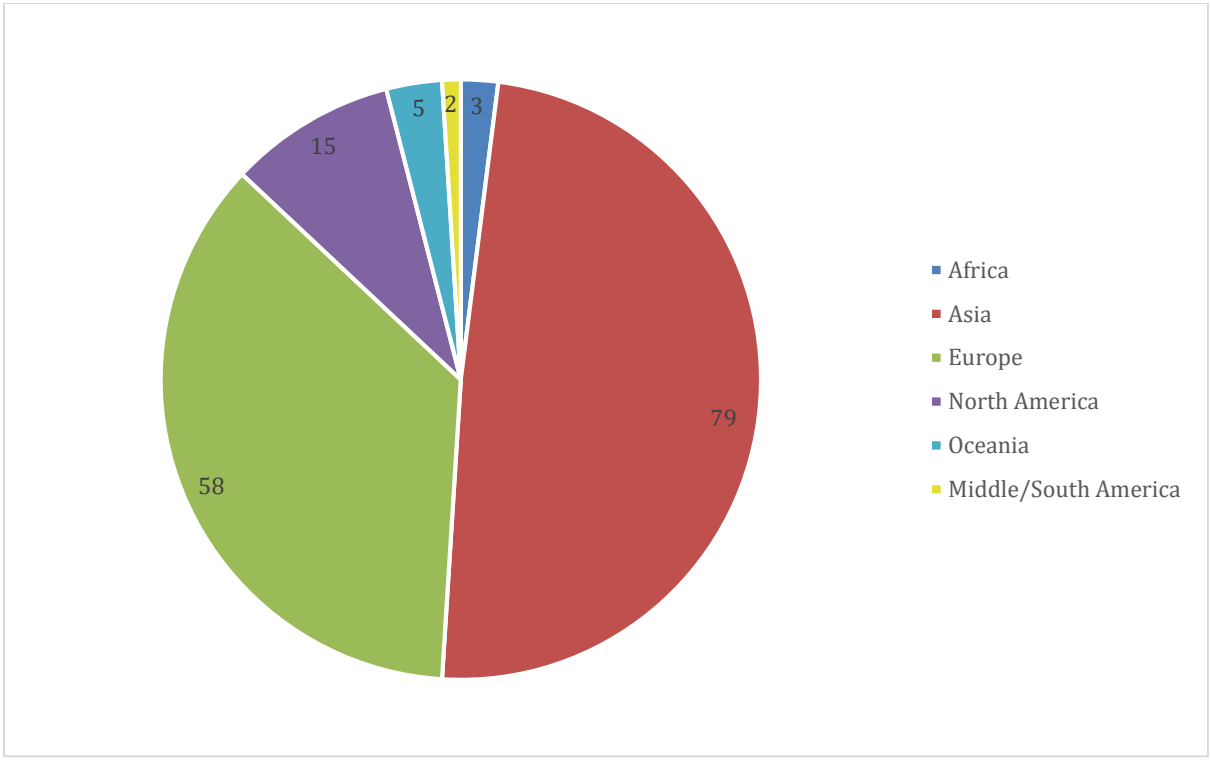

Figure 2-22: Geography analysis of Digital City implementation from Cocchia (2014)

The examples within Oceania from Figure 2-22 were all based on locations within Australia. Within New Zealand, more recent representations of digital cities included the Smart Cities Programme (LINZ, 2016, 2017) which developed and tested 13 projects across Auckland, Wellington, and Christchurch. The Smart Wellington program aims are, amongst other things, to develop a platform for the increased understanding of social systems, creation of better environments and to analyse means of recovering from a 7.8 M_w earthquake (New Zealand Government, 2018). In Christchurch, the Smart Cities Programme has a focus on sensor technology and obtaining real-time data, including an earthquake sensor network to provide valuable data for industry and academic research and to aid in improving seismic resilience and reducing risk (CCC, n.d.). An evaluation of the LINZ Smart Cities Programme can be found in Scally-Irvine and Louisson (2016).

Couclelis (2004) noted that major problems in Digital City development involve technical issues of data modelling and accuracy, arising from merging widely disparate data sources into a single integrated product, and privacy issues raised by comprehensive, high-resolution geographical databases. Maintenance was also an issue highlighted by Shiffer (1999) in keeping the platform current following its initial development, considering the task to be tedious, time-consuming, and costly, and underestimated at the outset. This thesis discusses methods for overcoming these issues in Chapter 5.

The common underlying outcome from the literature review is that the majority of digital cities developed to date are predominantly for the public domain comprising geographic search engines for marketing, retail, and commerce. Few examples were identified where the focus was on research, urban planning, or asset management, except for some of those currently in development within New Zealand. Ishida (1999) and Börner (2002) recognised the importance of digital cities for amongst other things, disaster protection and urban planning, but within this literature review, a study or proposal to develop a fully integrated Digital City for such a purpose has not been found. Equally, an observation by Nam and Pardo (2011) identified a noticeable discrepancy between theories and “visions” of, and the actual implementation and “how-to-do” of smart cities within the academic literature.

An important point raised by Chourabi *et al.* (2012) is the role of governance within Smart City initiatives and that a critical success factor in delivery of a Smart City was stakeholder relationships. Examples of e-government key projects studied by Scholl *et al.* (2009), found that ability to cooperate, support of leadership, structure of alliances, and working under different jurisdictions were the main issues impacting success. The implementation of smart governance infrastructure (Johnston and Hansen, 2011) is an important process in the development of a Smart City which includes citizen participation and private/public partnerships that should be accountable, responsive and transparent (Mooij, 2003).

With what is proposed in this study, the proposed model and workflow closely resembles the definition of Digital City by Wildfire (2018) who describes a Digital City as a combination of a "reactive" and a "predictive" model. Whilst the article by Wildfire (2018) presents definitions and terminologies for a "digital twin," a term usually used to describe individual processes, products, or service, a Digital City could be described as a collection of interdependent "digital twins." The underlying principle of the "Smart City: concept framework" by Wildfire (2018) (Figure 2-24) is that "the key drive in a city is to improve people's lives", and it is this philosophy that needs to be at the forefront of any Digital City development. The framework in Figure 2-24 illustrates service layers building from the data collection layer, the foundation of a well-organised platform of analytical tools, tailored to specific city issues that when combined with interoperability, unlocks additional insight.

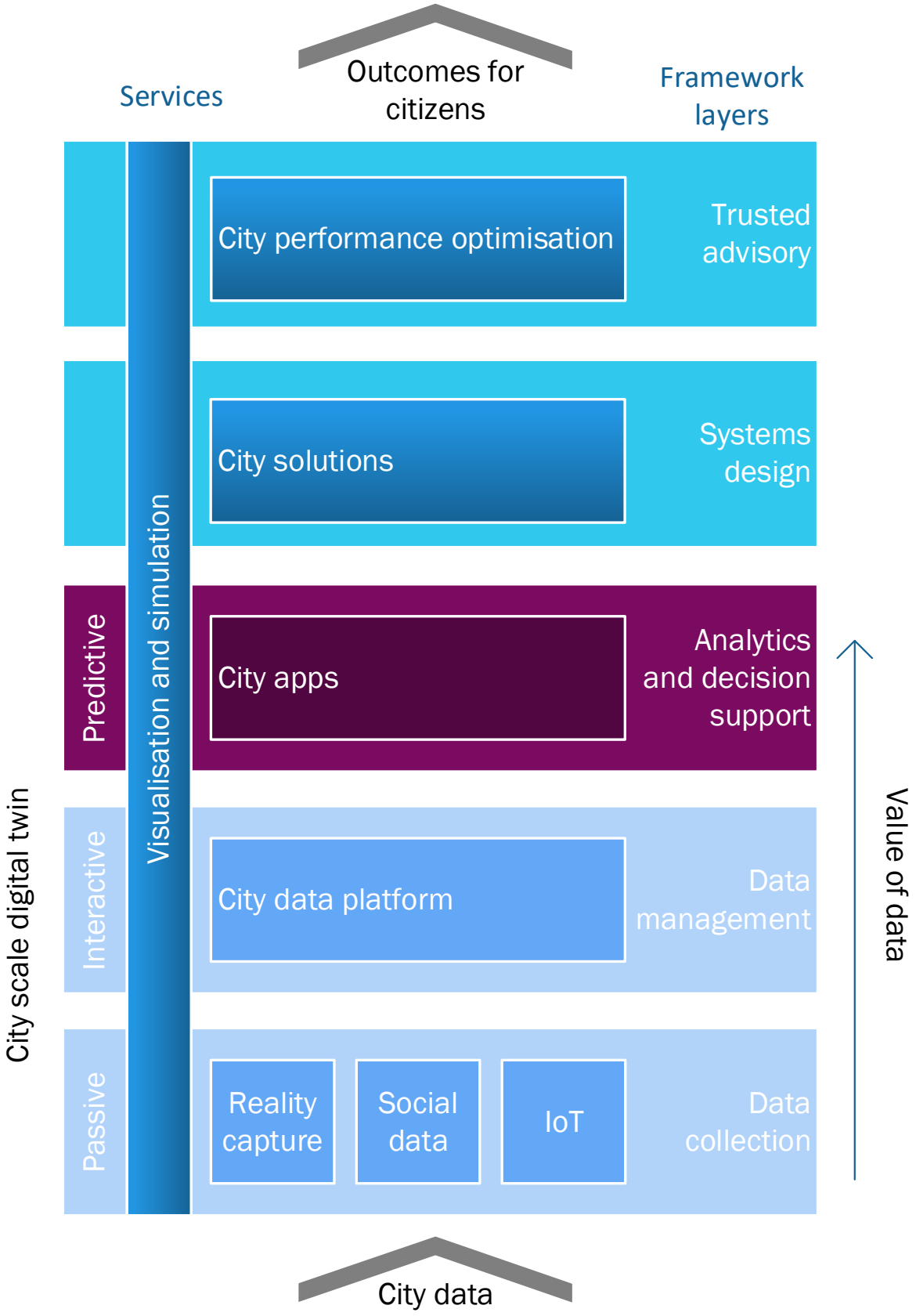

Figure 2-23: Digital City concept framework (from Wildfire, 2018)

The real power from a predictive model comes from, as the name suggests, predicting performance of the built and natural environment. This is best demonstrated from an integrated infrastructure perspective by the modelling by Bhamidipati *et al.* (2016) who developed interdependent relationship performance between several horizontal infrastructure assets (Section 2.2.1).

Predictive modelling can be further subcategorised into iterative/feedback loop and response models, and sandbox scenario testing. These method categories are designed as a method of resilience management, by using "real world" data in hypothetical scenarios, based on historic evidence. As has been discussed throughout this chapter, there are numerous examples of GIS use for this type of modelling and few for BIM, but it is the research by Grasso and Maugeri (2003); Xiong *et al.* (2015) and Xu *et al.* (2014) in their methods of assessing performance of multiple buildings for seismic hazards that are best placed for use in resilience assessment, and particularly applicable to this thesis. Whilst these methods generate 3D geometric shapes of buildings using just GIS data, the opportunity for improvement of this analysis by using BIM data is apparent. However, to demonstrate the true analytical properties of an integrated BIM and GIS system, the flood damage visualisation by Amirebrahimi *et al.* (2015) (Section 2.2.5.3), not only incorporates geospatial and building information data, but also factored financial data to determine the cost of repairs. A tool such as this would provide significant benefit for the likes of private insurers in the calculation of premiums. In addition, asset and facilities managers could also utilise financial data in an integrated system for capital works planning. All of these methods, with some modification, also have the ability to be used in Sandbox scenario testing where any of the information from any of the datasets can be modified to undertake sensitivity analysis on performance during hypothetical events. However, if the ETL type process were to be adopted to integrate the data and act as a "stream", strict editing rights would need to be enforced to ensure the source data isn't overwritten. The author of this thesis recommends that all analysis be undertaken in external computational engines, but that city authorities mandating federated data (assuming the governance issues raised by Chourabi *et al.*, 2012 are resolved) provide the tools to extract source data, as well as upload the results of any analysis.

The second type of model this thesis discusses is classified by Wildfire (2018) as a "reactive" model. This type of model provides feedback and visualisations that enhance real-time or near real-time interventions to improve the smooth day-to-day running of the city or asset. These concepts relate directly to an asset management FM/OM functionality, or potentially for use in a disaster scenario as an emergency response tool (Franchin and Cavalieri, 2013). This type of model could be accomplished by incorporating the methodologies proposed by Al-Kasisbeh and Abudayyeh (2018) and Schultz (2012) who were able to develop AM-type tools in GIS adopting both risk and resilience frameworks in their analysis. The benefit to a GIS/BIM integrated tool for a reactive model comes with the cost information in IFC semantics. If this information were incorporated into the model as Amirebrahimi *et al.* (2015) did with the flood analysis, then the functionality moves even closer towards a fully integrated FM/OM tool. The final piece to the puzzle with a fully integrated digital twin for FM/OM would come with the introduction of sensors and other smart technologies in the physical assets as described by Yalcinkaya and Singh (2014) (Section 2.2.2).

However, as Wildfire (2018) discussed, many of these concepts are currently more "blue sky thinking" as there are very few cities that are either developing city-scale models, or have the means to develop one due to their economy. A sense of realism should be applied and any planned developments should be scaled and designed with the city in mind. The biggest disconnect from truly realising a digital twin is the transfer of data during the project life-cycle, as highlighted throughout Chapter 2. Until the workflow of design to client handover of an as-built georeferenced BIM model is achieved, through collaboration with the entire infrastructure community, the goal of a Digital City delivering significant and tangible benefits to the people is still a far-off (virtual) reality.

2.2.6. Summary

This section presented common data formats in the digital engineering field, their applications (independently and collectively) in disaster risk and resilience management, and asset management/FM/OM, the means to integrate smart technologies, and the current knowledge gaps in the development of a fully federated Digital City. The methods addressed some of the fundamental principles of digital integration in their own fields, but no published article contained the one-stop-shop solution.

The remainder of this thesis takes the key findings of integration technologies, and working alongside NextSpace Ltd., aims to develop a hybrid integration solution. The technologies and methods from this Chapter that are used in the development of the geospatial workflow and implemented in the case study are:

- Semi-automatic translation ETL process for "streaming" and visualising data (Section 2.2.4.1).
- The use of WFS for "streaming" data and integrating IFC and CityGML data (Section 2.2.4.2)
- The use of an open web service for visualisation of the geospatial platform (Section 2.2.4.2).

One of the main objectives of Chapter 3 is to demonstrate a method that effectively negates data loss through the integration process, a limitation of many of the methods presented in Table 6. Secondly, this research proposes to implement a workflow for use in the assessment of urban risk and resilience, focussing on seismic hazards. The case study leverages off an existing computational engine (Section 3.2) and the geospatial workflow aims to expand on the points in Section 2.2.5.4 i.e. demonstrating an analysis workflow without having direct editing access to source data.

Finally, time and cost appear to be another significant area of concern with the development of a Digital City. Therefore, this research will discuss where time efficiencies can be made, particularly through collaboration with local and national government where nationally federated standards of digital data is an ongoing topic of discussion (Chapter 5).

2.3. Christchurch Case Study Area

2.3.1. Regional Tectonics

New Zealand lies along the boundary of the Australian and Pacific Plates. In the North Island, active tectonics are dominated by an oblique subduction along the Hikurangi trough, whilst in the South Island much of the relative displacement between these plates is taken up by the Alpine fault, an 850 km dextral-reverse transpressional fault within the axial tectonic belt known as the Southern Alps (Figure 2-24). The Alpine Fault is considered highly active with an average slip rate of 39 mm/year and the ability to produce Mw 7-8 earthquakes with a return period of 271 ± 73 years (Baratin *et al.*, 2018).

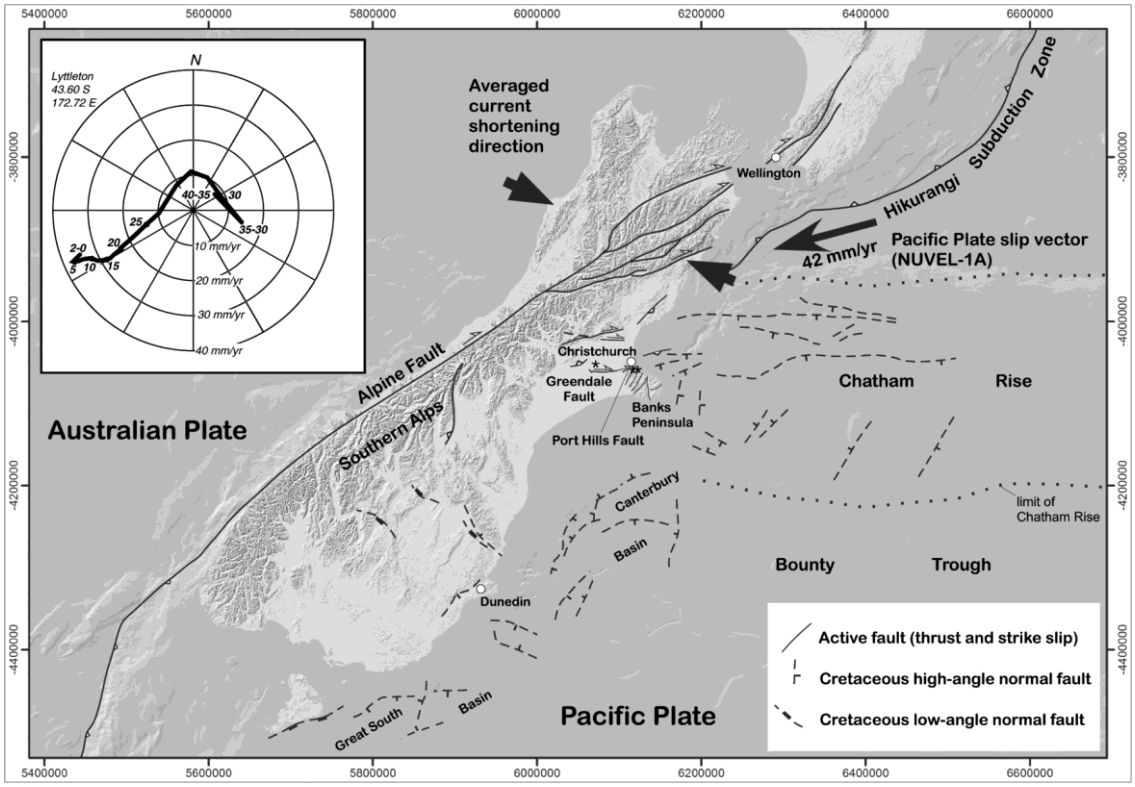

Figure 2-24: Tectonic setting of New Zealand (Ring and Hampton, 2012). Inset: motion of Pacific plate for a point at Lyttelton in an Australia plate fixed reference frame. The graph shows the azimuth changed from ~240° at 15 Ma to ~246° at 8 Ma and relative plate motion increased by ~10 mm a^{-1}.

Pre-CES GPS measurements indicated regional strain rates of ~2 mm/yr^{-1} shortening with a (σ_1) azimuth of 110-120° over an approximate 150 km wide region, known as the Canterbury Block. These rates are generally lower when compared to more tectonically active areas of the diffuse plate boundary zone, but higher than active "intraplate" settings in regions further from the plate boundary (Quigley *et al.*, 2016).

2.3.2. Geology of the Christchurch Area

Christchurch is located on the east coast of New Zealand's South Island within the Canterbury plains. The geology of the Christchurch area has been described by Brown and Weeber (1992) as a complex of alluvial sand, silt and gravel fan deposits, stemming from the eastward flowing Rakaia and Waimakariri rivers emerging from the foothills of the Southern Alps.

Whilst bedrock is often found at depths of between 300-800 m, the surface geology of Christchurch is predominantly Holocene alluvial gravel, sand, silt, and clay and peat deposits, split into two main regions; Central Christchurch and eastern Christchurch. Springston Formation deposits, a combination of overbank flood deposits of sand and silt, and river flood channels containing alluvial gravel, dominate the majority of Central Christchurch. The fine sediments form aquicludes and aquitards between the gravel aquifers. Due to the low-lying riverine and coastal environment, the water Table is generally less than three metres deep across the urban area.

In eastern Christchurch, where the water table is generally less than 1.0 m from the surface, the postglacial Christchurch Formation is prevalent comprising mainly sand (some deposits including shells), silt, clay and peat formed in estuarine, lagoonal, dune, and coastal swamp environments.

The Port Hills, located along the southeast edge of Christchurch form part of the Banks Peninsula, a now-extinct volcano of Tertiary basalt composition, overlain by windblown loess deposits. Figure 2-25 presents an excerpt from the geological map in Brown and Weeber (1992).

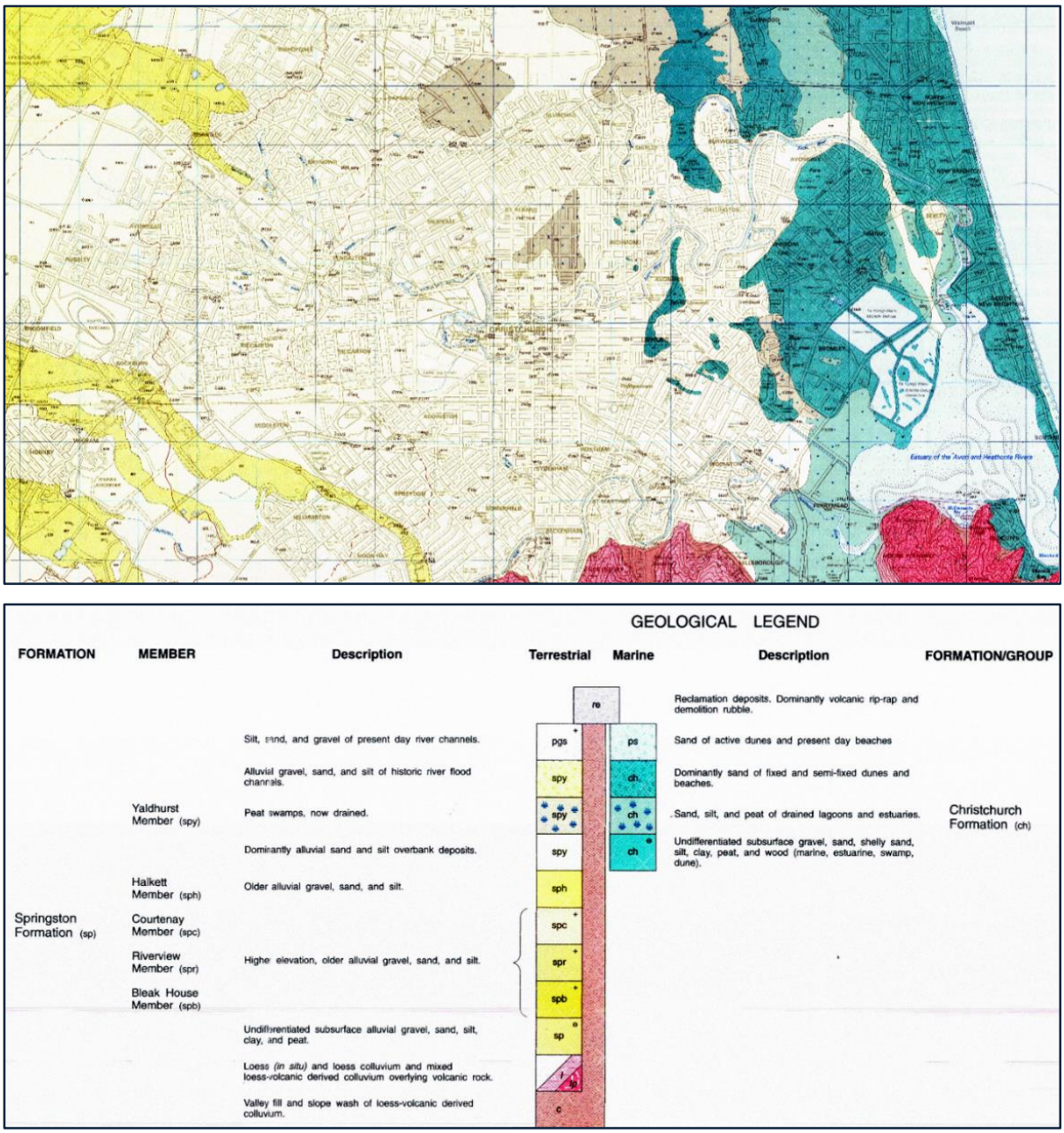

Figure 2-25: 1:25000 scale geological map extract (Brown and Weeber, 1992)

2.3.3. 2010-2011 Canterbury Earthquake Sequence

2.3.3.1. Overview – Seismology of the CES

During 2010 and 2011, Canterbury was subjected to six large earthquakes and thousands of aftershocks with moment magnitudes (M_w) as high as 6.2, which affected Christchurch, the second largest city in New Zealand, and surrounding communities. The causative faults of these earthquakes were either close to or within the city boundaries resulting in strong ground motions and causing widespread damage throughout the city. These earthquakes are termed the Canterbury Earthquake Sequence (GNS Science, 2011), hereinafter referred to as the CES.

The works by Bradley and Hughes (2012a, 2012b) and Bradley *et al.* (2014) characterise ground motion data (PGA and PGV) for the four main earthquake events (4th September 2010, 22nd February 2011, 13th June 2011, and 23rd December 2011), using recorded values at strong motion stations, as well as an empirical ground motion model to predict PGA values at locations away from those stations.

The initial shock, the largest in the sequence, struck at 04:36 on Saturday 4th September 2010. With its epicentre located near the town of Darfield, approximately 30 km west of Christchurch, a 7.1 M_w earthquake ruptured at a depth of approximately 10 km, along a previously unknown, east-west trending, strike-slip fault, now named the Greendale fault (hereafter referred to as the 4th September 2010 Darfield Earthquake). Local media reported the rolling motion lasting approximately 30-40 seconds and resulted in Central Christchurch experiencing moderate levels of ground shaking, liquefaction, and damage to lifelines. Widespread liquefaction and lateral spreading occurred in areas close to waterways within Christchurch and particularly the eastern suburbs, and the nearby towns of Kaiapoi and Taitapu (Cubrinovski and Green, 2010). Recorded ground motions close to the epicentre registered peak ground accelerations (PGAs) in the order of magnitude of 0.5-0.9 g. However, in these areas population density is generally low comprising predominantly rural farming infrastructure. Closer to the Christchurch Central Business District (CBD), ground motions were much lower with PGAs of 0.18 to 0.25 g, and a few cases with recordings of roughly 0.35 g (Bradley *et al.*, 2014).

On 22nd February 2011 at 12:51, a much more devastating 6.3 Mw earthquake struck along a blind oblique-thrust rupture of a generally north-east to south-west trending fault at the base of the Port Hills, 10 km south-east of Christchurch City (hereafter referred as the 22nd February 2011 Christchurch Earthquake). The increased devastation was due to the epicentre's location being much closer to the CBD and at a shallower depth (5-6 km). The severe shaking only lasted approximately 15 seconds but caused widespread damage to vertical and horizontal infrastructure and resulted in 185 fatalities. Compared to the 4th September 2010 Darfield Earthquake, the recorded PGAs were expectedly much higher for the 22nd February 2011 Christchurch Earthquake, which on average was approximately 0.5 g in both the horizontal and vertical direction within the Christchurch CBD (Giovinazzi *et al.*, 2011). However, closer to the epicentre, the highest PGA was recorded at the Heathcote Valley Primary School, measuring 1.7 g in the horizontal and 2.2 g in the vertical directions. These higher PGAs also led to the widespread occurrence of severe liquefaction and attendant manifestation of ejected sands and silts, and lateral spreading, relative to that experienced during the 4th September 2010 Darfield Earthquake. This liquefaction-induced permanent ground deformation caused much of the damage to structures and infrastructure lifelines across Christchurch. Figure 2-26 illustrates the PGA ground motions for the 4th September 2010 Darfield Earthquake and 22nd February 2011 Christchurch Earthquake where the data are shown with respect to the spatial distribution of PGA over the region. The largest PGV was recorded at the Greendale strong motion station (GDLC) and measured 115cm/s^{-1} during the 4th September 2010 Darfield Earthquake. Similar to the PGA maps produced in Figure 2-26, Bradley and Hughes (2012a, 2012b) and Bradley *et al.* (2014) produced similar illustrations for PGV, as shown in Figure 2-27.

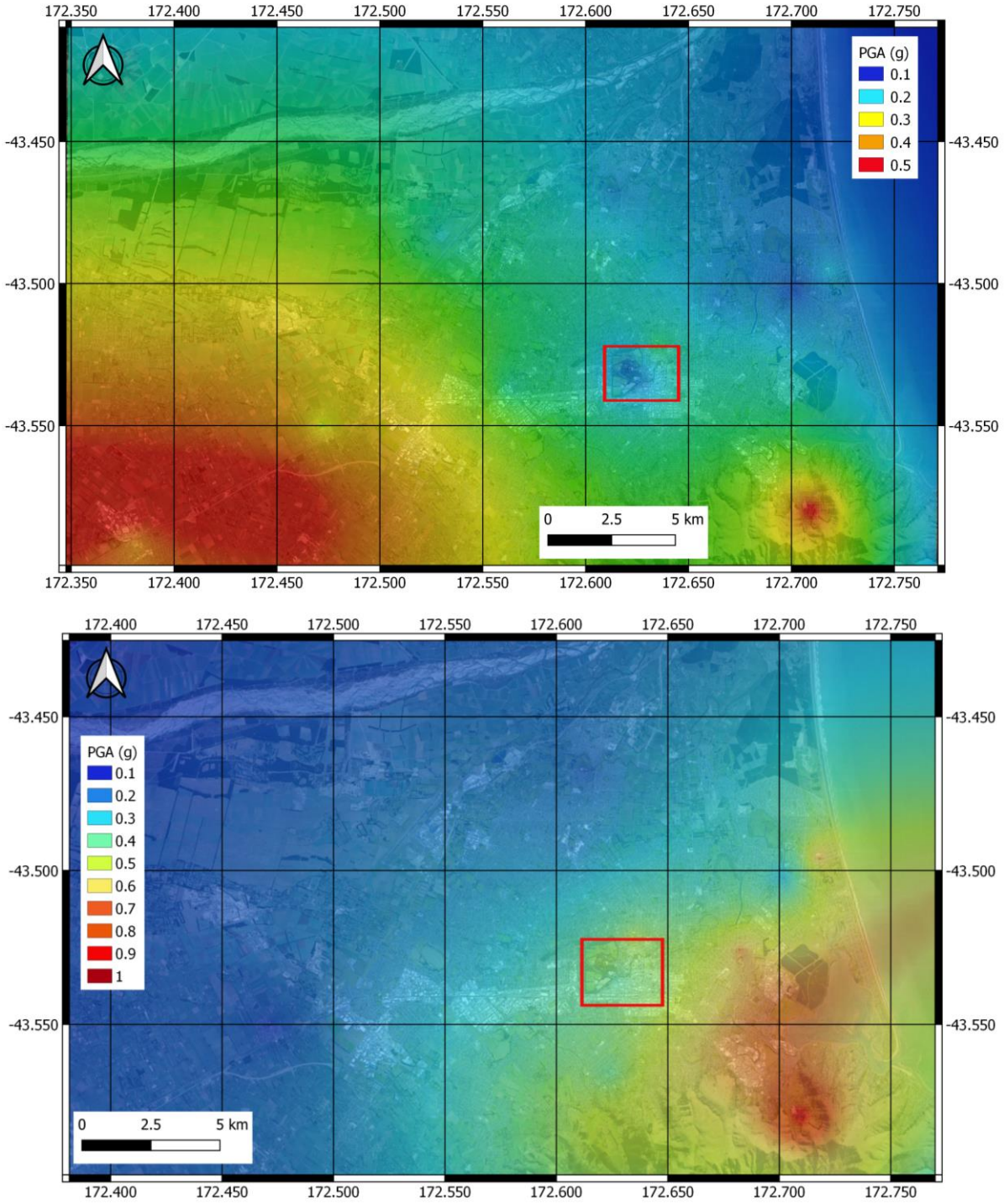

Figure 2-26: Interpolated PGA values from strong motion station measurements for the 4th September 2010 Darfield Earthquake (top) and 22nd February 2011 Christchurch Earthquake (bottom) (modified from Bradley and Hughes, 2012a; Bradley and Hughes, 2012b; Bradley et al., 2014). Red box outlines the Christchurch CBD.

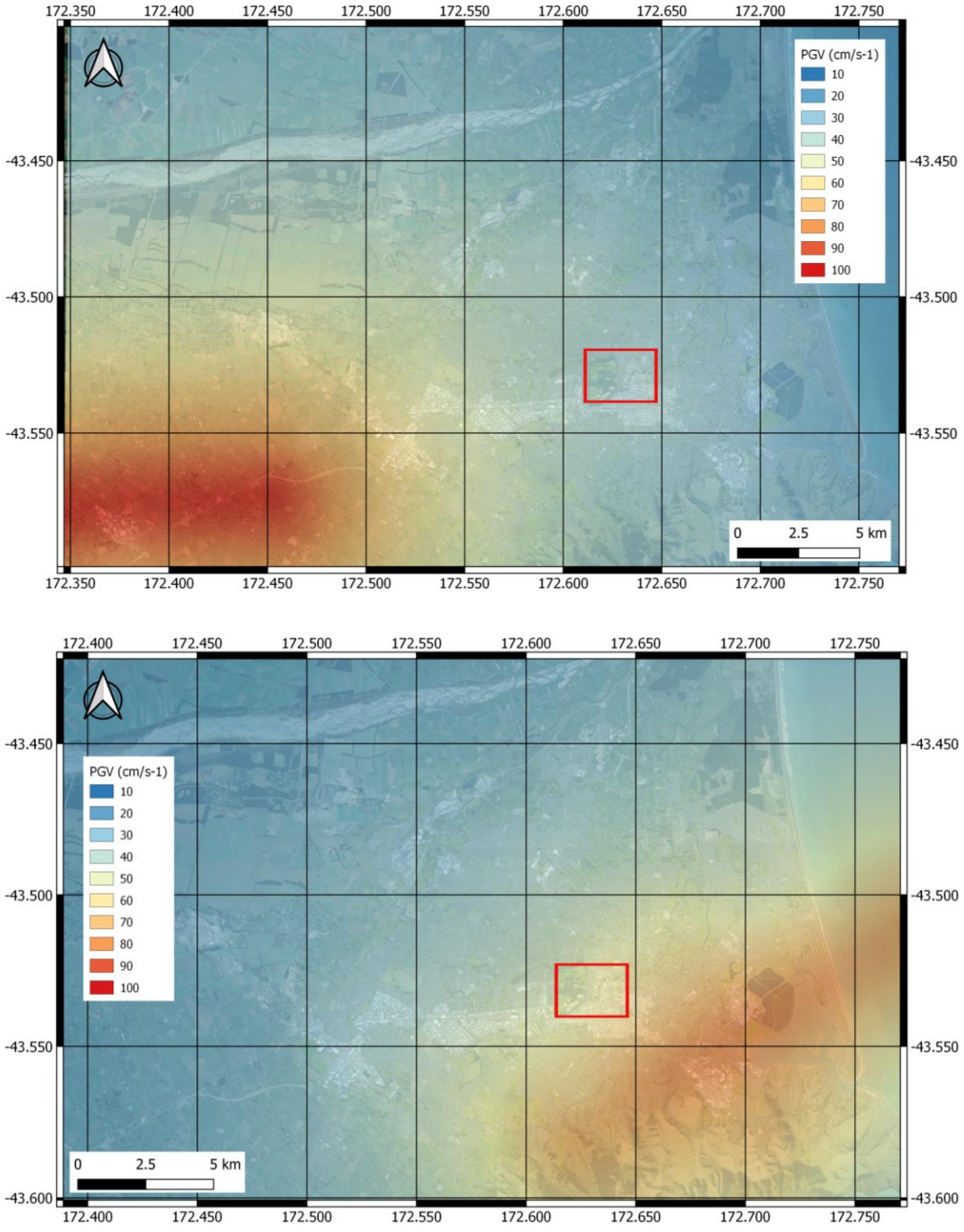

Figure 2-27: Interpolated PGV values for the 4th September 2010 Darfield Earthquake (top) and 22nd February 2011 Christchurch Earthquake (bottom) (modified from Bradley and Hughes, 2012a; Bradley and Hughes, 2012b; Bradley et al., 2014). Red box outlines the Christchurch CBD.

Following from the 22nd February 2011 Christchurch Earthquake, the subsequent major earthquakes occurred on 13 June 2011 with a magnitude 5.3 M_w rupturing at 13:00 and a second event at 14:20 with a magnitude of 6.0 M_w. The former event ruptured along a north-west to southeast trending fault within the Port Hills, the latter in a similar orientation to the 22nd February 2011 Christchurch Earthquake (Cubrinovski *et al.*, 2014). Due to the short time difference between the occurrences of these two earthquakes, they are generally reported and treated as a single event in the literature (and herein referred to as the 13th June 2011 Christchurch Earthquake). The 13th June 2011 Christchurch Earthquake caused further damage to previously damaged structures and additional ejected sand and silt caused by in some cases, as equally severe liquefaction as that experienced during the Christchurch earthquake. Maximum recorded PGAs for this event were in the order of 0.50 g in the Port Hills area, 0.35 g+ in the eastern suburbs of Christchurch, and approximately 0.20 g in the CBD (Eidinger and Tang, 2012).

The final major event towards the end of 2011 was also a double event similar to what occurred in the 13th June 2011 Christchurch Earthquake comprising a foreshock of magnitude 5.8 M_w occurring at 12:58 followed by the main shock of 5.9 M_w occurring 20 minutes later on 23 December 2011 (referred to as the 23rd December 2011 Christchurch Earthquake) (Bradley and Hughes, 2012b). For the foreshock, PGAs in the eastern suburbs were in the order of 0.35 to 0.98 g, whilst those in the CBD were much smaller measuring 0.15 to 0.20 g. The main shock recorded PGAs of similar magnitude to that of the foreshock being approximately 0.34 to 0.66 g and 0.15 to 0.25 g for the eastern suburbs and CBD, respectively (Eidinger and Tang, 2012). Whilst liquefaction was observed during this event to a much lesser extent than those previously, additional damage was caused by the collapse of previously damaged buildings in the CBD. Cubrinovski *et al.* (2014) presented a graphical representation of each of the major fault planes with regional surficial geology and seismicity also shown, in Figure 2-28.

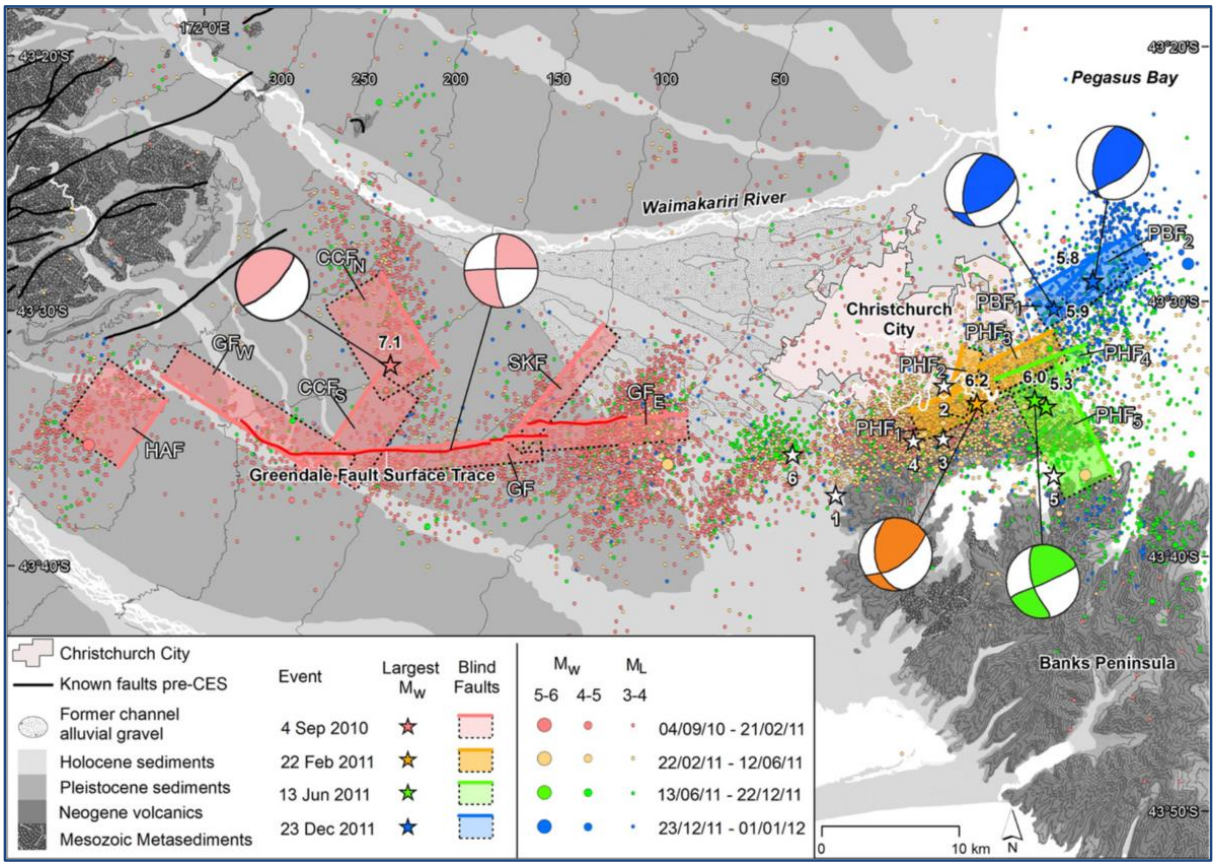

Figure 2-28: Causative fault planes of the CES (Cubrinovski et al., 2014) where star symbols represent the main earthquakes from the CES and dots represent aftershocks

2.3.3.2. Liquefaction and Ground Motion

Much of the damage to the city was caused by liquefaction that mainly occurred in saturated, unconsolidated alluvial and marine fine sediments in eastern Christchurch, in the region of late Holocene coastal progradation (Hughes *et al.*, 2015). Significant reconnaissance was undertaken by several parties and collated as part of a national database to document the location and severity of land damage across the major earthquake events (NZGD, 2016). The use of geospatial data including Interferometric Synthetic Aperture Radar (InSAR), Global Positioning System (GPS), and Light Detection and Ranging (LiDAR) have greatly improved the resolution of imagery that earthquakes and their environmental effects can be recorded (Quigley *et al.*, 2016). For example, LiDAR surveys carried out pre-CES in 2003 and post- earthquake surveys, approximately one month following each subsequent event throughout the CES, provided the means to quantify property subsidence for insurance assessments and reconstruction work.

From these data, Hughes *et al.* (2015), developed between-event maps showing total vertical elevation changes, elevation changes due to liquefaction, lateral ground movements due to liquefaction and vertical tectonic changes. The results showed that the 4th September 2010 Darfield Earthquake caused 74% of central and eastern Christchurch to subside, 60% of which did so by 0.2 m. Comparing this to the 22nd February 2011 Christchurch Earthquake where 83% of the same area subsided further, where 78% of this dropped an additional 0.3 m and localised areas exhibited settlement exceeding 1.0 m. The 22nd February 2011 Christchurch Earthquake was also categorised by almost 0.5 m of tectonic uplift of blind faults in the Avon-Heathcote Estuary.

These changes were the result of lateral spreading, topographic re-levelling, volume loss due to water, sand and silt ejecta to the ground surface and post-liquefaction volumetric densification (Cubrinovski *et al.*, 2015). This in turn has exacerbated longstanding flooding issues and vulnerability to tsunami and sea-level rise impacts (Hughes *et al.*, 2015). Figure 2-29(a and b) below collate some of the key findings from the field observations for the 4th September 2010 Darfield Earthquake and 22nd February 2011 Christchurch Earthquake as documented in NZGD (2016). As would be expected, the assessments carried out following the 4th September 2010 Darfield Earthquake, were incomplete prior to the occurrence of the 22nd February 2011 Christchurch Earthquake. By this point, a significantly larger workforce had mobilised to complete assessments across the city within a much shorter timeframe.

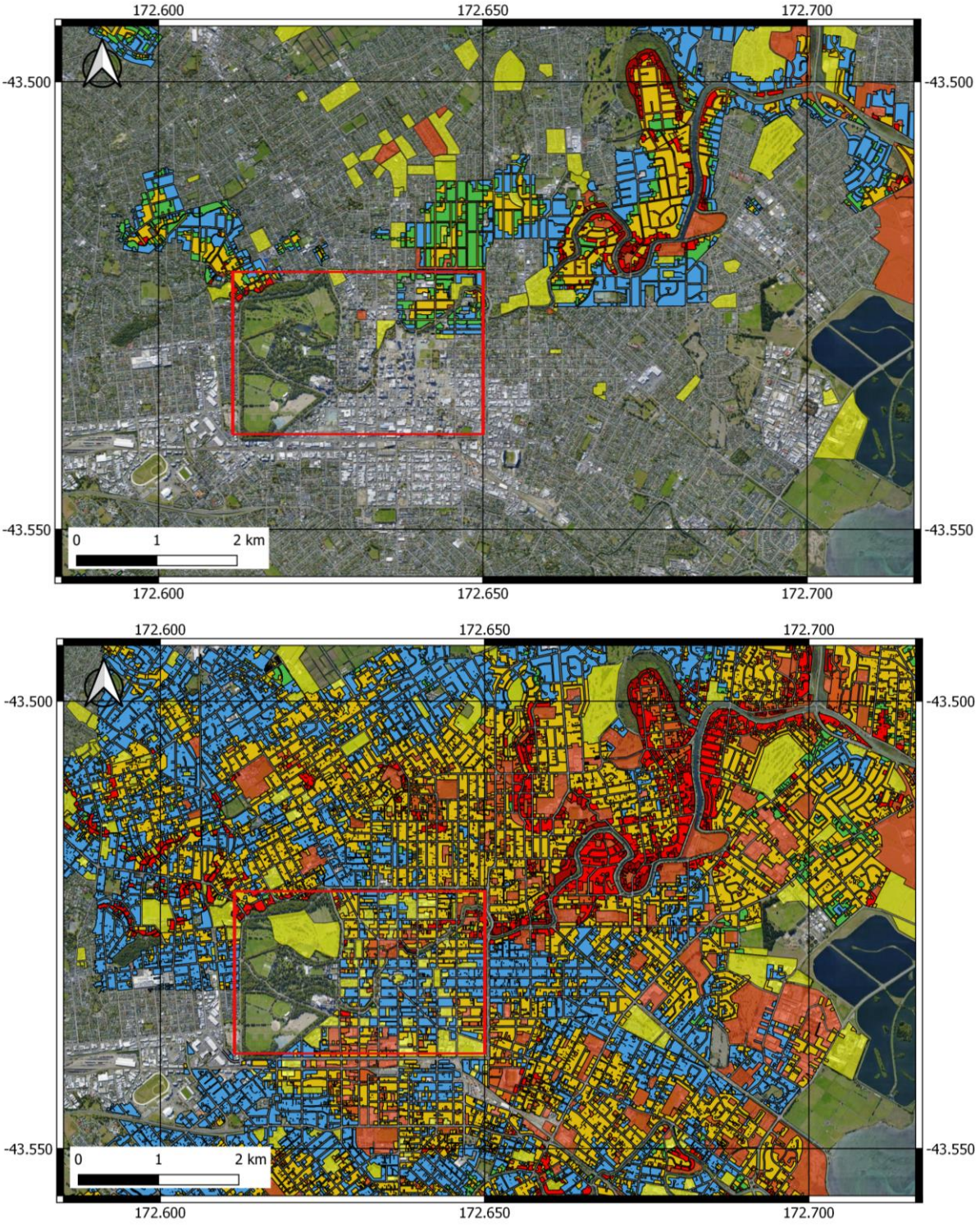

Figure 2-29: Exert of field observations and reconnaissance work where (top) represents data collected following the 4th September 2010 Darfield Earthquake, and (bottom) is from the 22nd February 2011 Christchurch Earthquake *(NZGD, 2016). Red box indicated Christchurch CBD.*

2.3.3.3. Impacts on Horizontal Infrastructure

Across the horizontal infrastructure networks, areas where liquefaction caused large ground deformations in the form of differential settlement and lateral spreading, resulted in vertical angular distortions and horizontal strains in the soil column, in which horizontal infrastructure networks are embedded (Bouziou and O'Rourke, 2017; Eidinger and Tang, 2012; O'Rourke *et al.*, 2014). These deformations often exceeded the design capacity of infrastructure components, resulting in faults which in turn induced major power outages and loss of functionality in the electricity network (Giovinazzi and Wilson, 2012; Giovinazzi *et al.*, 2011; Kwasinski *et al.*, 2014). Similarly, the water network capacities were insufficient to resist the movements and loads experienced, leading to widespread damage and failure/breaks. Information relating to event-specific damage in the potable water network is much more readily available than the wastewater, predominantly due to the shallow embedment depth of the former, leading to faults being clear between events (Cubrinovski *et al.*, 2014; O'Rourke *et al.*, 2014).

Most of the damage and impacts to lifelines from the CES was due to liquefaction-induced settlement and lateral spreading (Cubrinovski *et al.*, 2014; Giovinazzi *et al.*, 2011). Strong ground shaking played a modest role in the performance of lifeline-related buildings (e.g. substations, water treatment plants). Substantial damage occurred to potable water, wastewater and power distribution systems, moderate damage to telecommunications, railway, and the road/highway bridge networks, and light damage occurred to power transmission systems and gas distribution and liquid fuels (Eidinger and Tang, 2012). The damage caused to lifelines and infrastructure covered approximately one third of the city area. For further details on the taxonomy of the horizontal infrastructure, refer to Appendix A.1 and a more comprehensive review of horizontal infrastructure performance can be found in Appendix B.1.

2.3.3.3.1. 4th September 2010 Darfield Earthquake

The greatest impact on horizontal infrastructure was on the potable water and wastewater systems, where there was a loss of service, and discharge of wastewater. As would be expected for a reactive process to an earthquake event, and as documented in Cubrinovski *et al.* (2014), the availability and systematic recording of pipe damage and associated repairs were sparse.

However, the reconnaissance work by Cubrinovski and Green (2010) assessed some water network performance following the 4th September 2010 Darfield Earthquake, namely that the predominant damage mechanism to CCC's water and wastewater systems was ground movement and floating of manholes. Where breaks and joint separation occurred in the wastewater network, a significant influx of ejected sand was discovered, which hampered restoration of the service. CCC estimated that the volume of ejecta removed from pipes and pump stations was in the order of 9,000 m^3.

A secondary effect of broken pipes saw a 20% increase in flow rate into wastewater treatment plants due to an influx of groundwater into the pipe network. At the same time, Eidinger and Tang (2012) noted rapid depressurisation of major portions of the potable water network due to the large number of broken pipes in liquefaction zones (Figure 2-30) and power outages disrupting water supply from wells.

Figure 2-30: Broken water pipe barrel (Eidinger and Tang, 2012)

Figure 2-31 taken from Eidinger and Tang (2012) shows the extensive repairs undertaken in north-east Christchurch. Horseshoe Lake in Burwood was a suburb to have suffered some of the greatest liquefaction-induced pipe damage and CCC replaced many of the pipes in this area with high-density polyethylene (HDPE), prior to the 22nd February 2011 Christchurch Earthquake.

Newer facilities with flexible joints performed better than older rigid connections and all back-up power supplies at each of the pump stations worked as intended. Of note is the observation that asbestos cement (AC) pipes sustained significant damage when subjected to greater than 50 mm of settlement or 300 mm of lateral spreading. Typical repairs to the network included using external clamps or partial replacement with PVC pipe, cut into the damaged sections. By mid-October 2010, about 280 repairs to potable water and wastewater pipes had been carried out, at a cost of roughly NZ$12m.

Contrary to this, the electric power systems performed relatively well with performance attributed to improvements made in response to vulnerabilities highlighted in Christchurch Engineering Lifelines Group (1997). Other lifelines such a telecommunications and fuel also performed well. Due to the distance of the epicentre from Christchurch City, the 4th September 2010 Darfield Earthquake caused relatively minor damage overall to the network. Within the available literature, Watson (2010), Eidinger and Tang (2012), and Kwasinski *et al.* (2014) provide the best sources of information for recorded damage following the 4th September 2010 Darfield Earthquake. Eidinger and Tang (2012) estimated infrastructure damage in the range of NZ$1bn with Central Christchurch experiencing moderate levels of ground shaking, liquefaction and damage to lifelines.

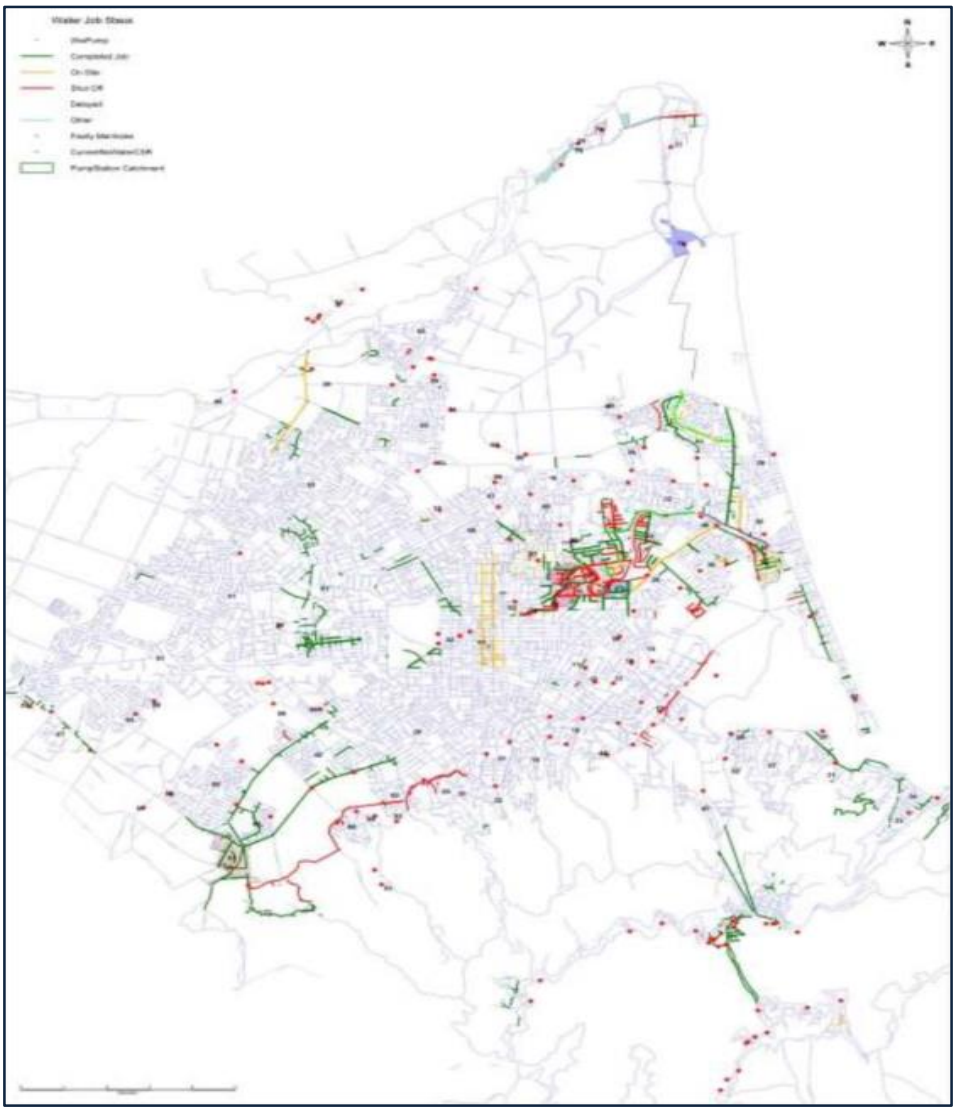

Figure 2-31: Map of water pipe repairs following the 4th September 2010 Darfield Earthquake (Eidinger and Tang, 2012)

2.3.3.3.2. 22nd February 2011 Christchurch Earthquake

Unlike the 4th September 2010 Darfield Earthquake, where the literature generally shows the electricity network to have performed better than the water network, following the 22nd February 2011 Christchurch Earthquake, both networks sustained significant damage. Eidinger and Tang (2012) estimated building and infrastructure damage was in the range of NZ$15bn- NZ$25bn, of which at least NZ$50m could be attributed to the electricity network (Giovinazzi *et al.*, 2011). Despite the total repair cost to the water network not being available, it is known that approximately NZ$125m was spent on CCTV assessments to determine extent of pipe damage (Cubrinovski *et al.*, 2014).

Following the 22nd February 2011 Christchurch Earthquake, the albeit short-term lessons learnt from the 4th September 2010 Darfield Earthquake were quickly applied in the recording and assessment of damage. Across the water network, 3,000 pipe repairs were completed by approximately 300 pipe repair crews taking six weeks to complete the works (Eidinger and Tang, 2012). CCC and SCIRT mobilised to digitally record faults and repairs to the water network, for the 36,000 potable water and wastewater service requests, lodged in the five months following the 22nd February 2011 Christchurch Earthquake (Giovinazzi et al., 2011).The full records of damage and repairs are presented in Bouziou and O'Rourke (2017) and Eidinger and Tang (2012), the former of which is presented in Figure 2-32.

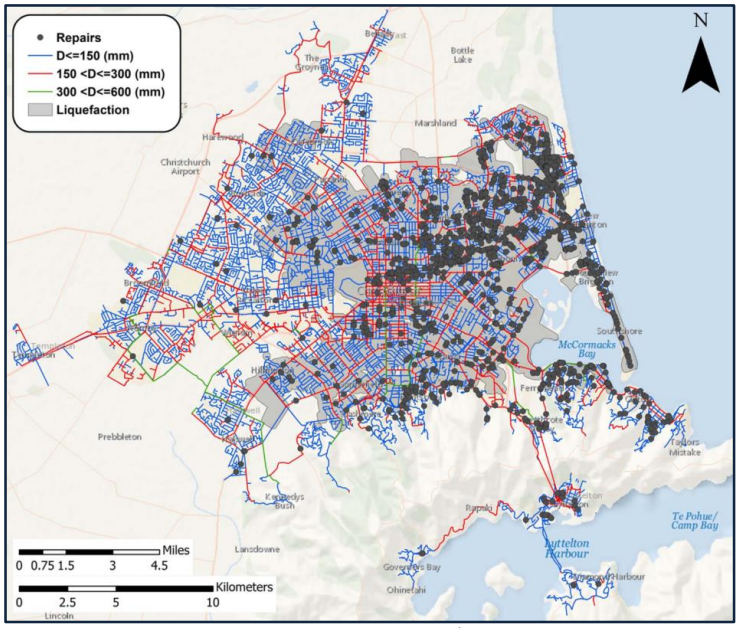

Figure 2-32: Water distribution system during the 22nd February 2011 Christchurch Earthquake (Bouziou and O'Rourke, 2017)

With respect to the potable water network, Cubrinovski *et al.* (2011) noted approximately 78 km of potable pipe length were damaged with 80% of these in areas of observed liquefaction. Eidinger and Tang (2012) indicated 20 out of 160 wells were reported as damaged including collapsed casing pipes, and damage caused by liquefaction-induced settlement and lateral spreading. However, Giovinazzi *et al.* (2011) reported that by August 2011, construction of 12 km of pressure mains, repair of 60 supply wells, and renewal of 150 km and 100 km of potable water mains and submains, respectively had been undertaken. Of interest is the observation by Eidinger and Tang (2012) where the HDPE potable water pipes installed in Horseshoe Lake following the 4th September 2010 Darfield Earthquake, suffered no leaks from the 22nd February 2011 Christchurch Earthquake.

Giovinazzi *et al.* (2011) reported that it took approximately one month for 95% of the city to regain its potable water supply, whilst Eidinger and Tang (2012) estimated the restoration of the wastewater network in eastern Christchurch alone took up to one year. Throughout the literature, poor performance of the network was attributed to damage from cracking and joint and laterals failures. This included wastewater pipes stretching at bridge crossings caused by lateral spreading, breaks at connection pipelines due to the combination of concrete vault buoyancy and liquefaction-induced settlement, and loss of critical services like pump stations and wastewater treatment plants. Similarly, like the entry of sand and silt into the network following the 4th September 2010 Darfield Earthquake, inspection, and repair of the pipes following the 22nd February 2011 Christchurch Earthquake was hampered by further blockages.

2.3.3.4. Impacts on Vertical Infrastructure

Christchurch City, prior to the CES, comprised some 185,000 buildings, 155,000 of which were residential dwellings generally of lightweight construction. In the commercial/industrial sectors of the city, approximately 4800 brick and masonry buildings, at least 600 of which were recorded as unreinforced masonry (URM) structures. During the CES, some of these URMs suffered complete or partial collapse and the majority suffered moderate to extensive damage (Cubrinovski and Green, 2010; Kam *et al.*, 2011). Generally, reinforced concrete (RC) and steel structures performed better than masonry and brick buildings, with only a small number of them considered unsafe for occupancy. Liquefaction and lateral spreading as well as shaking caused damage to approximately 20,000 residential structures, none of which collapsed or are known to have caused fatalities (Cubrinovski *et al.*, 2011; Orense *et al.*, 2011). However, around 7,000 of these were abandoned due to serious damage, predominantly in the eastern suburbs of Christchurch, labelled the "Residential Red Zone." Further information on the taxonomy of the vertical infrastructure is summarised in Appendix A.2 and a more detailed review of vertical infrastructure performance is presented in Appendix B.2.

2.3.3.4.1. 4th September 2010 Darfield Earthquake

As discussed in Section 2.3.3.3.1, the distance of the epicentre from Christchurch City played a significant factor in the extent of damage. Whilst it is well documented that suburbs in the eastern extents of Christchurch, areas close to waterways, and towns north of Christchurch such as Kaiapoi were adversely affected, predominantly due to the poor ground conditions (Buchanan and Newcombe, 2010), the majority of Christchurch sustained relatively minor damage overall (Cubrinovski and Green, 2010; Cubrinovski and Orense, 2010). Bruneau *et al.* (2010) noted that had it not been for the failures of unreinforced masonry buildings and damage resulting from liquefaction, the response and recovery requirements would have been minor. One reserve bank report estimated the cost of repairs and rebuilding at around NZ$5bn (Parker and Steenkamp, 2012), which is approximately five times less than the damage that would be caused by later earthquake events.

Generally, damage in the CBD was limited to older brick and masonry buildings where brick facades collapsed, cascading bricks onto the streets. Several of the historic buildings, including churches built of stone were severely damaged, as were many of the old homesteads centred much closer to the epicentre. Generally, retrofitted URM buildings performed well with damage limited to parapet and chimney collapse. However, the predominant failure types of non-retrofitted URM buildings were parapet, chimney, and out-of-plane façade wall failure, and in-plane damage (Dizhur *et al.*, 2010).

Buchanan and Newcombe (2010) noted that for the most part, residential dwellings performed very well. The key damage themes were lateral spreading and liquefaction-induced settlements, the collapse of brick chimneys (noted as generally the worst-case examples of shaking induced structural damage), and like the older brick and masonry buildings in the CBD, the older double brick construction and heavy brick veneer residential dwellings also sustained extensive damage.

2.3.3.4.2. 22nd February 2011 Christchurch Earthquake

With respect to the extent of damage sustained to the buildings within the CBD, there are several published articles with differing views. Kam *et al.* (2011) presented statistics of CBD building damage following the 22nd February 2011 Christchurch Earthquake, similar to that undertaken for the 4th September 2010 Darfield Earthquake described above and notes a split of 58% and 42% for commercial and residential buildings, respectively, within the CBD. However, the categories of safety placards do not distinguish between residential and commercial buildings and upon review of the graphical representations from the paper, the revised statistics show that of the 2,721 buildings assessed, 52% were deemed green, 24% yellow (restricted use), and 24% Red (unsafe), as per the BSE categorisation. Whilst the percentages reported almost match, the number of buildings vastly differs in Stevenson *et al.* (2011) who presents a total of 3,621.

Kam *et al.* (2011) also goes on to discuss a further breakdown into the categories of buildings within the CBD and their extents of damage, the results of which are presented in Figure 2-33. The graphs show that of those buildings that were deemed unsafe, approximately half were unreinforced masonry, and equally, a similar percentage of those that were identified as having performed well were of timber-framed construction.

Despite the statistics from Uma *et al.* (2013) being from December 2011, they do present a geospatial distribution of the building classifications, and are presented in Figure 2-34.

Residential dwellings were as equally affected as commercial buildings with approximately 15,000 structures subjected to settlement and lateral spreading caused by liquefaction. (Cubrinovski *et al.*, 2011). Following the assessments of residential buildings after the 4th September 2010 Darfield Earthquake, Buchanan *et al.* (2011) assessed the performance after the 22nd February 2011 Christchurch Earthquake. Their work identified that whilst the common residential construction types performed extremely well for life safety, thousands had sustained structural and non-structural damage. Other generalised damage patterns identified were: plasterboard performed better than lath and plaster; NZS3604 slab-on-grade foundations had insufficient stiffness to bridge severe land deformation; and irrespective of type, reinforced foundations performed considerably better than those that were not reinforced.

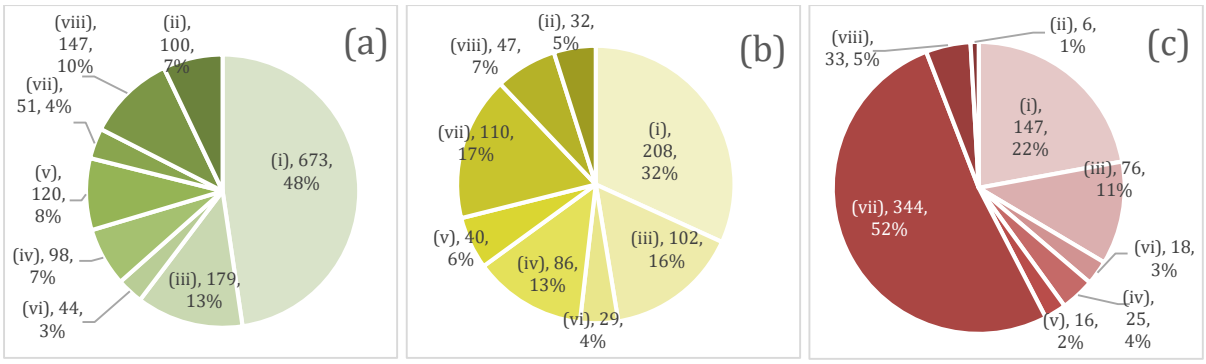

Figure 2-33: Comparison of CBD building construction type and the extent of damage following the February 2011 Christchurch Earthquake *categorised as (a) green – safe for occupancy, (b) yellow – restricted use, and (c) red - unsafe. Roman numerals represent the following: (i) – timber framed, (ii) – steel framed, (iii) – concrete framed, (iv) – infilled concrete frame, (v) – tilt-up concrete, (vi) – concrete walls, (vii) – unreinforced masonry, (viii) – reinforced masonry.*

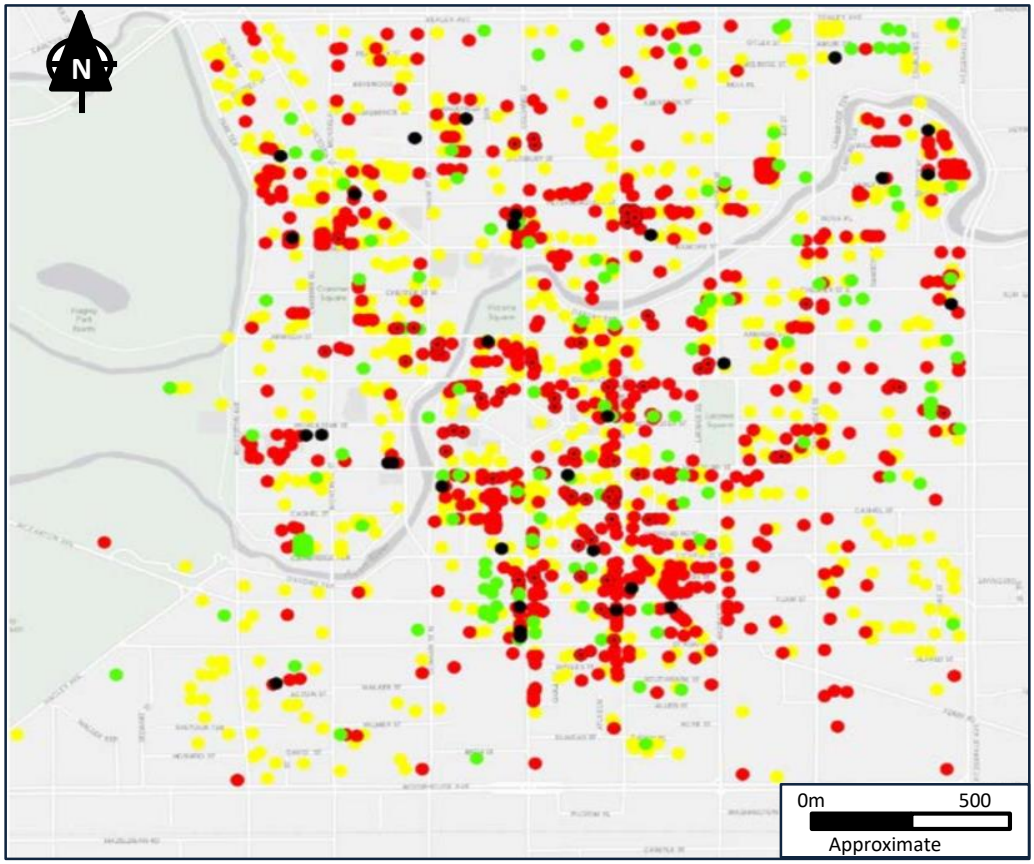

Figure 2-34: Distribution of CBD building damage following the 22nd February Christchurch Earthquake (Uma *et al.*, 2013). *Note: black dots indicate sites that were not recorded, and red dots with a black point indicate those buildings that were at risk due to either ground failure or adjacent buildings.*

2.3.4. Summary

This section presented an overview of land and infrastructure performance during the Canterbury Earthquake Sequence (CES). The available literature shows that generally, assessment and reporting of damage was more prevalent following the 22nd February 2011 Christchurch Earthquake and that on balance, damage was significantly greater than the 4th September 2010 Darfield earthquake due to the location of the epicentre. The manifestation of liquefaction and lateral spreading was severe towards the east of the city due to the presence of sand and silt formed in estuarine, lagoonal, and coastal swamp environments that are particularly susceptible to liquefaction, paired with the shallow ground water table.

For these reasons the case study site, the Taiora QEII recreation and sports centre has been chosen (Chapter 4). The site is known to have experienced severe liquefaction following the 22nd February 2011 Christchurch Earthquake, the previous sports centre building was severely damaged to the point it required demolishing, and there was a loss of service to the potable water network. Also, due to the availability of damage information relating to the potable water network and its taxonomy, the case study utilises a serviceability loss model (Section 3.2) developed by Bellagamba *et al.* (2018a) to demonstrate the implementation of the geospatial workflow.

Chapter 3
—The Proposed Geospatial Workflow

Contents

3.1. Introduction

Through the ongoing development of digital technologies and Smart Cities, Christchurch City Council (CCC) has identified the prospect to better collate both their own asset data, and building information, supplied by designers as part of the consenting process. To that end, this thesis, in collaboration with NextSpace Ltd. and CCC, presents a proof of concept to combine detailed designer-supplied BIM data with CCC assets (initially the 3 Waters network stored in GIS-based databases), into a geospatially referenced platform, currently codenamed *Bruce*.

In addition to the integrated platform, this current research integrates datasets and identifies how a detailed digital twin of Christchurch could be utilised in citywide analysis with a focus on risk management and urban resilience (discussed in Chapter 5). As highlighted in Chapter 2, unlike most other natural hazards that have occurred in recent times, the CES allowed Christchurch to become a city-wide research laboratory with vast quantities of data being collected and catalogued for each main earthquake event. Whilst not exhaustive, the real-time observations of earthquake-induced land and infrastructure damage have been utilised in many publications and research, including a PhD thesis by Liu (2016), which developed a decision support framework for the wastewater network. However, for this thesis, the Bellagamba *et al.* (2018a) potable water network serviceability loss model (SLM) has been used, based on the more comprehensive performance dataset that was available (Section 2.3.3.3.2 and Appendix B.1.2), in the demonstration of the proof of concept.

The subsequent sections in this Chapter introduce the following:

- The SLM and *Bruce*,
- The workflow undertaken to collate the data into *Bruce*,
- The extraction of all relevant data,
- The subsequent process for reading and analysing the outputs in the SLM.

Whilst this research focusses on seismic analysis, the future works discussion in Section 5.4 highlights potential uses in other natural hazard analysis, and other infrastructure analysis, such as the wastewater model by Liu (2016).

3.2. Serviceability Loss Model

Bellagamba *et al.* (2018a) developed a series of fragility functions to model Christchurch's buried potable water network performance following the 22nd February 2011 Christchurch Earthquake. By assessing the damage records as summarised in Appendix B.1.2 and applying four parameters; PGV, Cyclic Resistance Ratio (CRR), pipe material (limited to brittle or ductile), and pipe diameter, a series of failure rate functions were derived, assuming a Poisson distribution of pipeline failures (reported failures per km), with a specific functional form:

$$\ln(\lambda) = f_0 + \sum_{i=1}^{n}[C_i(h_i)] + \epsilon \quad (1)$$

where:

$ln(\lambda)$is the natural logarithm of the failure rate

f_0*(PGV)* is the so-called backbone function depending on PGV

$C_i(h_i)$ is the correction term corresponding to the i[th] known model parameter, dependent on parameter vector h_i

n is the number of known parameters

ϵ is a zero-centred normally distributed random variable representing uncertainty of the model

The failure rate functions were validated by Bellagamba *et al.* (2018a) in a retrospective analysis using a 2000 run Monte-Carlo Simulation (MCS), with each run consisting of the following five-step process:

1. Generate a spatially correlated, multivariate random field to sample ground motion residuals.
2. Compute PGV intensity at each strong ground motion station utilising simulated median and generated residuals for the 22nd February 2011 Christchurch Earthquake (Figure 2-27 and section 2.3.3.1).
3. Evaluate mean failure rate and standard deviation for each pipeline based on experienced ground motion intensity and known characteristics of the failure rate model (PGV, CRR, pipe material, and pipe diameter).
4. Sample the failure rate for each pipeline.
5. Simulate the number of failures for each pipe segment.

From this model, a comparison of simulated versus recorded pipe failures across the network was conducted, grouped by the SCIRT repair catchments, as shown in Figure 3-1 (*a* and *b*).

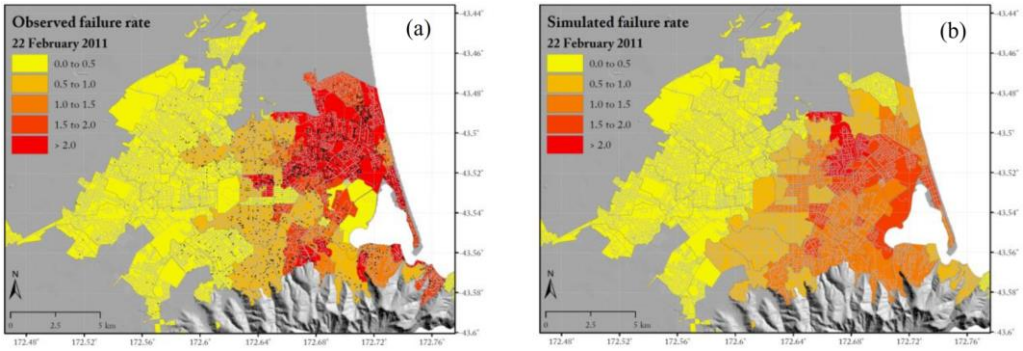

Figure 3-1: Spatial distribution of potable water network failure rates (from Bellagamba et al., 2018a) where (a) is the observed failure rate and (b) is the simulated failure rate

Figure 3-1 (*a* and *b*) demonstrates that generally, the model can replicate the performance of the potable water network well. There are exceptions where the use of CRR under-predicts pipe failure in areas where soils are susceptible to severe liquefaction, such as the Residential Red Zone or in areas of rock fall and slope instability. Bellagamba *et al.* (2018a) noted that the use of these fragility functions and methodology could be applied to other distributed infrastructure components, a topic later discussed in Section 5.4.

Bellagamba *et al.* (2018b) compared the MCS results with the inferred co-seismic performance, using global and specialised community-orientated metrics. The prediction results, which form the basis of comparison for this thesis, illustrate similarities with co-seismic performance. The model shows that a significant number of buildings with a predicted probability connection loss of ≥0.5 are presented as disconnected from the water supply network (Figure 3-2 *a* and *b*). Readers are encouraged to review these papers further for details on the development and implementation of the fragility functions.

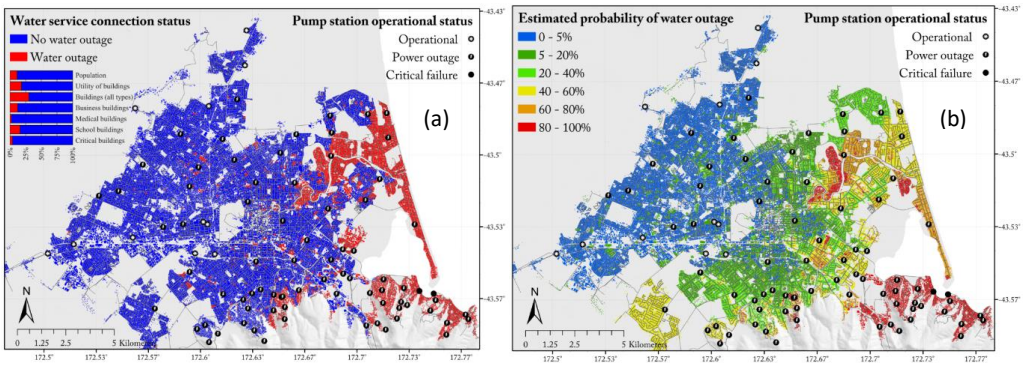

Figure 3-2: Comparison of inferred co-seismic performance (a) and estimated water outage (b) (from Bellagamba et al., 2018b)

3.3. NextSpace and NSIS, Codenamed *Bruce*

3.3.1. Introduction to *Bruce*

The Christchurch City Council and NextSpace Ltd. have collaborated to develop *Bruce*, an integrated GIS and BIM web-based system to collate multi-source data into a 3D model (digital twin) of Christchurch's built environment. One of the main objectives of *Bruce* is to demonstrate its capabilities as a combined asset management, consenting, and contract management and design tool. *Bruce* also presents significant research opportunities for investigating urban resilience to earthquake hazards. This research thesis has presented the opportunity to further develop data integration of research model outputs and *Bruce*.

Generally, within an organisation such as CCC, the current method of storing, managing and exposing numerous data sources and control points is complex, complicating the process of accessing and amalgamating data (Figure 3-3a). *Bruce's* use of a bidirectional link manager and universal data access language allows for the easy transference and accessibility of data, irrespective of their format, meaning that *Bruce* can recognise and transpose data from existing tools and sources. By acting as the connection between existing data, *Bruce* enables stakeholders to share, view, and manage; large datasets that are both current and relevant (see Figure 3-3b).

(a)

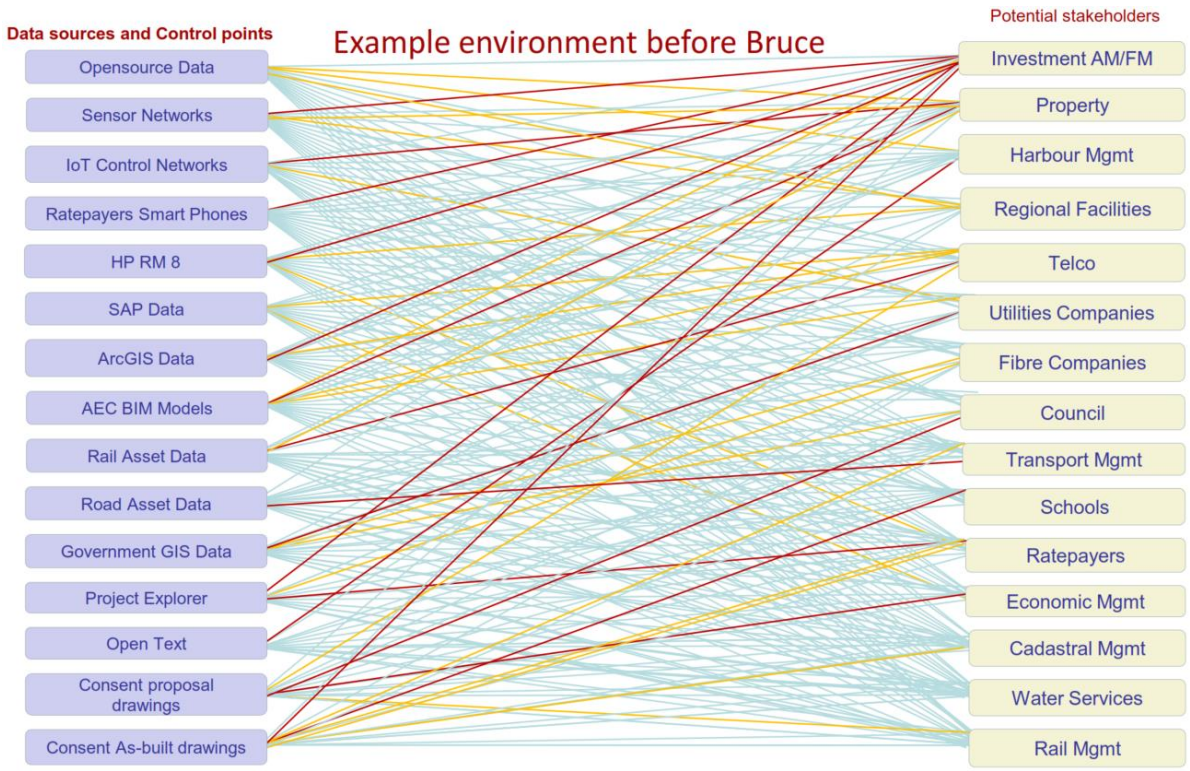

(b)

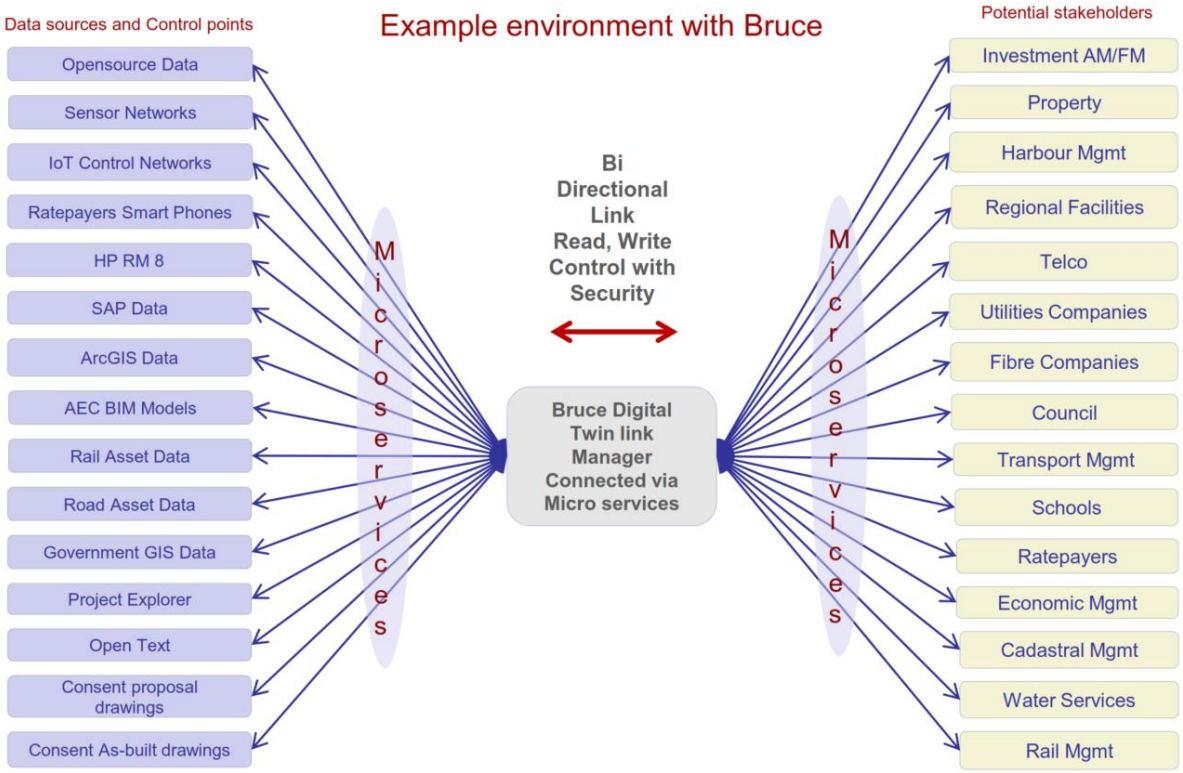

Figure 3-3: Smart City data management where (a) is a generalisation of current complex data sharing models and (b) is a model using Bruce (Nextspace Limited, 2018)

As updates and modifications are made to the source data, they are seamlessly and automatically updated within the interface, meaning that an action need only be carried out once for all linked sources to recognise the change. This significantly reduces time, cost, effort and the potential for errors. However, to achieve this, strict adherence to format versions and protocols around the meaning and use of "revisions" and "versions" is required.

The methodology seen in Figure 3-3 (b) further develops the work by Lapierre and Cote (2007) and continues to overcome the BIM and GIS ontology integration issues identified in Section 2.2.4, whereby for one to view the multi-format datasets, no conversion from one platform to another is required. Whilst visually, *Bruce* provides a representation of the connectivity between building and utilities, the current model does not contain metadata and unique values for these connections, predominantly due to an inconsistency in provision of this data because of a lack of a national mandate. For the purpose of the analysis in this thesis, the lack of this connection data does not have an impact on the methodology, as it is not one of the input parameters. However, as is discussed later in this thesis (Section 5.4.2), this data would be vital if the SLM were to be improved by modelling settlement of buildings, as these connections become points of weakness where the heavier building is more likely to settle more than the utility. Similarly, they provide an additional damage mechanism and potential for service loss within the private laterals, another functionality the current SLM does not have.

For researchers, *Bruce* is a powerful data storage facility, acting as a one-stop-shop for an array of potential analyses (later discussed in Section 5.4). The section below provides a high-level overview as to how *Bruce* reads and displays the various data sources and how it acts as a "streaming service" for stakeholders to obtain required information.

3.3.2. Overview of the Bruce Interface and its Connection to Data

The User Interface (UI) developed by NextSpace Ltd is an html JavaScript platform allowing the user to quickly and efficiently design data schemas, connect them to various data sources, and perform static and real-time streaming of those data. The UI-associated administration tool provides the means to filter, manage, sort, and edit assets and data schemas; it also enables mapping multiple schemas into many to one, and many to many relationships between existing entity types and imported data. The four main classification categories within Bruce for managing various integratable file formats are (see also Figure 3-4):

- *Entity Type*: Classification system for grouping similar entities together e.g. horizontal infrastructure, vertical infrastructure, building parcels, land information.
- *Entity*: These are each of the files/objects uploaded into *Bruce* e.g. an as-built BIM model, or a raster image file. Within each entity, different LODs can be assigned and viewed separately i.e. a high-resolution 3D-BIM of the building exterior, or a low-resolution 3D-BIM of the internal structural elements such as bracing/framing. All entities are given unique IDs for cataloguing and cross-referencing.
- *Layer*: Assigned to each entity type to allow for sub-classes e.g. vertical infrastructure may have layers associated with foundations, structural framing, or building exterior layers. Each layer can have multiple entities within them.
- *Menu Items*: Each UI can have a tailored menu system, relevant to the user. For each menu item, different file types can be assigned such as a *Bruce* entity, .kml file, or WFS feeds.

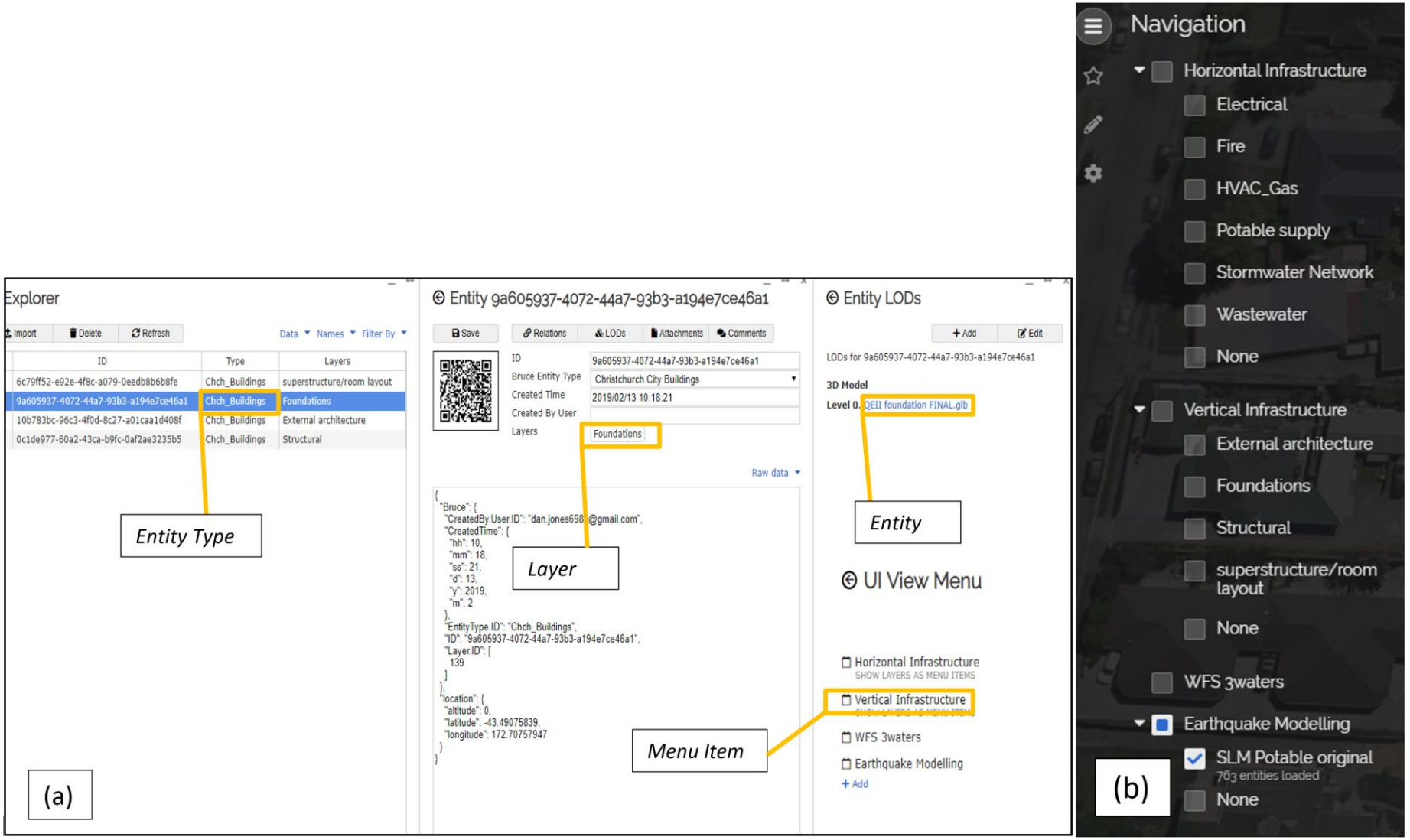

Figure 3-4: Bruce classification category examples where (a) shows the Bruce admin tool and its menus for UI development and (b) presents the translation to the UI

Within the UI, *Bruce* has several open-source base maps and digital elevation models (DEMs). This enables detailed geospatial data visualisation and qualitative evaluation of entities with respect to one another. Examples of this are discussed in Section 5.2. As part of this thesis, entity types that are not project/user-specific have been developed within *Bruce*, that can be applied to a national database, such as the entity types for vertical and horizontal infrastructure. The detailed formats of these are shown in Figure 3-5.

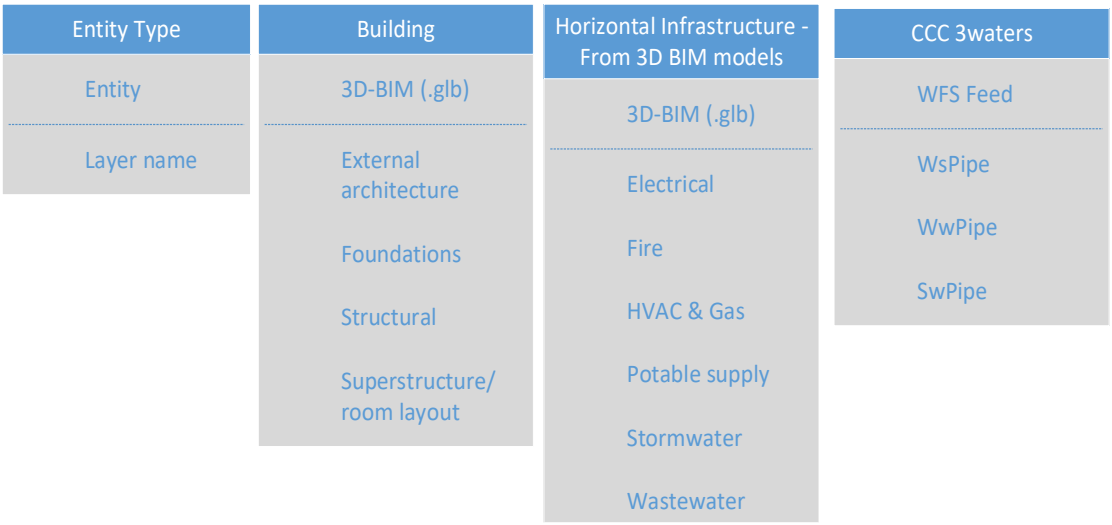

Figure 3-5: Hierarchy of vertical and horizontal infrastructure within Bruce

Each schema within *Bruce* can be specific to a created entity. Alternatively, to ensure consistency, a city/nationwide schema set could be established with entities mapped to them. For example, in the case of a nationwide database, a "building" schema could be created whereby a many-to-one relationship is established for "foundations". This would allow the schema mapping of all variations of "foundations" labelling within each regional council's database and would ensure consistency across the country. Another feature of many-to-one and one-to-many schema is the ability to extract and display metadata relevant to user needs, and is fully customisable across accounts and users (discussed further in Chapter 5). An account in *Bruce* can be defined as an organisational level UI that comprises multiple users with different access requirements. For example, CCC is the account owner, but the building consent team will have a different set of read/write privileges of data, to the asset management team, within the CCC UI. This is demonstrated in Figure 3-6 where a BIM sample metadata output shows "User A" has a schema referencing fields 1 and 3, but the schema of "User B" has fields 2 and 4. Within *Bruce*, as previously mentioned in 3.3.1, the original data remains unchanged from the source, but tailored schema are developed between each user's "view" to create project/user-specific interfaces.

Unique ID	Field 1	Field 2	Field 3	Field 4
	Depth	Diameter	System Type	Family and Type
(CCD2F1EF-09F6-45D6-8BC7-93120F1AA826):#2886	77.50	25.83	Piping System: Potable Cold Water	Ball_Valve-Bronze-Standard_Port-WATTS-B6000-0.25_Thru_4.00_Inch-Threaded: 1"
(CCD2F1EF-09F6-45D6-8BC7-93120F1AA826):#2709	216.00	72.00	Piping System: Potable Cold Water	Ball Valve - 50-150 mm: 50 mm
(CCD2F1EF-09F6-45D6-8BC7-93120F1AA826):#2890	77.50	25.83	Piping System: Potable Cold Water	Ball_Valve-Bronze-Standard_Port-WATTS-B6000-0.25_Thru_4.00_Inch-Threaded: 1"
(CCD2F1EF-09F6-45D6-8BC7-93120F1AA826):#2811	160.48	53.49	Piping System: Potable Cold Water	050-075_009-QT-S: 3/4" 009-M3-QT-S

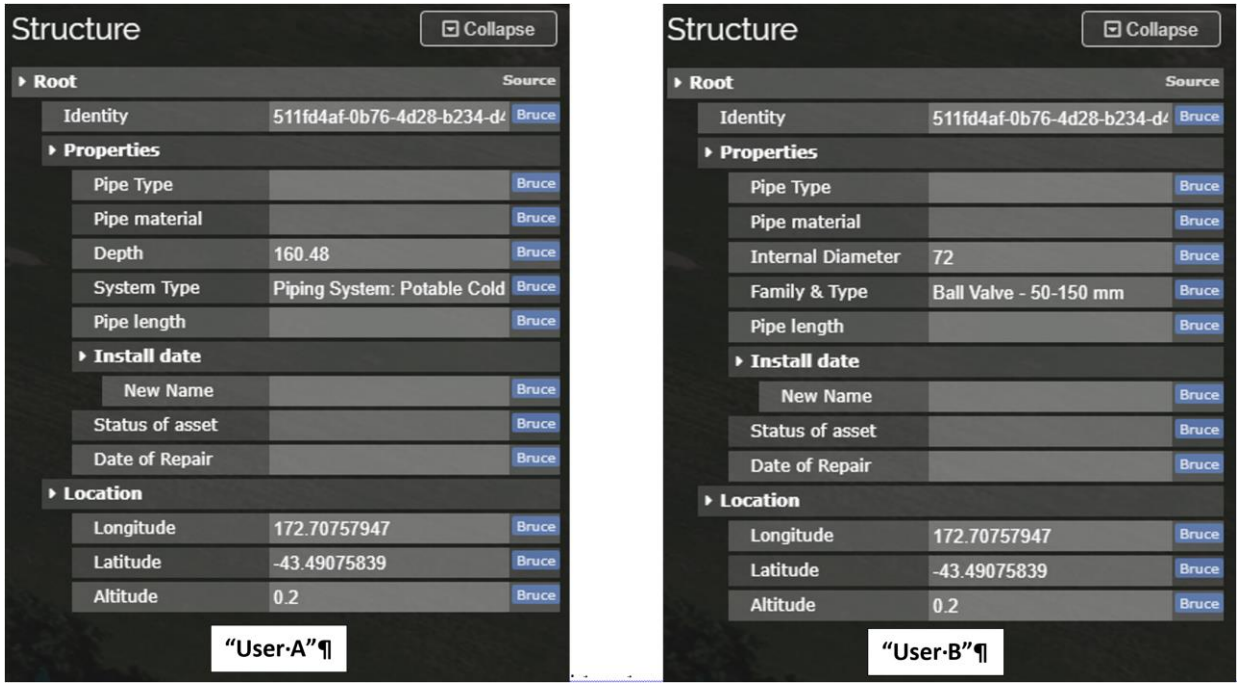

Figure 3-6: (above) sample output of metadata from BIM (below) example schema for "User A" and "User B" demonstrating Bruce's' ability for tailored user views. Note how the Schema from "User A" captures fields 1 and 3, and "User B" has fields 2 and 4.

Currently, the main data sources relevant to Christchurch in the *Bruce* UI include the CCC WFS feed relating to the 3 Waters network and several CCC-owned vertical infrastructure assets in as-built BIM formats. The 3 Waters WFS feed is configurable, enabling user-specific schema mapping to equivalent *Bruce* entities whilst identifying geospatial and geometry data from within the WFS fields to display as points, lines/polylines and polygons. Real-time updates of source data and any associated revisions are possible through automation of ETL (Extract Translate Load) processes, if workflows and protocols are followed. At present, *Bruce* has a workflow involving .kml, .kmz, .glb, and .ifc file extensions. This process has been used as part of the case study presented in Chapter 4.

The primary purpose of *Bruce* is to manage existing data connections and provide a process for separating, opening, and editing data, whilst ensuring robustly links are maintained in *Bruce* between the source data and any subsequent visual proxy formats. This process is explained further in Chapter 4. *Bruce* also has the means to create relationships between entities by applying rules and searching for attributes within multiple datasets. Equally, the search and rule functions can be based on fuzzy data and complete nearest neighbour searches on features such as ends of pipes. The predominant hindrance with any rule-based query is inconsistency in naming conventions, which again highlights the need for a standardised protocol.

3.4. Geospatial Workflow Model

Using the nomenclature from Section 2.2.4, *Bruce* can be considered a combination of several processes. At its core, it is a hybrid data level and process level integration tool.

Beginning with the data sources and control points at the top of the workflow, these represent each of the connections between the various datasets and *Bruce* through micro services (the "streaming" component) as shown in Figure 3-3b. *Bruce* uses semi-automatic conversion, translation, and extension methods to translate semantic data into a *Bruce*-specific schema, that attempts to closely resemble the source schema as much as possible. During this time, the source data is also given a Unique ID, the initial part of the ETL process presented in Section 2.2.4.1.

From these connections, a "mirror" of the data is transposed, retaining all semantics and format of the original data, minimising data loss whilst translating the "mirror" into a suitable format for the html JavaScript platform to process. This is achieved in a similar manner to Lapierre and Cote (2007), in that *Bruce* uses WFS as a means of linking to some of the source data (in the example of this thesis, the CCC 3 waters network data, discussed later in Chapter 4). The semantic and geometric data are separated as shown by the first blue process boxes in the workflow below, using a methodology comparable to Amirebrahimi *et al.* (2015) as shown in Figure 2-20.

The outputs from the first process are shown in the workflow as a .glb geometry file and a .csv/.txt file, which contains attribute and semantic information from the BIM IFC data. The geometric outputs are assigned to an entity type (Figure 3-5). Where *Bruce* differs from the methodologies presented in Chapter 2 is through the ability to separate the geometric data into sub layers, based on the semantic data, for interrogation. This becomes a key feature, particularly with ensuring the semantic data is consistent or at least mapped to a consistent schema when developing a Digital City (Section 2.2.5.4), a topic discussed in detail in Chapter 5.

The next stage of the workflow combines the translated semantic and geometric data into *Bruce* so that within the visualisation tool, the two datasets are linked. This also closes out the ETL process whereby the unique ID assigned to the translated file is linked back to the source data for cross-referencing and for monitoring revisions and updates. Once the integrated datasets are in *Bruce*, *Bruce* has the functionality to query and filter any of the semantic data that has been indexed for external analysis in computational engines, examples of which are presented in the green boxes at the end of the workflow.

Finally, to close out the workflow, outputs from computational engines can be uploaded back into *Bruce* for visual interrogation and for use in compounded analysis (i.e. these results could be exported by another researcher and incorporated with other semantic data, thereby providing a reiterative research engine).

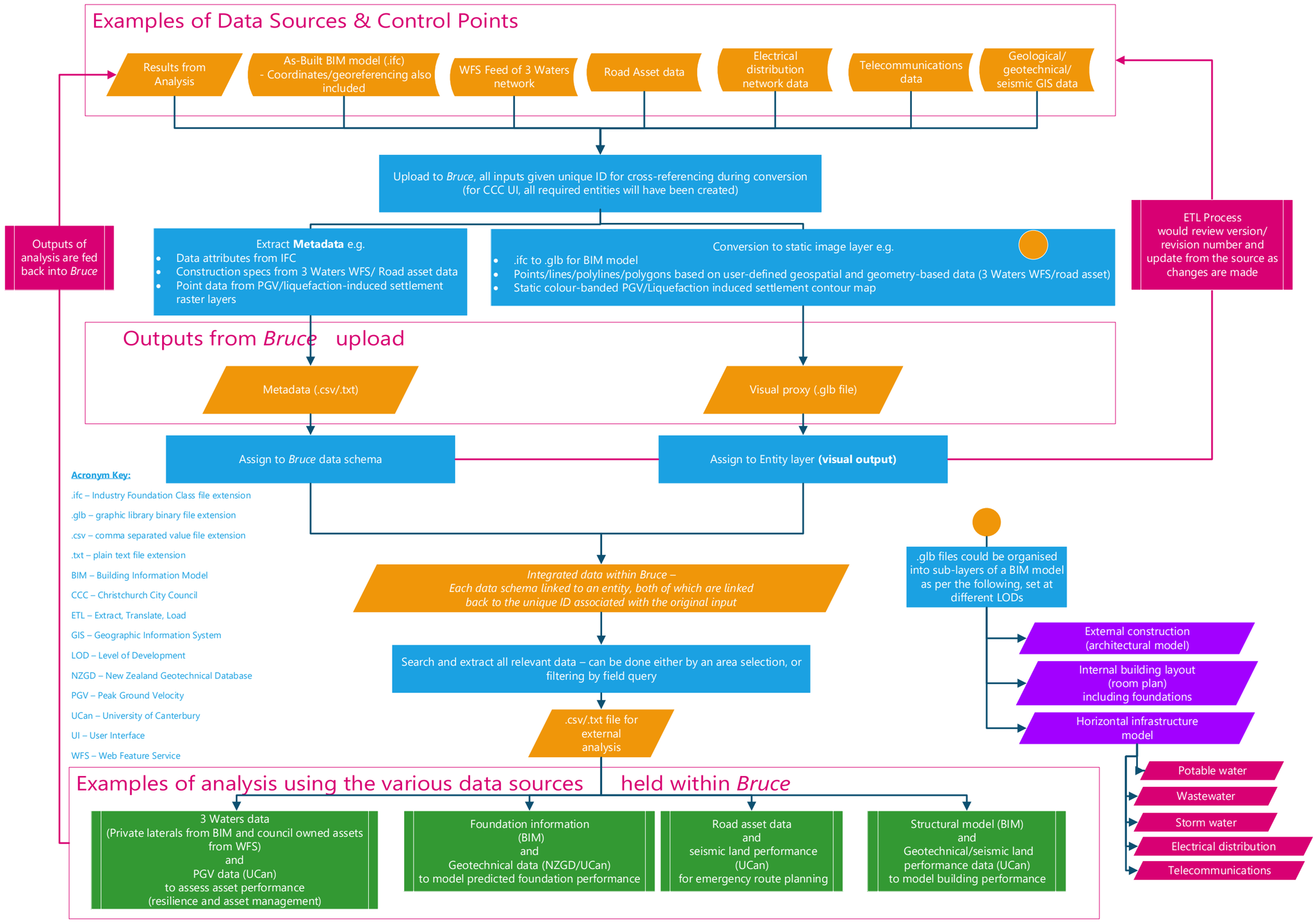

Figure 3-7: Geospatial workflow

Chapter 4
—Taiora: QEII Recreation and Sport Centre – A Case Study

Contents

4.1. Introduction

To demonstrate the proposed workflow, a site has been chosen where building and infrastructure data were readily available and in a format suitable for integration into *Bruce*. To that end, the new Taiora: QEII Recreation and Sport Centre, which opened in 2018, was selected. The CCC provided as-built BIM data that contained the majority of the main building, and some of the horizontal infrastructure exiting the building. Along with this, a connection to the 3 Waters WFS feed was established to obtain network data surrounding the case study site. The raw data posed several challenges posed by: file format, geo-referencing and incomplete data, all of which required manual manipulation by the author in order to be usable. Further detail regarding these issues is discussed in Section 5.2.

Once data had been appropriately formatted, X. Bellagamba (from Bellagamba *et al.* 2018a) was consulted to confirm the parameters for the serviceability loss model (SLM), ensuring a tailored schema could be developed to extract required data from *Bruce.* Also as part of this consultation, X. Bellagamba also provided an excerpt of his original analysis to enable comparison with the new analysis undertaken as part of this case study.

4.2. Inputs

4.2.1. BIM Data

The as-built BIM model was modified from its original Revit Project File extension (.rvt) to an eventual SAP Visual Enterprise Binary (.rh) format within SAP Visual Enterprise Author (VEA) (V9.0.600.6989), and was exported from VEA as binary versions of Graphic Library Transmission Format (glTF) files, known as .glb (Graphic Library Binary). The .glb files (herein referred to as entities) provide a means of sharing 3D models between different platforms; they are an interoperable format for transmission and loading into *Bruce,* due to the optimised download speed and load time configuration for use in mobile and web-based 3D modelling programs (Sharpened Productions, 2018).

As discussed in Section 4.1, the QEII BIM data, provided by CCC, were partially complete and had to be supplemented with .pdf plans of as-built surveys of some of the 3 Waters network. From this, the author of this thesis had to teach himself to manually create 3D models of remaining omitted 3 waters network data in SAP VEA. This was achieved by superimposing the laterals .pdf plans underneath the .rh file of the QEII building to complete the network between building and street level, for a complete digital twin of the site. These were then also exported as .glb files.

To geospatially reference the .glb files of both the building and the horizontal infrastructure in *Bruce,* the .pdf plans that contain geographic projection coordinates were scaled and underlain beneath the 3D building model in SAP VEA. Axis origin points for each .glb entity were positioned over a known geospatial location, which, for the case study, was a storm water manhole cover to the north-west corner of the building.

Upon completion of geospatially referencing all .glb entities, the entities were uploaded into the *Bruce* web platform via a drag and drop process, and assigned to corresponding layers within the "Vertical Infrastructure" and "Horizontal Infrastructure" entity types, as per Figure 3-5. The Vertical Infrastructure entity type is currently defined by four layers, "external" (Figure 4-1), "internal" and "foundations" (Figure 4-2) and "structural". Figure 4-3 presents the electrical, fire, potable water and wastewater infrastructure entities within their matching layers of the "horizontal infrastructure" entity type, and the 3 Waters network from the BIM model, showing the internal network connected to the private laterals is shown in Figure 4-4.

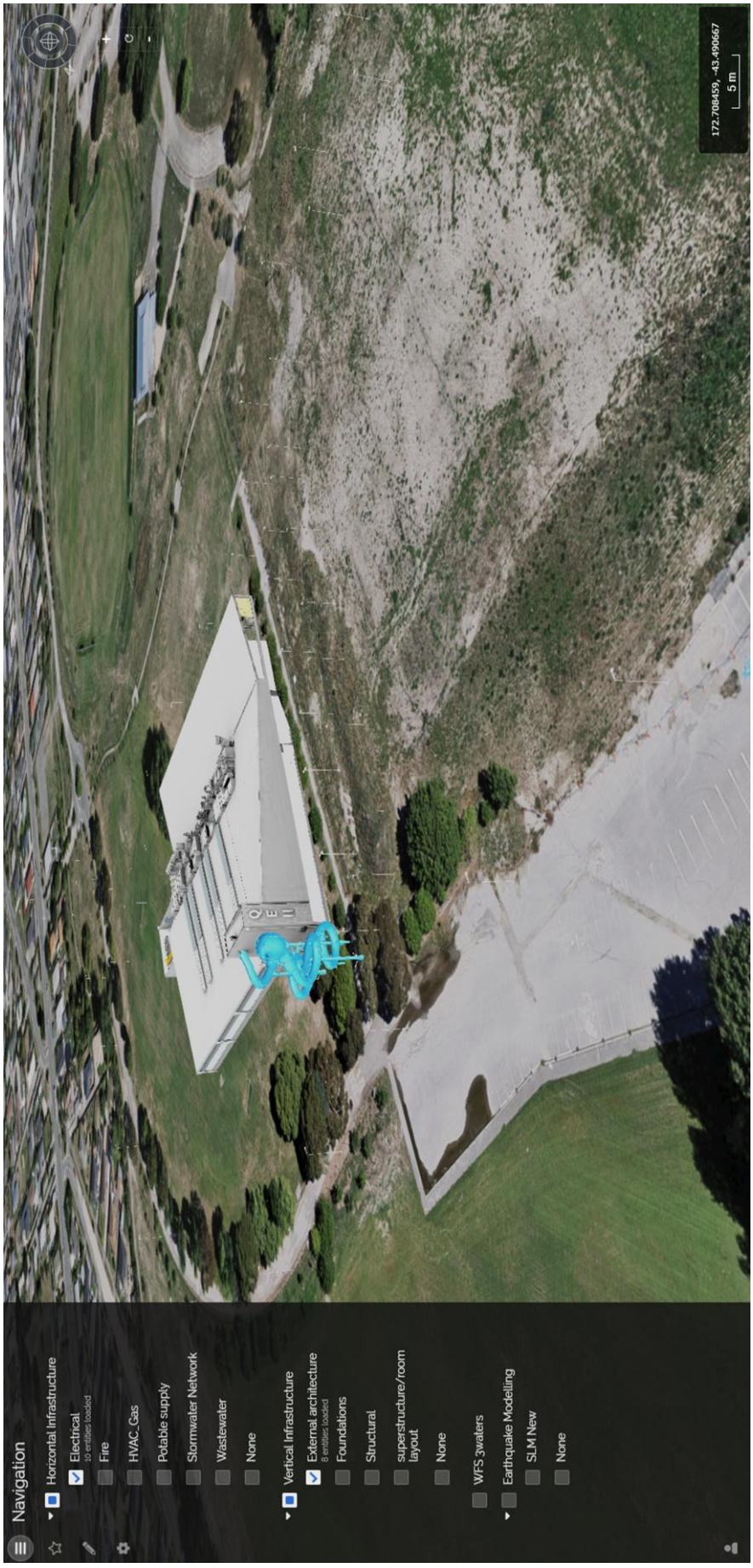

Figure 4-1: External model of QEII in Bruce

Figure 4-2: Internal room layout model of QEII in Bruce

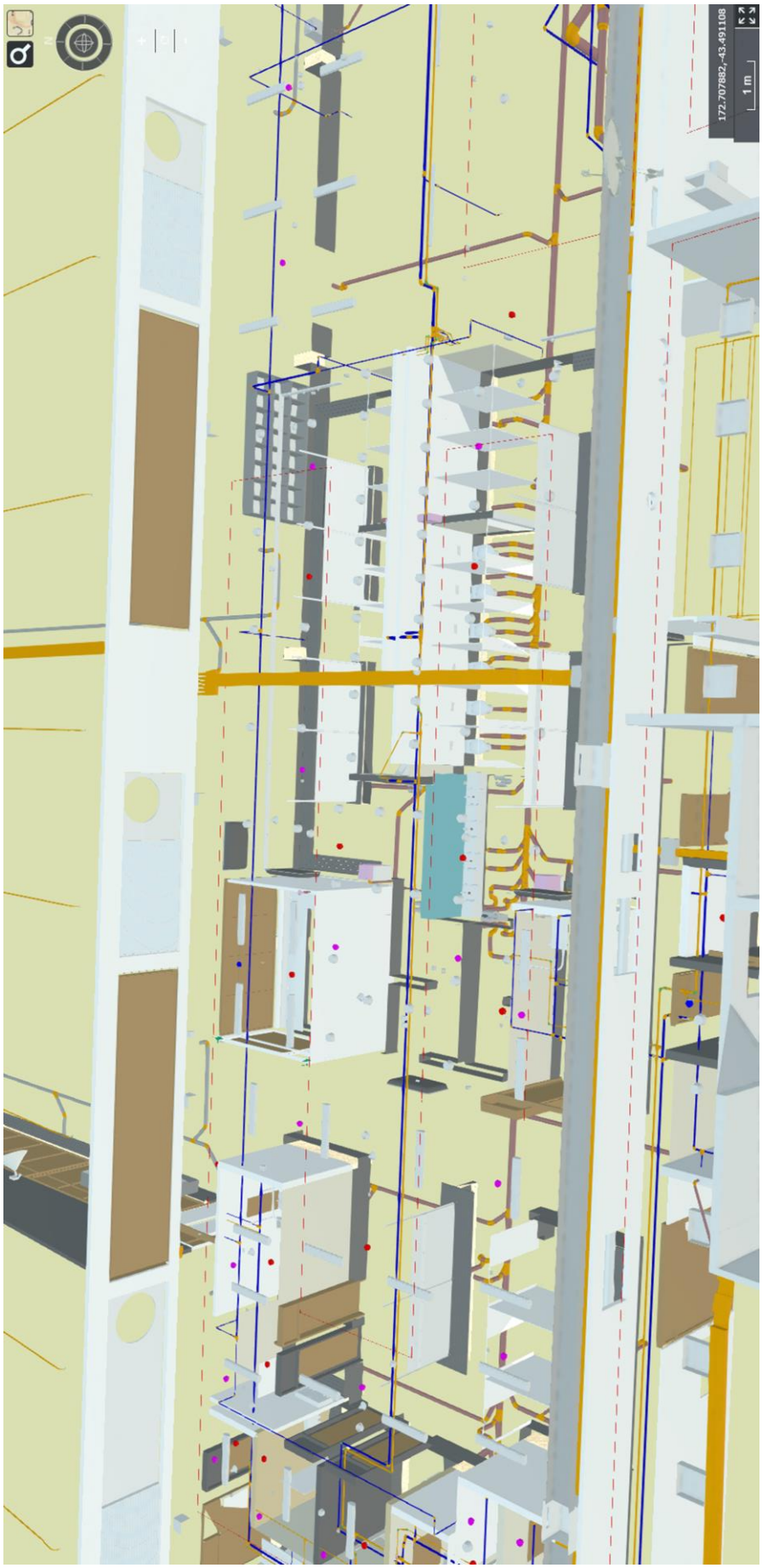

Figure 4-3: Room model of QEII in Bruce showing internal services (in this view filtered for 3 waters, electrical and fire). Foundations have been removed to show wastewater network beneath the foundations.

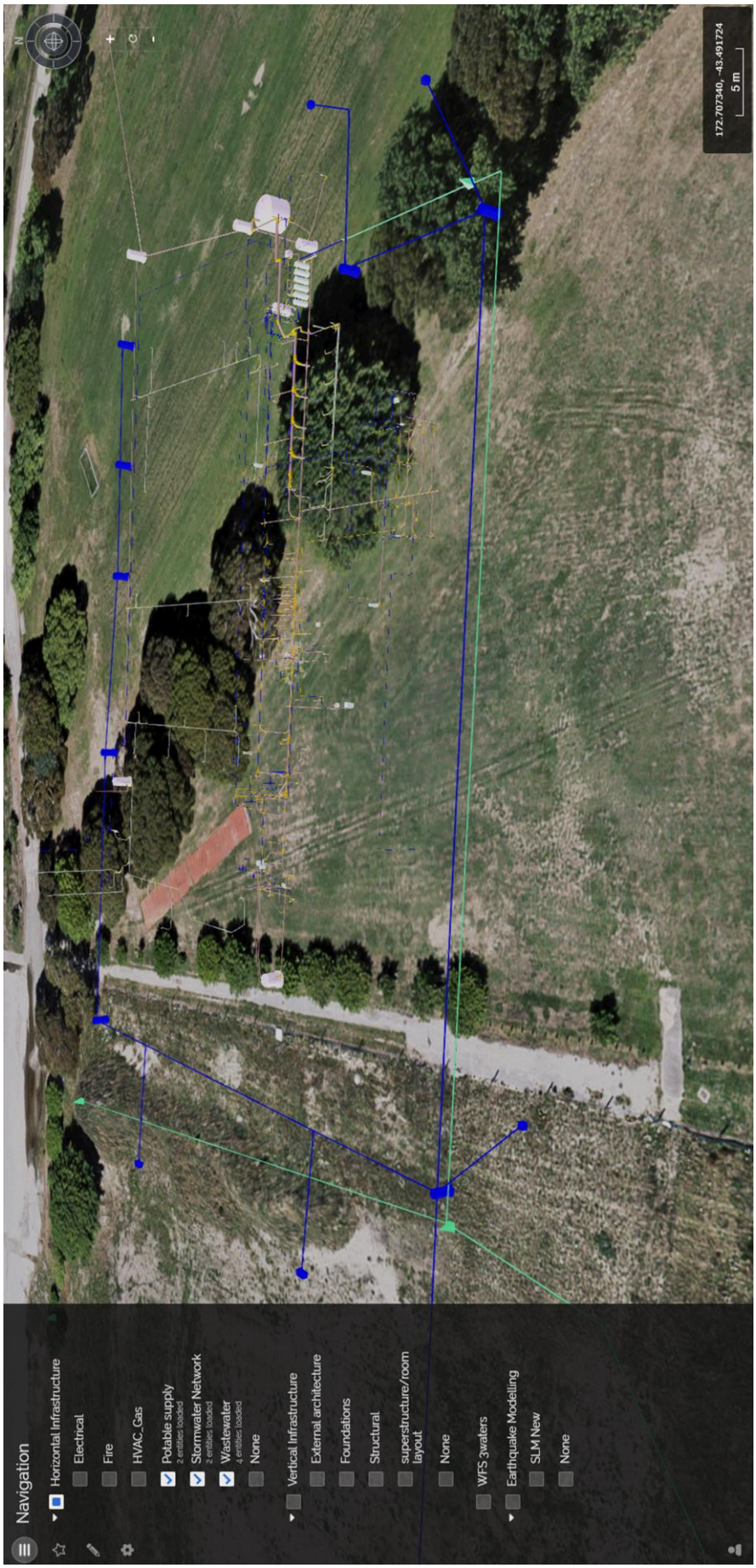

Figure 4-4: BIM data of 3 Waters network (internal QEII and partially complete external network)

4.2.2. GIS Data

As of March 2019, NextSpace Ltd. were still completing work on the CCC 3 Waters WFS feed to update the connection to *Bruce,* and integrating the points/lines/polylines/polygons conversion tool, as defined in Figure 3-7. As a temporary measure to overcome this for the analysis presented here, .csv extractions from the WFS feed were carried out, filtered by a specified area surrounding the case study site.

The exported .csv file was in an unsuitable format for *Bruce* and the SLM. Each set of coordinates were in a string of text in a single spreadsheet cell for each pipe, and needed to be separated so that each coordinate pair were in their own row (Figure 4-5 and Figure 4-6). This required a significant amount of post-extraction manipulation in Excel. Once this was achieved, the amended .csv file was in a format suitable for upload into *Bruce*.

Pipe ID	Geometry (NZTM2000)
1304	1576153.02375115 5183623.21161937 1576151.78124746 5183623.13462408
1305	1576143.6094993 5183623.23141695 1576151.78124746 5183623.13462408

Figure 4-5: Pipe ID and coordinate format of WFS feed .csv extraction

Pipe ID	Easting (NZTM2000)	Northing (NZTM2000)
1304	1576153.02375115	5183623.21161937
1304	1576151.78124746	5183623.13462408
1305	1576143.6094993	5183623.23141695
1305	1576151.78124746	5183623.13462408

Figure 4-6: Pipe ID and coordinate format of WFS feed, post-manipulation

From this, each set of co-ordinate reference points for each pipe were grouped with a *points to path* processing tool in QGIS (V3.4.4-Madeira) to create polylines representing each pipe. These were saved as three static .kml files grouped by network type (potable water, wastewater and storm water) and uploaded into *Bruce*. During this process, the .kml files were exported with a different Coordinate Reference System (CRS), as the raw data uses New Zealand Transverse Mercator (NZTM) as the geographic projection; *Bruce*, however, uses WGS84 as the default projection. Following the workflow in Figure 3-7, .kml files that were created were mapped to a schema in *Bruce* so that the .csv metadata could be filtered and extracted. The results of this part of the workflow are shown in Figure 4-7.

Figure 4-7: WFS feed of 3 Waters network

4.2.3. Integrating GIS and BIM in *Bruce*

During this data preparation phase, duplicates of the 3 Waters private connections were created in both .glb and .kml due to the WFS feed being updated. As an additional exercise both sets of data were uploaded to *Bruce* to test the degree of accuracy of each source.

The results presented in Figure 4-8 show there are some minor disparities between locations of several of the pipes across the two data sources. The four predominant reasons for these discrepancies are:

1. Inaccuracies with orientating and scaling as-built .pdf plans as part of the manual drawing process required for the private connection data (discussed in detail in Section 5.2).
2. Margin of error with the coordinate referencing of the WFS feed, particularly the older pipe network. The BIM data/.pdf plans have a higher degree of accuracy than the WFS data, based on the provided surveyed plans of the manhole covers.
3. Errors caused during the conversion between coordinate systems. The coordinate system in the .pdf plans (used for the geolocation of both the building and the connected utilities) was Mount Pleasant Circuit 2000, whereas the coordinate system used in *Bruce* is WGS84.
4. Once the .glb files were uploaded into *Bruce*, the QEII building and all infrastructure had to be manually rotated to line up with its as-built orientation.

Figure 4-8: Comparison of private connection accuracy between BIM data and WFS feed. Red circle indicates building connection to lateral supply pipe.

As discussed in Section 3.3.2, it is proposed that future works between NextSpace Ltd. and CCC involve the design of a standardised *Bruce* schema that will be defined based on the mandated requirements of as-built BIM data, supplied as part of the consenting process. This will include the provision of fully georeferenced data to overcome the challenges/issues faced above. However, for the purposes of this thesis and demonstrating the workflow, a manual schema for the potable water network has been developed within the *Bruce* admin UI to show the link between IFC metadata and how it is presented in *Bruce* (Figure 4-9).

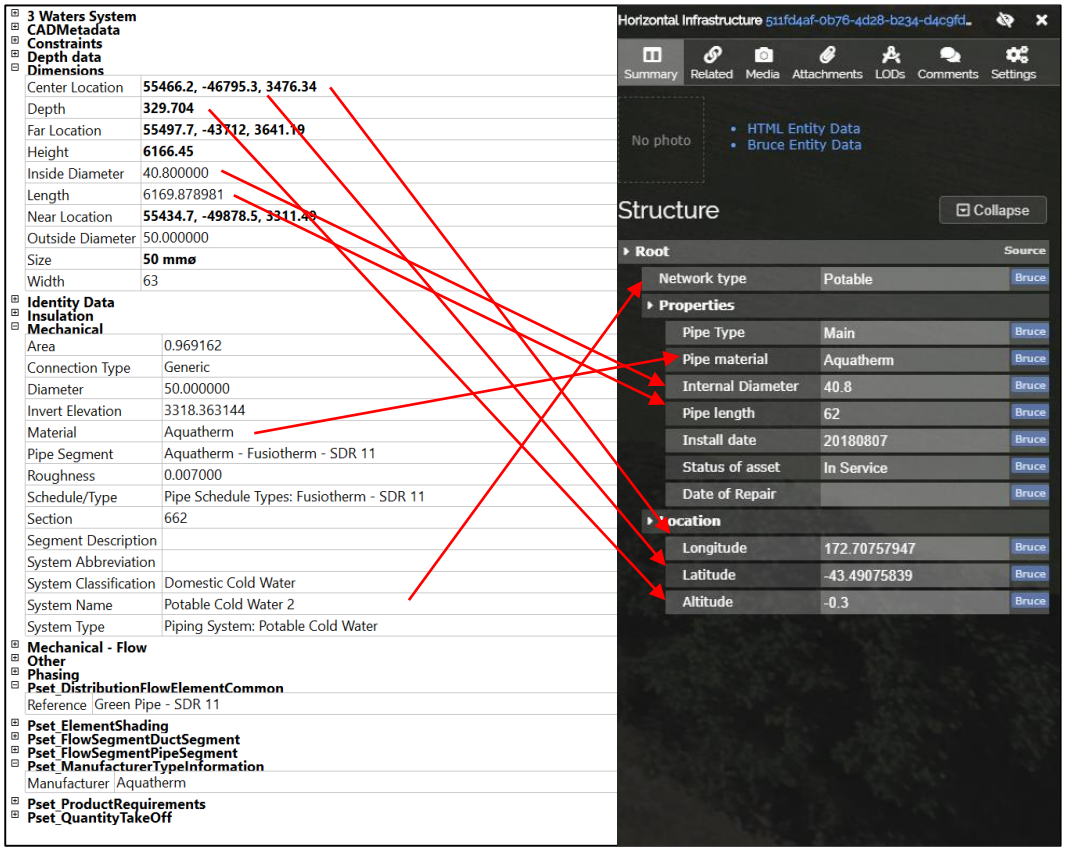

Figure 4-9: Potable water network schema created in Bruce and matched to QEII BIM data

4.2.4. Serviceability Loss Model Inputs

The fragility functions and decision support algorithms developed by Bellagamba *et al.* (2018a; 2018b; see Section 3.2), use, along with PGV and CRR, a number of pipe characteristics in global and community-based metrics to assess performance and recovery of the water supply network. Pipe characteristics include diameter, material, and embedment depth, the latter of which is used to determine the Liquefaction Resistance Index (LRI) value (subsequently used in the calculated CRR value). Global metrics measure population, utility of buildings and the number of buildings deprived of water, meanwhile specialised metrics quantify the business, medical, school, and critical buildings deprived of water. The majority of these parameters can either be directly obtained or easily modified from the data contained within *Bruce.* From the BIM and 3 Waters data, the following attributes were extracted directly from *Bruce*:

1. Latitude and longitude for each end of each pipe, or where there is a change in orientation,
2. Latitude and longitude for the case study building,
3. Pipe diameter.

"Material type" was able to be directly obtained and used without transformation from the WFS feed as this was the same database used for the original analysis by Bellagamba *et al.* (2018a). However, for "material type" from the BIM data, post-extraction manipulation was required due to the highly detailed description, into either the "brittle" or "ductile" variants for the fragility function model. Similarly, the LRI had to be determined post-extraction based on pipe embedment depths provided within the data.

The main point of difference with the data available within *Bruce* that was unavailable during the Bellagamba *et al.* (2018b) analysis is the topology of private connections between street-level services and the building. Prior to the introduction of the proof of concept in this thesis, these data types at an individual building level were almost non-existent in a digital format, and this concept forms part of the nationalised mandate later discussed in Chapter 5.

To prepare the data for use in the SLM, point IDs and Pipe IDs were assigned. At least two consequent points (Pt ID) that do not have to be collinear define each pipe, but where pipe junctions occur, points have to be repeated as demonstrated by Pt ID 110 and Pt ID 23 in Figure 4-10 below. Generally, for the data used as part of this analysis, Pt IDs are assigned to each set of coordinates for each end of a pipe, unless an individual pipe length exceeds 100 m (one of the limitations of the model) and so an additional Pt ID is added (demonstrated by Pt ID 24 in Figure 4-10).

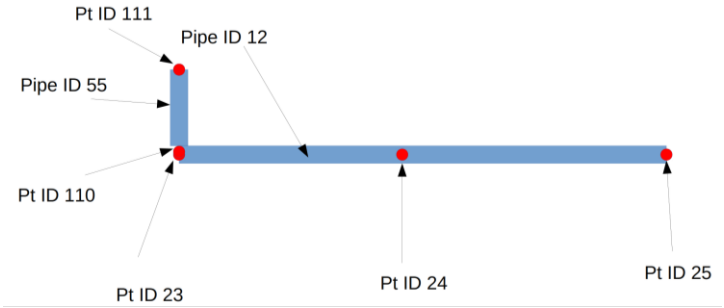

Figure 4-10: Pipe network preparation for Serviceability Loss Model

The final conversion process requires the creation of a .shp file for the new QEII building to which the population and utility values are assigned. Coordinates are taken directly from within *Bruce,* as is the calculated footprint area. It is hoped that in the near future, as part of the national mandate, building use will be one of the key identifiers incorporated into the schema along with up-to-date census data, allowing the utility and population data also to be directly extracted from *Bruce.* All data required for the SLM was packaged up as .csv files and submitted to Xavier Bellagamba for analysis.

4.3. Analysis and Results

To demonstrate the implementation of the workflow in Figure 3-7 and highlight its capabilities as an urban resilience modelling tool, the analysis conducted in this thesis has focused on the potable water network to assess and compare the performance of the case study site during the 22nd February 2011 Christchurch Earthquake. The original building and services that existed at the time of the 22nd February 2011 Christchurch Earthquake were eventually replaced due to the extent of damage they sustained. So as a means of comparison, the new building, and utilities were modelled under the same seismic conditions to assess if there would be an improvement in performance following upgrades to the network. Figure 4-11 and Figure 4-12 show the pre and post-CES potable water network and building stock topology, respectively, the former categorised by material type (Table 9) showing the evolution of the network following the earthquakes. The author, utilising the as-built BIM model, created the building footprint for the new QEII building (orange building in north-east corner of red box in Figure 4-12) manually. However, it is anticipated that as part of ongoing development of *Bruce* and the national database, an autonomous process for identifying, drawing and updating building footprints will be completed.

Table 9: Definition of pipe acronyms

Pipe type	Acronym
Asbestos Cement	AC
American Petroleum Institute (welded steel line)	API
Cast Iron	CI
Ductile Iron	DI
Galvanised steel	GALV
High-density Polyethylene	HDPE
Low-density Polyethylene	LDPE
Medium-density Polyethylene 80 (80 referring to the minimum required strength of 8.0MPa)	MDPE80
Modified Poly Vinyl Chloride	MPVC
Polyethylene	PE
Polyethylene 100 (100 referring to the minimum required strength of 10.0MPa)	PE100
Poly Vinyl Chloride	PVC
Steel	STEEL
Unplasticised Poly Vinyl Chloride	UPVC

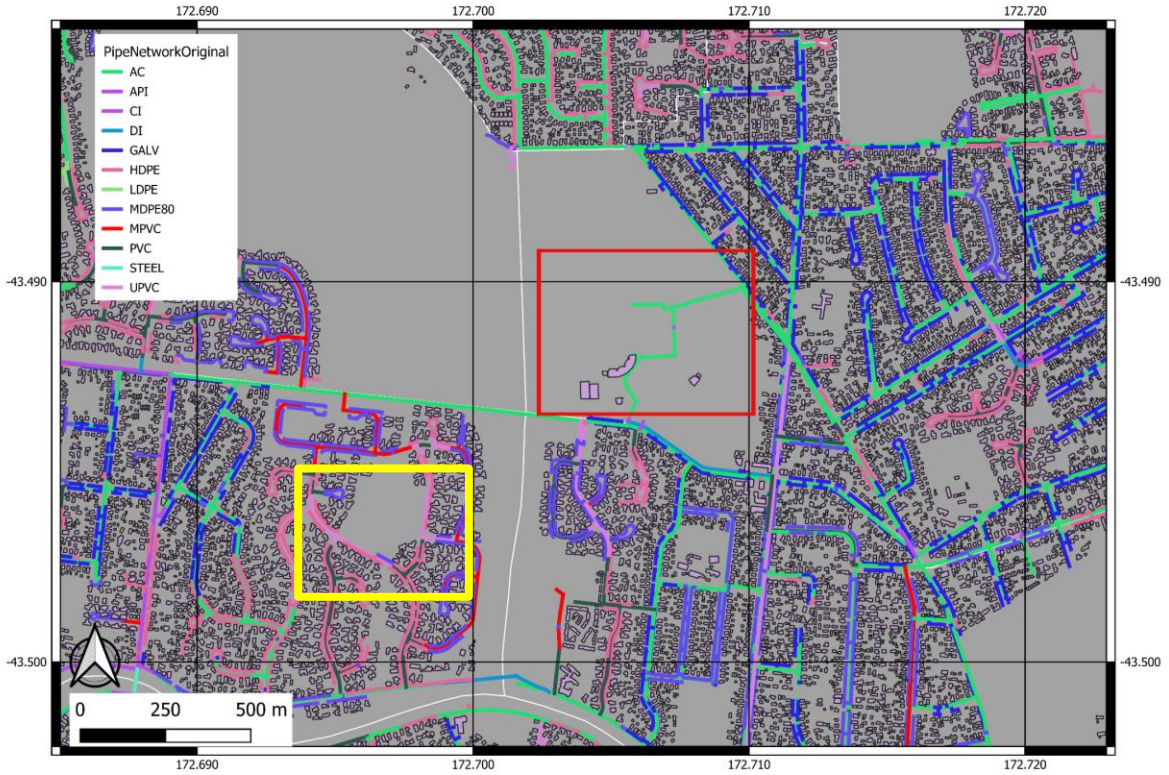

Figure 4-11: Pre-CES potable water supply topology and building stock distributed. Red box indicates case study area. Yellow box indicates data discrepancy in Residential Red Zone.

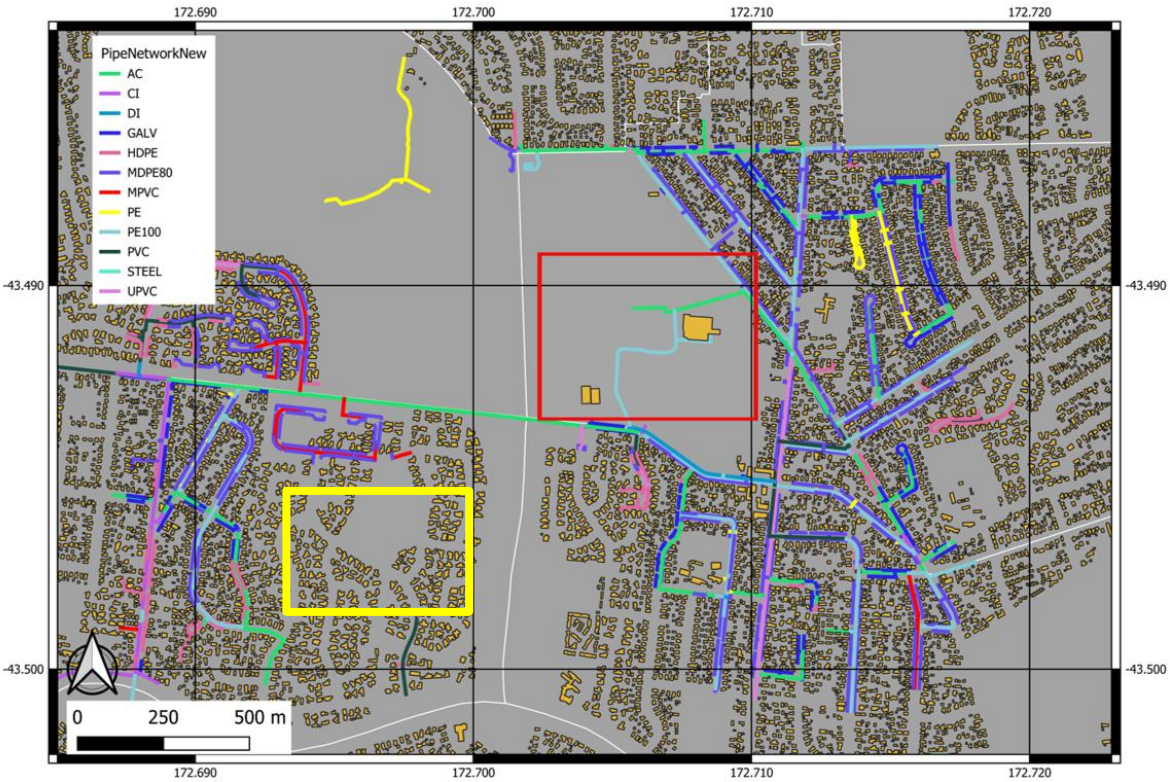

Figure 4-12: Post-CES potable water supply topology and building stock distributed. Red box indicates case study area. Yellow box indicates data discrepancy in Residential Red Zone.

One key observation demonstrating a need for continued data review of an integrated system is shown by the yellow boxes in Figure 4-11 and Figure 4-12 whereby the potable water network data have been updated to reflect pipes removed in the Residential Red Zone. Houses and infrastructure in the Residential Red Zone were removed due to the land being unsuitable for construction. Whilst Figure 4-12 correctly depicts a lack of services in the area, the representation of building footprints in the yellow box demonstrates how this data source requires updating. This error in data highlights the need for a QA process not just within each entity itself, but also of relationships between different entities.

Using the method Section 4.2, X. Bellagamba was provided the latest potable water network data exported from Bruce for the case study site. From this, X. Bellagamba replicated the processes for the SLM as described in Section 3.2 to model the performance of the latest potable water network data under 22nd February 2011 Christchurch Earthquake conditions. A comparison of the case study area was made using an excerpt from Bellagamba *et al.* (2018b) and the new analysis. The excerpt from Bellagamba *et al.* (2018b) and the analysis results were provided as .shp files which then had to be manually converted by the author to .kml extensions (using QGIS V3.4.4-Madeira) for upload into Bruce (Figure 4-13). The SLM results of the pre and post-CES building arrangements are presented in Figur and Figure 4-15.

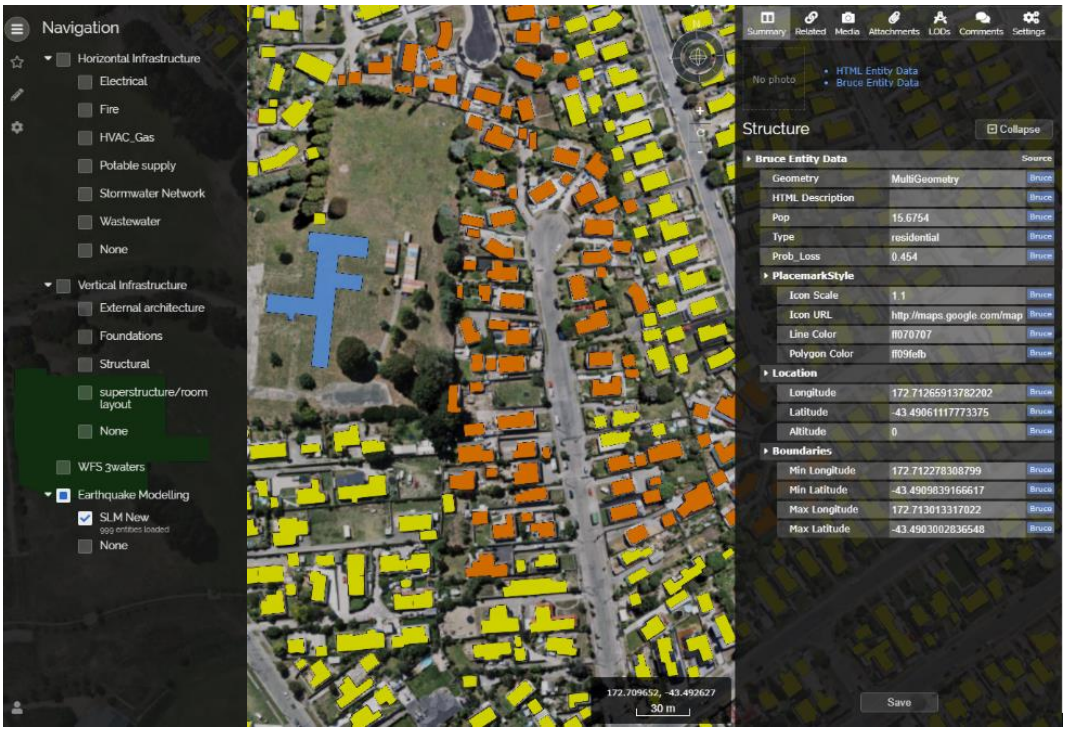

Figure 4-13: SLM results within Bruce

Figure 4-14: SLM results for pre-CES building arrangement of case study site (from Bellagamba et al., 2018b)

Figure 4-15: SLM results for post-CES building arrangement of case study site. 3 Waters network also shown where red lines are wastewater, blue lines are storm water, green is potable water. Yellow box indicates site boundary.

Figur and Figure 4-15 demonstrate that were the new building and supply water network subject to the exact same conditions as the 22nd February 2011 Christchurch Earthquake, they would perform better than the pre-CES configuration. The probability of water outage has dropped significantly from 65% to 29.5%, and it is considered that the predominant reason for this is the change in pipe material type from AC to PE100 (Figure 4-11 and Figure 4-12.) This change with respect to Equation (1) in Section 3.2 changes the binary parameter identifying whether a pipe is brittle or ductile (in this case the brittle AC pipe being replaced for a ductile PE100 pipe). A second change in the case study site potable water network topology is the pipe diameter whereby the original network had typical pipe diameters of 150 mm, whereas the newer pipelines comprise 180 mm diameter pipes.

The detailed foundation data were also omitted from the input as-built BIM data with respect to potential ground improvement work that was required in line with building consent requirements. Based on the observed performance of the site during the CES, it is expected that some ground improvement method was implemented. If these data had been available, the CRR component of Equation (1) in Section 3.2 could have also been modified to reflect the change and would have likely resulted in a further reduction in estimated probability of failure.

4.4. Conclusions

As of March 2019, *Bruce* schemas (derived either manually or by direct data/schema transfer from IFC files) are linked to a single entity. This means that if an individual .glb file contains multiple elements (i.e. one .glb file of the complete internal potable water pipe network for a building), and then a schema will be linked to this entity as a whole. It is not possible to select an individual pipe within a building unless that single pipe is its own entity. *Bruce* has not been set up this way as it would result in a significant number of entities being created for a single building and would likely impose substantial demand on *Bruce.*

One of the main lessons from this analysis was understanding the level of detail required from the UI of an integrated model, and where data can be grouped within a single entity. For example, it might be sufficient to have a single schema for the entire internal potable water network within a building, as all building elements (e.g. pipes, fittings, fixtures) associated with the schema have their own dimension coordinates tied to the original file. Therefore, the function in the UI displaying data associated with an individual pipe would not be necessary, if accurate geospatial data tied to each element were available for exporting and use in external analysis. Based on the BIM model for QEII, geospatial data assigned to each building element is achievable if set up correctly. However, this requires consistency in labelling of individual building elements and high quality data management to be maintained. This is highlighted in the internal potable water network QEII BIM data where examples of pipes labelled as “potable cold water” were joined with fittings labelled as “non-potable.” Whilst this presents an issue when extracting the complete potable water network data from *Bruce,* and one that needs addressing (further discussed in Section 5.2.1), loss of service due to a pipe break within the building is currently unable to be modelled in the SLM and so had no impact on the analysis.

As identified in Figure 4-11 and Figure 4-12 in Section 4.3, the building footprint data had not been updated from the pre-CES distribution to post-CES. This was due to this dataset being provided as part of the excerpt from Bellagamba *et al.* (2018b), and not from the original source that was used by Bellagamba *et al.* (2018b). The absence of this “raw” data linkage also resulted in the need to draw manually the new QEII building footprint, as discussed in Section 4.3.

Chapter 5
—Discussion and Summary

Contents

5.1. Introduction

The aim of this thesis, as outlined in Section 1.3.1, was to develop and implement a workflow for integrating data of multiple ontologies, and utilising them in analysis for characterising the resilience of a digital twin of part of Christchurch City. To achieve this aim, with the assistance of CCC and NextSpace Ltd., a conceptual framework was developed to; identify processes required for integrating and "streaming" geospatial and non-geospatial data into a platform, and how one would visualise and access the combined data (Chapter 3). To test this workflow, as-built BIM data from CCC's QEII facility were provided and augmented with the WFS data for the reticulated water network in the NextSpace integrated platform known as *Bruce.* From this, the serviceability loss model (SLM) developed by Bellagamba *et al.* (2018a; 2018b) was chosen as the analysis method to test the workflow's applicability in urban resilience assessment. A review of the required parameters for the model was undertaken, with a tailored schema developed in *Bruce* to extract the corresponding data associated with these parameters, from all data sources linked to *Bruce*. Finally, the data exported from *Bruce* was used in the SLM to compare the post-CES QEII facility and its infrastructure, with its pre-CES counterpart (Chapter 4).

This research demonstrates that the design of the new QEII facility and its infrastructure have improved resilience to a seismic event equivalent to the 22nd February 2011 Christchurch Earthquake (when compared to its predecessor). In addition, the integrated tool provides the ability to perform this type of analysis using a centralised database of building and infrastructure information, whereas previously, multiple sources were required to carry out the same analysis. Despite this success, this research was not completed without its challenges and on-the-fly adaptation being required to achieve results, along with the several identified limitations (Section 5.2). A lessons-learned exercise provides the opportunity for reflection, and identification of areas for improvement across the entire workflow as well as highlighting key areas of recommended future research (Sections 5.3 and 5.4). Concluding remarks are presented in Section 5.5.

5.2. Limitations of the Model and Challenges Faced

This section critically reviews the quality of the inputs to the model, the ability to implement the workflow, and discusses the challenges faced throughout the completion of this research. This will provide discussion points for areas of improvement and recommendations for future research (Section 5.4).

5.2.1. Data Accuracy

The first identified issue in the QEII BIM data was with naming convention of building elements. Inconsistency and lack of a QA process implemented on the BIM data has resulted in examples of potable water pipes connected to each other with pipefittings labelled as "non-potable" in the BIM metadata. Whilst having no impact on the visual output associated with the BIM, the errors within the metadata mean that if a query or filtering exercise were to be conducted to select/export only the potable network, the incorrectly named fittings would be omitted and therefore not show the complete network. To overcome this, draughtsman/architects are going to be required to become data managers if the provision of a granular, accurate metadata schema associated with a BIM model is going to be mandated and required on all consentable designs. Through communication with CCC, it is their intent to mandate the provision of a fully geospatially referenced BIM model as part of the building consent process, and the implementation of Industry Foundation Class (IFC) standards (see Section 2.2.5) would help draughtsman/architects overcome a significant number of the inconsistency issues highlighted. These inconsistences will also affect asset managers during the lifecycle of a building when provided with the as-built BIM data, particularly through facilities management if the incorrect non-graphic data or dimension data is provided and this would have a significant impact on accurately estimating costs of works orders and maintenance projects (Section 2.2.5.2). A secondary impact of inconsistencies is on earthquake impacts analysis, such as assessing ground shaking thresholds for triggering a loss of service within a building, where accuracy of the internal building network becomes vital.

Secondly, during the UI development in *Bruce*, it became apparent that using the latest DEM was an important consideration of an integrated tool. The CES caused differential ground movement and subsidence, but the DEM used in *Bruce* was not up-to-date to reflect these changes. The results were issues with depth offset of pipes where they appeared to breach the ground surface. This issue was further compounded in the case study where the DEM in *Bruce* was of a partially regraded site (following demolition of the previous structures).

Along with the DEM issue, another additional step required during the development of the workflow, which it is hoped could be negated during future refinements to *Bruce* (Section 5.4), relates to the consistent projection system used for surveying. In addition to the complications of some data being provided in non-BIM format (predominantly .pdf plans), the files provided used multiple projection systems (Mount Pleasant Circuit 2000 and NZTM). Following the superimposing of .pdf plans onto the .rh file in VEA (Section 4.2.1 and further discussed in Section 5.2.2), the coordinates had to be converted manually into WGS84, prior to upload into *Bruce*. Even after undertaking this process there were disparities identified, particularly between the WFS feed and the manually drawn 3 Waters network as shown in Figure 4-8. Whilst it has been identified that some of these disparities are likely the result of the manual drawing process, errors were exacerbated by the inconsistent use of geospatial projections.

The final data accuracy issues that were highlighted during implementation of the workflow became known during the WFS feed and BIM integration in *Bruce.* First, there were maintenance issues for the WFS source data linked to *Bruce*; there were examples of pipes inside the case study site that were still categorised as “in service” when it was known that these had been removed. This presents an example of an ongoing review and update requirement of the integrated tool, and that owners of the platform may wish to stipulate regular updates from users as part of a terms of use agreement, similar to the NZGD (NZGD, 2016), to ensure the latest data are always present (examples of platform maintenance are discussed in Section 5.4.1). This leads to the second maintenance issue/consideration identified during the workflow. Following initial data extraction by the author for analysis, CCC uploaded the QEII laterals connecting the building and street-level infrastructure pipes as part of an update to the WFS feed (due to the site being owned by CCC who also manage the 3 Waters network WFS feed). The update to the WFS feed provided the comparison with the BIM model in the identification of geospatial projection conversion issues discussed above, but it also emphasised the need to include a date stamp or identifier to alert the user of the data’s age within *Bruce,* especially when undertaking analysis.

5.2.2. Completeness of Data

As described in Section 4.2.1, CCC provided partial as-built BIM data, limited to most of the main QEII building, the wastewater network, and an isolated potable water pipe exiting the building (but not connected to any other potable lateral). Through liaison and coordination with the designers (architects, engineers, etc.) of the QEII sports and recreation centre, the remaining missing BIM data were obtained; however, this was in .pdf format comprising 2D plans of the 3 Waters network. From this, 3D models of remaining omitted 3 Waters network data were created (Section 4.2.1). This process led to many challenges such as accurate scaling and rotating of.pdf plans in VEA, which was the likely cause for many of the offsets/orientation issues shown in Figure 4-8. Similarly, as part of the manual drawing process, the pipes were not drawn with their corresponding depths (however, this information was contained within the depth metadata for the model). Therefore, visually this may contribute to pipes breaching the surface, as highlighted in Section 5.2.1. This process strayed from the workflow, as per Figure 3-7. “Business as usual” would comprise the provision of all project-related horizontal and vertical infrastructure in a georeferenced as-built BIM. This would be provided at the first level of the workflow, as part of the consenting process.

Until such time when BIM data contains a geographical projection, such as IFC4 (BuildingSMART, n.d.-a), in a national mandate for building consent applications, the methodology for providing a georeferenced location will continue to be a semi-manual process (as demonstrated by the method described in Sections 4.2.1 and 4.2.3).

5.2.3. Implementation of Workflow and Analysis

Prior to implementing the analysis, the.csv file from the WFS feed was in an unsuitable format for *Bruce* and the SLM, as described in Section 4.2.2. For the SLM analysis, the exported .csv file from *Bruce* required each coordinate pair to be assigned a ptID and Pipe ID (Figure 4-10). Once this was achieved, the amended .csv file was in a format suitable for use in the SLM.

As previously stated in Section 3.3.1 , the SLM is unable to model potential breaks at the building/lateral connection (identified by the red circle in Figure 4-8). A potential modification to the SLM in order to undertake analysis on these connections is discussed further in Section 5.4. However, based on the available literature in Appendix B, there is limited information on the performance of these connections during the CES, making it difficult to replicate in the SLM. The most likely source of available information relating to this performance will be in the earthquake damage engineering reports associated with each building.

Once analysis had been completed in the SLM, the final phase of the workflow in Figure 3-7 demonstrates the integration of results back into *Bruce* for review, and highlights the ability of *Bruce* to serve as a centralised research repository. However, the outputs from the SLM were in a .shp format, one not currently supported in *Bruce* and so conversion of these files to the .kml file extension was required and undertaken in QGIS (V3.4.4-Madeira) and ArcGIS. Similar to the process required for the WFS feed conversion to a .kml extension (Section 4.2), the outputs from the SLM were in the NZTM geographic projection but through conversion to .kml were translated to the WGS84 projection, prior to upload to *Bruce.* The report by Kenley and Harfield (2018) has explored the use of virtual location hubs as a means of overcoming this issue of multiple projections, along with integration of location data from topological, geospatial, and geometric sources, whilst negating the need for asset users to undertake significant modifications to their “business-as-usual” processes. The research by Kenley and Harfield (2018) relates predominantly to roads and horizontal infrastructure, but the application of its use with BIM is also discussed. This concept is explored further in Section 5.4.1 as an improvement/modification to *Bruce*.

During the timeframe of this thesis research, there was significant development and improvements made to *Bruce*, based on the usability and implementation of the workflow from Figure 3-7. Improvements included overcoming some of the initial limitations with *Bruce,* such as the ability to upload the .kml outputs from the SLM analysis back into *Bruce* (Figur and Figure 4-15). However, the main benefit to real-time development of *Bruce* during this thesis was the ability to perform live trials of schema layouts and relationship mapping, through identification of key IFC metadata fields within the QEII BIM data, such as those shown in Figure 3-6. When reviewing the various metadata fields, consideration was given to other possible schema layouts that could be adopted for different analyses to the SLM undertaken in this thesis. These concepts are discussed further in Section 5.4.2.

The challenges and subsequent methodologies required to overcome these challenges, as discussed in the preceding three sections, are due to incomplete BIM data at the time of this thesis. Because there is no national mandate for BIM, unlike in parts of Europe and Asia, there is inconsistency between consent documentation within both CCC and across New Zealand. Similar steps are being taken in New Zealand to those countries already with a mandate, with development of The New Zealand BIM Handbook (BIM Acceleration Committee, 2016), but currently this is the extent of nationalising a standard of practice. Once these protocols and requirements are enforced, the need to manually add data, as was required for this thesis, would be negated.

5.3. Implications for Urban Resilience

One of the fundamental benefits identified through this work is how a city-wide digital twin presents the opportunity for digital integration of a city's assets into a single-source viewing platform such as *Bruce*, and integration of both risk and resilience frameworks. The examples of analysis shown in Figure 3-7 demonstrate how a digital twin allows for cataloguing and assessment of a city's as-built infrastructure taxonomy (assuming the databases are maintained) with a focus on the associated interdependency matrices (Figure 1-2). In parallel to this and as part of the post-disaster matrix assessment, *Bruce* provides the ability to manipulate the ontology of a city's building/infrastructure for use in a cost-benefit analysis of improvements to critical systems and lifelines as part of operations and maintenance budgeting, whilst modelling the impact of high risk, low probability events (Section 1.2.2).

The applicability of the data in *Bruce* and the various analyses that can be conducted is not just limited to academic researchers and asset managers for urban resilience assessment. Other stakeholders include:

- The Insurance Council who could assess liability to aid with premiums calculations,
- Infrastructure lifelines groups, the MCDEM, and emergency services for hazard response and route planning.
- All building consent authorities (if the platform was held nationally) as a national repository of all building consents.

Urban resilience is not just limited to seismic hazards, and as discussed in Section 2.2.5.3 and demonstrated by the workflow, any combination of datasets can be extracted from the digital twin of Christchurch in *Bruce*. Equally, other datasets can be imported. For example, tide information could be included and this, exported with finished floor heights of buildings, could be used in flood and sea-level rise analysis with the results imported back into *Bruce* as a visual input showing affected properties. Similar visuals and analyses could also be developed for tsunami and storm events.

5.4. Model Refinements and Future Work

This thesis has developed and demonstrated the implementation of a geospatial workflow that integrates digital technologies for use in assessing urban resilience. The integrated platform's ability to visualise and store these datasets, and to their use in external analysis, shows significant potential with the results of the SLM analysis. This highlights the usefulness and ease of having the latest available data in a centralised location. However, the SLM is a representation of just one form of analysis that can be undertaken using a subset of data contained within *Bruce*. This research also shows how the *Bruce* UI can be customised for how data are accessed and displayed (or hidden) depending on, user requirements, project scope/objective, and security (e.g. privacy restrictions, read/write privileges). The following sections present areas of ongoing improvement to *Bruce* from its initial first version, as well as proposed topics of research that could utilise the capabilities that *Bruce* has.

5.4.1. Improvements to *Bruce*

The workflow developed in this research enables an array of analyses to be conducted, utilising any combination of data contained within *Bruce*. Presently, data in *Bruce* are limited to vertical and horizontal infrastructure in both BIM and GIS formats, (the latter limited to the 3 Waters network outside of private laterals) as used in Chapter 4. The first step to producing a complete digital twin of a city is to ensure all infrastructure is represented in *Bruce*, including the electrical distribution networks, telecommunications, and roads. As discussed in Appendix A, ownership and management of the horizontal infrastructure varies between purely government-owned and partially/fully privatised. Therefore, coordination, "buy-in," and any intellectual property or security protocols need to be carefully considered as part of the integration and ongoing ownership of *Bruce*.

The analysis undertaken by Bellagamba et al. (2018a; 2018b) utilised ground motion data and geotechnical parameters (CRR and LSI) from secondary sources (currently unavailable in *Bruce)*, that are only applicable to Christchurch. However, research by Grasso and Maugeri (2003) demonstrated the means of assessing the seismic geotechnical hazard of historical buildings by using the nearest available geotechnical data (taken from a dataset of 910 boreholes). An area of future development for *Bruce,* utilising both the work by Grasso and Maugeri (2003) and the comprehensive New Zealand Geotechnical Database (NZGD, 2016), might include the integration of data from the NZGD in order to be able to perform similar analysis, anywhere in New Zealand where such data are available.

A proposed QA methodology for *Bruce* could utilise evolving artificial intelligence (AI) technologies, which include the ability to perform verification/error identification analysis of BIM models whereby erroneous features such as “vertical floors” and structural beams with no function are identified (L. Ross, personal communication, October 4, 2018). This could be implemented into *Bruce* as a means of quickly identifying errors for large volumes of data over a wide area, for example identifying all unconnected pipes, or infrastructure clashes where building elements intersect (i.e. a potable water pipe passing through a wastewater pipe because depths of the two have been incorrectly entered).

Similarly, as part of the QA process within *Bruce*, contractors and subcontractors could be provided the means to update as-built data in *Bruce,* whilst undertaking a works order for maintenance to a buried utility. Contractor/subcontractor-specific profiles (a feature which is already present in *Bruce*) could be assigned and either data are updated directly into *Bruce* via desktop computer or, through the development of a smartphone/tablet-based app, data are populated whilst on site and submitted with a geospatially referenced location to *Bruce.* Once data have been uploaded, there is then the option of notifying the *Bruce* account owner (such as CCC) of new/updated data for review prior to release into *Bruce*. Alternatively, the data would seamlessly *update Bruce* directly from the app, but still notify the account owner of the new data for them to verify and amend accordingly.

As previously noted in Section 4.2, there were some completeness and accuracy issues relating to the Coordinate Reference Systems (CRS) used between the different datasets and a predominantly manual process was required in order to collate them in *Bruce*. NextSpace Ltd. have proposed to soon embed a tool in *Bruce* that can either autonomously recognise all input geographic coordinates and convert to WGS84, or have the user select the input reference system prior to conversion. Concerning BIM data, to geospatially reference these data, at least one known coordinate will be required. Section 2.2.4.2 discussed the development of IFC4, which includes new fields for geospatial referencing ("IfcGeographicElement" and "IfcGeographicElementType") which, if implemented, would assist with the integration of a BIM model into *Bruce*. However, to geospatially reference all elements of a BIM model, either all elements will require the "IfcGeographicElement" and "IfcGeographicElementType" fields to be populated, or the use of a secondary tool to translate geometric data into geospatial, similar to the research by Kenley and Harfield (2018) and Deng *et al.* (2016).

Still to be identified as a mandated requirement of an as-built BIM model are metadata standards associated with fittings/valves connecting the building to private laterals, categorised as exterior nodes by Hijazi *et al.* (2011) and mapped in GIS by Schultz (2012) (However, the latter were grouped to the relevant pump station and not given their own referenced individual entity). This may appear a trivial component to a BIM model designer/contractor. However, as shown by the analysis in this thesis and discussed further in the following section, these metadata become vital in a modified SLM analysis of city-wide urban resilience for service loss due to breaks at these connections.

Finally, a more commercially-based use potentially applicable from an integrated tool such as *Bruce* would utilise the accurate subsurface infrastructure network information as a pre-excavation safety tool. For those undertaking operation and maintenance works to subsurface infrastructure, conventionally requests are submitted for generally outdated and incomplete 2D plans. By licensing read-only access to works-specific data within *Bruce*, the degree of risk for a service strike is reduced. It is acknowledged that this would not negate the need to do on-site assessment, such as ground penetrating radar, but would provide additional confidence in pre-excavation health and safety management plans. Additionally, accountability would be a significant consideration if damage to a utility were to occur. The benefit of *Bruce* is that it is fully auditable as to when data were uploaded and by whom, linking this back to the proposed future improvement relating to contractors/subcontractors updating data whilst on-site through use of an app.

5.4.2. Future Research Utilising *Bruce*'s Capabilities

For transparency, the following recommended research topics are designed to use the existing/proposed data housed within *Bruce* and that *Bruce's* functionality should be treated as a data portal, not a computational engine.

As described in the preceding section, the methodology by Bellagamba *et al*. (2018a; 2018b) utilises a Christchurch-specific geotechnical performance metric in the SLM. In order to modify this analysis and make it applicable to other parts of New Zealand or internationally, a different ground condition parameter would be required. To achieve this, ground investigation data from the NZGD and other data, such as the PGA/PGV data from Section 2.3.3.1, could be linked to *Bruce* (using the method in Figure 3-3). This would provide the ability to export both datasets from *Bruce*, and undertake citywide liquefaction analysis (in an external computational engine) for the 22nd February 2011 Christchurch Earthquake. By adopting a similar method as Grasso and Maugeri (2003), of utilising the nearest geotechnical and PGA/PGV data to each object (e.g. building or utility), predicted liquefaction-induced settlement could be calculated. In addition to this, the data contained within BIM models and WFS feeds would allow a more accurate determination of embedment depth of pipes which in turn, with geotechnical investigation data (e.g. CPTS, boreholes, test pits) would enable targeted liquefaction analysis of critical embedment zones. From this, a new series of fragility functions would be derived using the remaining parameters from the SLM (Section 3.2) and tested against both the observed and simulated failure rate from Figure 3-1. If this methodology demonstrates a better correlation, then a series of simulations could be modelled for an AF8 event utilising ongoing research (MCDEM, 2019). Presently, both the original SLM and the proposed modified SLM do not account for lateral spreading and so further research would be required to determine how this could be factored into modelling, as it was a known issue in the horizontal infrastructure during the CES (Appendix B).

Applying as-built foundation data contained within *Bruce* and combining with the proposed liquefaction analysis above, a similar set of city-wide fragility functions could be derived for building performance, leveraging off data gathered on building performance during the CES (Section B.2 Henderson, 2013). Again, if this is proven to model observed performance with an acceptable degree of accuracy, then as per the recommendation for AF8 scenario analysis of horizontal infrastructure, the same could be applied to vertical infrastructure utilising all BIM-derived as-built foundation data in *Bruce*. Building foundation performance using AF8 ground motion with the integrated CPT and borehole data in *Bruce* could produce liquefaction susceptibility maps for Christchurch, with a focus on the critical foundation embedment zones. Combining this analysis with the known/estimated building foundation embedment depth from the BIM data, would provide the ability to model building foundation performance for a simulated event with respect to liquefaction-induced bearing capacity failure. It is acknowledged that currently in Christchurch, there are very few examples of as-built BIM models for commercial structures and none identified for residential buildings, so performing this type of analysis presently is in its infancy. It is also recognised that generally this would only be available to new builds that have BIM models generated. However, whilst there are examples of retrospective BIM models being generated for existing structures using 3D scanner technologies and point clouds (Centofanti *et al.*, 2011; Dore and Murphy, 2012; InteliBuild, 2016; Yang *et al.*, 2012), these only provide representations of above-ground superstructures. Unless invasive investigations are carried out to determine the foundation characteristics, these would have to be assumed in any analysis. The same also applies for buried lifeline systems and it is recognised that the costs associated with retrospective data collection for an entire city's network is likely to be a very costly exercise.

Combining the analysis for foundation performance with the recommended improvement to *Bruce* for building to lateral connections, as per the research by Hijazi *et al.* (2011), would provide the means to model service loss due to building movement at these connections, and where there are physical breaks within the horizontal infrastructure networks. Research would be required into retrospectively categorising the types of failures that occurred at the building/lateral connections for particular earthquake events during the CES. However, this is very difficult to assess, as it is highly unlikely that this type of damage and performance information is readily available at an individual building level. An alternative methodology might include determining the yield point of various material or connection types, and testing magnitudes of deflection when subjected to varying degrees of shaking. Again, this carries a high degree of uncertainty due to the inability to compare with observed performance during the CES. In the event that a suitable model is developed, citywide analysis could be conducted using the various integrated datasets within *Bruce*. For example, a simplistic model could analyse that if predicted settlement of building/lateral connection "A" is X mm, and X mm>Y mm, where Y is the maximum degree of deflection for connection type "B", then pipe connection fails = loss of service. All connection types could be classified using the BIM data whereby they are mapped to a schema that identifies them as "exterior nodes" in line with Hijazi *et al.* (2011).

A secondary function of mapping/classifying all exterior nodes is the ability to undertake urban resilience modelling for various hazard or service outage scenarios. For example, if a fully realised digital twin of a city were able to identify affected buildings from a break in the network immediately adjacent to a pump station, this would provide the means to identify suburbs/regions/streets at highest risk according to the size and characteristics of the affected population.

The above proposed research topics are focussed on the currently available digital twin data within *Bruce* in both a BIM and GIS format and the SLM analysis method, which has focussed on the potable network performance. As discussed throughout this thesis, there is published and ongoing research into the performance of the other horizontal infrastructure networks such as telecommunications, electrical distribution networks, and wastewater (Cavalieri *et al.*, 2014a; Cavalieri *et al.*, 2014b; Cubrinovski *et al.*, 2014; Giovinazzi *et al.*, 2011; Kwasinski *et al.*, 2014; Massie and Watson, 2011; New Zealand Lifelines Council [NZLC], 2017; O'Rourke *et al.*, 2012). Once the digital representations of these networks are included in a platform such as *Bruce*, similar integrated analyses can be conducted for these datasets. Equally, whilst this thesis has concentrated on seismic analysis of the built environment with respect to urban resilience, *Bruce* lends itself as a tool for alternative hazard analysis such as river and surface flooding, tsunami and sea-level rise, along with impacts of technological failures.

Finally, one of the overarching benefits of *Bruce*, combining all the above improvement and future research suggestions, is how it can be used as a highly detailed asset management tool. Along with assessment of assets, *Bruce* is also able to model the performance in response to various hazard analyses through being able to query and filter data geospatially. Whilst this may already be achievable in pure GIS environments, *Bruce* differs in its highly detailed 3D environment, providing an almost lossless BIM model in a geospatial environment. This was demonstrated in the case study where the BIM data for QEII had private lateral connection data, providing a direct linkage between privately and publicly owned assets.

5.5. Concluding Remarks

This thesis has made a methodological contribution to digital engineering and urban resilience assessment with a focus on seismic hazards by demonstrating a workflow for integrating different infrastructure datasets into a single-source platform and analysing their performance during the 22nd February 2011 Christchurch Earthquake.

The fundamental concern with analysis on a large scale such as this is quality and accuracy of data entered into the model. The benefits to having regional or national government maintaining a city/national digital twin include their resources such as in-house expertise (GIS experts and building consent officers who would be reviewing the BIM mandated consent data), and that regional and district councils own much of the horizontal infrastructure assets, making it easier to integrate with platforms such as *Bruce*. However, in order to "build" an accurate digital twin, vast amounts of data need to be collated into a single viewing/analysis platform, a task that could be problematic when coordinating external stakeholders.

This leads into the next biggest challenge, which will be buy-in from the other infrastructure asset owners such as electrical distribution and telecommunications. *Bruce* has demonstrated that it can provide secure linkages to source data, but hesitation to contribute data may arise from encroaching into the realms of sensitive/confidential information. However, the uniqueness of a tool such as *Bruce* is its adaptability and ability to be tailored on an individual account, user, and project basis. Since *Bruce* has the means to map relationships to the source data (such as the WFS feed) whilst also storing some data on its own cloud-based storage facilities, project and/or user-specific UIs and access/editing rights can be assigned, maintaining security and accountability. Equally, the benefits to a collaborative and single integrated platform containing all vertical and horizontal infrastructure data are demonstrated by the analysis undertaken in this thesis. Using just one of the lifeline systems connected to a single building in the model, and illustrating the ease of extracting integrated data and how to analyse loss of service during a seismic event, highlights the capabilities of *Bruce* and its other potential applications. *Bruce* can be used as an asset management modelling tool for assessing asset degradation of an entire network, or identify the weakest areas of the network that could benefit from being repaired or upgraded, and provide confidence in cost as part of operations and maintenance budgeting.

The response by emergency services, MCDEM, and the efforts of the utilities companies to restore service in the wake of an event such as the CES was testimony to the rapid recovery of those key lifeline facilities. However, one of the key observations was the delay in visible manifestation of a network break, particularly in the electrical distribution network, and the deeply embedded 3 Waters infrastructure (predominantly wastewater). Therefore, as a means of modelling urban resilience, the performance of Christchurch during a magnitude 8.0 M_w earthquake (such as an Alpine Fault type event;MCDEM, 2019) could be conducted in multiple computational engines, utilising any number of the data sources in *Bruce.* The data exported from *Bruce*, combined with the vast damage records collected during the CES, could be used to develop a range of fragility functions, providing the ability to assess the as-built infrastructures expected performance during an AF8 type event.

At present both the SLM and *Bruce* are specific to Christchurch, particularly the SLM as it uses a geotechnical parameter only applicable to Christchurch. As discussed in this thesis, the model could be revised to utilise non-geographic specific parameters such as predicted liquefaction-induced settlement, which would allow fragility functions to be developed for other major populated centres both domestically and internationally, provided similar datasets were either already available, or able to be collected prior to an event occurring.

References

"67 Important GIS Applications and Uses". (2015). 67 Important GIS Applications and Uses. Retrieved from https://grindgis.com/blog/gis-applications-uses

"About Level of Details". (2016). About Level of Details. Retrieved from http://semanti.city/tag/level-of-detail/#prettyPhoto

"Citygml wiki". (2017). Citygml wiki - Basic Information. Retrieved from http://www.citygmlwiki.org/index.php?title=Basic_Information

"Major areas of GIS application". (n.d.). 1-6 Area of GIS Applications. Retrieved from http://wtlab.iis.u-tokyo.ac.jp/wataru/lecture/rsgis/giswb/vol1/cp1/cp1-6.htm

"Marvelous Design Revit House Plans..." (Producer). (2018). Marvelous Design Revit House Plans Download Free Download CAD Or PDF Arch10A3343. [Image] Retrieved from http://thisabundantlifeblog.com/55928/revit-house-plans-download-free/marvelous-design-revit-house-plans-download-free-download-cad-or-pdf-arch10a3343/

AIA. (2019). *G202-2013, Building Information Modeling Protocol Form*. Retrieved from https://www.aiacontracts.org/contract-documents/19016-project-bim-protocol

Aien, A., Rajabifard, A., Kalantari, M., & Shojaei, D. (2015). Integrating legal and physical dimensions of urban environments. *ISPRS International Journal of Geo-Information, 4*(3), 1442-1479.

Al-Kasisbeh, M. R., & Abudayyeh, O. (2018). *Municipality Asset Management: Asset Types and Effective Management Decision Using GIS*. Paper presented at the Construction Research Congress 2018: Infrastructure and Facility Management, New Orleans, Louisiana.

Alirezaei, M., Noori, M., Tatari, O., Mackie, K. R., & Elgamal, A. (2016). BIM-based damage estimation of buildings under earthquake loading condition. *Procedia Engineering, 145*, 1051-1058.

Amirebrahimi, S., Rajabifard, A., Mendis, P., & Ngo, T. (2015). A data model for integrating GIS and BIM for assessment and 3D visualisation of flood damage to building. *Locate, 15*(2015), 10-12.

Anthopoulos, L. G., & Fitsilis, P. (2010). *From digital to ubiquitous cities: Defining a common architecture for urban development*. Paper presented at the Sixth International Conference on Intelligent Environments Kuala Lumpur, Malaysia.

Anthopoulos, L. G., & Tsoukalas, I. A. (2006). The implementation model of a Digital City. The case study of the Digital City of Trikala, Greece: e-Trikala. *Journal of e-Government, 2*(2), 91-109.

Apollo Projects (Producer). (2018). Taiora: QEII official opening! [photograph] Retrieved from https://www.apolloprojects.co.nz/news/taiora-qeii-opens-today

Autodesk. (2018). What is BIM? Retrieved from https://www.autodesk.com/solutions/bim

Baratin, L., Chamberlain, C. J., Townend, J., & Savage, M. K. (2018). Focal mechanisms and inter-event times of low-frequency earthquakes reveal quasi-continuous deformation and triggered slow slip on the deep Alpine Fault. *Earth and Planetary Science Letters, 484*, 111-123.

Barbat, A. H., Carreño, M. L., Pujades, L. G., Lantada, N., Cardona, O. D., & Marulanda, M. C. (2010). Seismic vulnerability and risk evaluation methods for urban areas. A review with application to a pilot area. *Structure and Infrastructure Engineering, 6*(1-2), 17-38.

Barclay, S. (2010, September 27). 8 Natural Disasters of Ancient Times. Retrieved from https://listverse.com/2010/09/27/8-natural-disasters-of-ancient-times/

Becerik-Gerber, B., Jazizadeh, F., Li, N., & Calis, G. (2011). Application areas and data requirements for BIM-enabled facilities management. *Journal of construction engineering and management, 138*(3), 431-442.

Bellagamba, X., Bradley, B. A., Wotherspoon, L. M., & Hughes, M. W. (2018a). *Development of fragility functions for buried pipelines based on New Zealand data.* Paper presented at the 16th European Conference on Earthquake Engineering, Thessaloniki, Greece.

Bellagamba, X., Bradley, B. A., Wotherspoon, L. M., & Lagrava, W. D. (2018b). A decision-support algorithm for post-earthquake water services recovery and its application to the 22 February 2011 M_w 6.2 Christchurch earthquake. *Submitted for publication*, 10.

Bhamidipati, S., van der Lei, T., & Herder, P. (2016). A layered approach to model interconnected infrastructure and its significance for asset management. *European Journal of Transport and Infrastructure Research, 16*(1), 254-272.

BIM Acceleration Committee. (2016). *The New Zealand BIM Handbook: A guide to enabling BIM on building projects (2nd ed.)*. Retrieved from https://www.biminnz.co.nz/bim-tools/

BIMForum. (2018). *Level of Development (LOD) Specification Part I & Commentary: For Building Information Models and Data - Public Comment Draft*. Retrieved from https://bimforum.org/lod/

Börner, K. (2002). Twin Worlds: Augmenting, Evaluating, and Studying Three-Dimensional Digital Cities and Their Evolving Communities. In M. Tanabe, P. Van den Besselaar, & T. Ishida (Eds.), *Digital Cities II: Computational and Sociological Approaches* (pp. 257-269). Germany: Springer.

Bouziou, D., & O'Rourke, T. D. (2017). Response of the Christchurch water distribution system to the 22 February 2011 earthquake. *Soil Dynamics and Earthquake Engineering, 97*, 14-24.

Boyes, G., Ellul, C., & Irwin, D. (2017). *Exploring BIM for Operational Integrated Asset Management-A Preliminary Study Utilising Real-world Infrastructure Data*. Paper presented at the ISPRS Annals of the Photogrammetry, Remote Sensing and Spatial Information Sciences.

Bradley, B. A., & Hughes, M. W. (2012a). Conditional Peak Ground Accelerations in the Canterbury Earthquakes for Conventional Liquefaction Assessment–Technical Report for the Ministry of Business. *Innovation and Employment Department of Building and Housing Te Tari Kaupapa Whare*, 22.

Bradley, B. A., & Hughes, M. W. (2012b). *Conditional Peak Ground Accelerations in the Canterbury Earthquakes for Conventional Liquefaction Assessment: Part 2*. Retrieved from Christchurch New Zealand:

Bradley, B. A., Quigley, M. C., Van Dissen, R. J., & Litchfield, N. J. (2014). Ground Motion and Seismic Source Aspects of the Canterbury Earthquake Sequence. *Earthquake Spectra, 30*(1), 1-15. doi:10.1193/030113eqs060m

Brown, L. J., & Weeber, J. H. (1992). *Geology of the Christchurch Urban Area:-Scale 1: 25,000*: Institute of Geological & Nuclear Sciences.

Bruneau, M., Anagnostopoulou, M., MacRae, G., Clifton, C., & Fussell, A. (2010). Preliminary report on steel building damage from the Darfield earthquake of September 4, 2010. *Bulletin of the New Zealand Society for Earthquake Engineering, 43*(4), 351-359.

Bruneau, M., Chang, S. E., Eguchi, R. T., Lee, G. C., O'Rourke, T. D., Reinhorn, A. M., Shinozuka, M., Tierney, K., Wallace, W. A., & Von Winterfeldt, D. (2003). A framework to quantitatively assess and enhance the seismic resilience of communities. *Earthquake Spectra, 19*(4), 733-752.

Buchanan, A., Carradine, D., Beattie, G., & Morris, H. (2011). Performance of houses during the Christchurch earthquake of 22 February 2011. *Bulletin of the New Zealand Society for Earthquake Engineering, 44*(4), 342-357.

Buchanan, A., & Newcombe, M. (2010). The performance of residential houses in the Darfield (Canterbury) earthquake. *Bulletin of the New Zealand Society for Earthquake Engineering, 43*(4), 387-392.

BuildingSMART. (n.d.-a). IFC4. Retrieved from http://www.buildingsmart-tech.org/ifc/IFC4/final/html/link/ifcbuildingelement.htm

BuildingSMART. (n.d.-b). Technical Vision. Retrieved from https://www.buildingsmart.org/standards/technical-vision/

Cavalieri, F., Franchin, P., Buritica, A. M., Cortes, J., & Tesfamariam, S. (2014a). Models for Seismic Vulnerability Analysis of Power Networks: Comparative Assessment. *Computer-Aided Civil and Infrastructure Engineering, 29*(8), 590-607. doi:10.1111/mice.12064

Cavalieri, F., Franchin, P., & Pinto, P. E. (2014b). Fragility Functions of Electric Power Stations. In K. Pitilakis, H. Crowley, & A. M. Kaynia (Eds.), *SYNER-G: Typology Definition and Fragility Functions for Physical Elements at Seismic Risk: Buildings, Lifelines, Transportation Networks and Critical Facilities* (pp. 157-185). Dordrecht: Springer Netherlands.

CCC. (2010). *Christchurch City Fact Pack 2010*. Retrieved from Christchurch, New Zealand: https://ccc.govt.nz/assets/Documents/Culture-Community/Stats-and-facts-on-Christchurch/fact-packs/FactPack2010-docs.pdf

CCC. (2018). Network Utility Operators. Retrieved from https://www.ccc.govt.nz/consents-and-licences/construction-requirements/network-utility-operators

CCC. (n.d.). Smart Cities Programme. Retrieved from https://www.ccc.govt.nz/the-council/future-projects/smart-cities-programme/

Centofanti, M., Continenza, R., Brusaporci, S., & Trizio, I. (2011). The Architectural Information System SIArch3D-Univaq for analysis and preservation of architectural heritage. *International Archives of the Photogrammetry, Remote Sensing and Spatial Information Sciences, 38*(5), 9-14.

Charalambos, G., Dimitrios, V., & Symeon, C. (2014). *Damage assessment, cost estimating, and scheduling for post-earthquake building rehabilitation using BIM*. Paper presented at the Computing in Civil and Building Engineering, Orlando, Florida.

Chen, L. C., Wu, C. H., Shen, T. S., & Chou, C. C. (2014). The application of geometric network models and building information models in geospatial environments for fire-fighting simulations. *Computers, Environment and Urban Systems, 45*, 1-12.

Chourabi, H., Nam, T., Walker, S., Gil-Garcia, J. R., Mellouli, S., Nahon, K., Pardo, T. A., & Scholl, H. J. (2012). *Understanding smart cities: An integrative framework.* Paper presented at the 45th Hawaii International Conference on System Science (HICSS), Hawaii.

Christchurch Engineering Lifelines Group. (1997). *Risk & realities: a multi-disciplinary approach to the vulnerability of lifelines to natural hazards* (Centre for Advanced Engineering & Christchurch Engineering Lifelines Group Eds.). Christchurch, New Zealand: Centre for Advanced Engineering, University of Canterbury

Cocchia, A. (2014). Smart and digital city: A systematic literature review. In R. P. Dameri & C. Rosenthal-Sabroux (Eds.), *Smart city* (pp. 13-43). Germany: Springer.

Combaz, E. (2014). *Disaster resilience: Topic Guide*. Birmingham, UK: GSDRC, University of Birmingham Retrieved from https://gsdrc.org/wp-content/uploads/2014/02/GSDRC_DR_topic_guide.pdf.

Couclelis, H. (2004). The construction of the digital city. *Environment and Planning B: Planning and design, 31*(1), 5-19.

Cubellis, E., & Carlino, S. (2004). Management of historical seismic data using GIS: the island of Ischia (Southern Italy). *Natural hazards, 33*(3), 379-393.

Cubrinovski, M., Bradley, B. A., Wotherspoon, L. M., Green, R. A., Bray, J., Wood, C., Pender, M., Allen, J., Bradshaw, A., Rix, G., Taylor, M., Robinson, K., Henderson, D. R. K., Giorgini, S., Ma, K., Winkley, A., Zupan, J., O'Rourke, T. D., DePascale, G., & Wells, D. (2011). Geotechnical aspects of the 22 February 2011 Christchurch earthquake. *Bulletin of the New Zealand Society for Earthquake Engineering, 44*, 205-226.

Cubrinovski, M., & Green, R. A. (2010). Geotechnical reconnaissance of the 2010 Darfield (New Zealand) earthquake. *Bulletin of the New Zealand Society for Earthquake Engineering, 43*, 243-320.

Cubrinovski, M., Hughes, M. W., Bradley, B. A., Noonan, J., Hopkins, R., McNeill, S., & English, G. (2014). *Performance of Horizontal Infrastructure in Christchurch City through the 2010-2011 Canterbury Earthquake Sequence*. Retrieved from Christchurch, New Zealand: https://ir.canterbury.ac.nz/bitstream/handle/10092/9492/12649178_Cubrinovski_CchchHorizontalInfrastructurePerformance_2014.pdf?sequence=1&isAllowed=y

Cubrinovski, M., Hughes, M. W., Bradley, B. A., Noonan, J., McNeill, S., English, G., & Sampedro, G. (2015). *Horizontal Infrastructure Performance and Application of the Liquefaction Resistance Index Methodology in Christchurch City through the 2010-2011 Canterbury Earthquake Sequence*. Retrieved from University of Canterbury Department of Civil & Natural Resources Engineering: https://ir.canterbury.ac.nz/bitstream/handle/10092/15093/Cubrinovski%20et%20al%202015.pdf?sequence=2&isAllowed=y

Cubrinovski, M., & Orense, R. (2010). 2010 Darfield (New Zealand) Earthquake-Impacts of liquefaction and lateral spreading. *Bulletin of the International Society for Soil Mechanics and Geotechnical Engineering, 4*(4), 15-23.

Cubrinovski, M., & Taylor, M. (2011). Liquefaction Map of Christchurch based on drive-through reconnaissance after the 22 February 2011 eathquake. In: University of Canterbury.

de la Torre, C., & Bradley, B. A. (2018). *Modelling Nonlinear Site Effects in Physics-Based Ground Motion Simulation*. Paper presented at the Geotechnical Earthquake Engineering and Soil Dynamics V: Seismic Hazard Analysis, Earthquake Ground Motions, and Regional-Scale Assessment, Austin, Texas, United States of America.

de Laat, R., & Van Berlo, L. (2011). Integration of BIM and GIS: The development of the CityGML GeoBIM extension. In T. H. Kolbe, G. König, & C. Nagel (Eds.), *Advances in 3D geo-information sciences* (pp. 211-225): Springer.

Deloitte Access Economics. (2015). *Four years on: insurance and the Canterbury earthquakes*. Retrieved from https://www.vero.co.nz/documents/newsroom/deloitte-vero-four-years-on-insurance-canterbury-earthquakes-report-february-2015.pdf

Deng, Y., Cheng, J. C., & Anumba, C. (2016). Mapping between BIM and 3D GIS in different levels of detail using schema mediation and instance comparison. *Automation in Construction, 67*, 1-21.

Ding, P., Lin, D., & Sheng, H. (2003). Digital City Shanghai: Concepts, Foundations, and Current State. In P. Van den Besselaar & S. Koizumi (Eds.), *Digital Cities III. Information Technologies for Social Capital: Cross-cultural Perspectives* (pp. 141-165): Springer.

Dizhur, D., Lumantarna, R., Ismail, N., Ingham, J. M., & Knox, C. (2010). Performance of unreinforced and retrofitted masonry buildings during the 2010 Darfield earthquake. *Bulletin of the New Zealand Society for Earthquake Engineering, 43*(4), 321-339.

Dore, C., & Murphy, M. (2012). *Integration of Historic Building Information Modeling (HBIM) and 3D GIS for recording and managing cultural heritage sites*. Paper presented at the 8th International Conference on Virtual Systems and Multimedia (VSMM), Milan, Italy.

Eastman, C., Lee, J. M., Jeong, Y. S., & Lee, J. K. (2009). Automatic rule-based checking of building designs. *Automation in Construction, 18*(8), 1011-1033.

Eidinger, J. M., & Tang, A. K. (2012). *Christchurch, New Zealand Earthquake Sequence of M_w 7.1 September 04, 2010 M_w 6.3 February 22, 2011 M_w 6.0 June 13, 2011: Lifeline Performance* (Vol. 41): American Society of Civil Engineers, Reston, VA.

El-Mekawy, M., Östman, A., & Hijazi, I. (2012a). An evaluation of IFC-CityGML unidirectional conversion. *International Journal of Advanced Computer Science and Applications, 3*(5), 159-171.

El-Mekawy, M., Östman, A., & Hijazi, I. (2012b). A unified building model for 3D urban GIS. *ISPRS International Journal of Geo-Information, 1*(2), 120-145.

Ergazakis, K., Metaxiotis, K., & Psarras, J. (2004). Towards knowledge cities: conceptual analysis and success stories. *Journal of knowledge management, 8*(5), 5-15.

Esri. (2018). What is GIS? Retrieved from https://www.esri.com/en-us/what-is-gis/overview

Ettouney, M. M. (Producer). (2016, 25 March 2019). Resilience and Risk Management. [Presentation slides] Retrieved from https://cdn.ymaws.com/www.nibs.org/resource/resmgr/Conference2016/BI2016_0113_ila_ettouney.pdf

Ettouney, M. M., & Alampalli, S. (2016). *Risk Management in Civil Infrastructure*. Boca Raton: CRC Press.

Fazal, S. (2008). *GIS Basics*. New Delhi, India.: New Age International Publishers.

Fosu, R., Suprabhas, K., Rathore, Z., & Cory, C. (2015). *Integration of Building Information Modeling (BIM) and Geographic Information Systems (GIS)–a literature review and future needs*. Paper presented at the Proceedings of the 32nd CIB W78 Conference, Eindhoven, The Netherlands.

Franchin, P., & Cavalieri, F. (2013). Seismic vulnerability analysis of a complex interconnected civil infrastructure. In S. Tesfamariam & K. Goda (Eds.), *Handbook of seismic risk analysis and management of civil infrastructure systems* (pp. 465-514e): Elsevier.

Giovinazzi, S., & Wilson, T. (2012). *"Recovery of Lifelines" following the 22nd February 2011 Christchurch Earthquake: successes and issues*. Paper presented at the 2012 Annual Technical Conference "Implementing Lessons Learnt", Christchurch, New Zealand. Paper 090 retrieved from https://ir.canterbury.ac.nz/bitstream/handle/10092/7297/12641200_Giovinazzi%20and%20Wilson%202012%20-%20NZSEE%20Conf%20-%20Recovery%20of%20Lifelines%20following%2022%20Feb%20EQ%20-%20successes%20and%20issues.pdf?sequence=1&isAllowed=y

Giovinazzi, S., Wilson, T., Davis, C., Bristow, D., Gallagher, M., Schofield, A., Villemure, M., Eidinger, J. M., & Tang, A. K. (2011). Lifelines Performance and Management Following the 22 February 2011 Christchurch Earthquake, New Zealand: Highlights of Resilience. *Bulletin of the New Zealand Society for Earthquake Engineering, 44*(4), 402-417.

GISGeography. (2018). The Remarkable History of GIS. Retrieved from https://gisgeography.com/history-of-gis/

GISGeography. (2019a). 1000 GIS Applications. Retrieved from https://gisgeography.com/gis-applications-uses/

GISGeography. (2019b). What is Geographic Information Systems (GIS)? Retrieved from https://gisgeography.com/what-gis-geographic-information-systems/

Grasso, S., & Maugeri, M. (2003). *A GIS model application supporting the analysis of the seismic hazard for the urban area of Catania (Italy)*. Paper presented at the Proceedings of the 13th European Conference on Soil Mechanics and Geotechnical Engineering, Geotechnical Problems with Man-made and Man Influenced Grounds, Prague.

Grasso, S., & Maugeri, M. (2009). The road map for seismic risk analysis in a Mediterranean city. *Soil Dynamics and Earthquake Engineering, 29*(6), 1034-1045.

Grignard, A., Taillandier, P., Gaudou, B., Vo, D. A., Huynh, N. Q., & Drogoul, A. (2013). *GAMA 1.6: Advancing the art of complex agent-based modeling and simulation*. Paper presented at the International Conference on Principles and Practice of Multi-Agent Systems, Dunedin, New Zealand.

Gunes, A. E., & Kovel, J. P. (2000). Using GIS in emergency management operations. *Journal of Urban Planning and Development, 126*(3), 136-149.

Hagedorn, B., & Döllner, J. (2007). Integrating urban GIS, CAD, and BIM Data by service-based virtual 3D city models. In M. Rumor, V. Coors, E. M. Fendel, & S. Zlatanova (Eds.), *Urban and Regional Data Management;* (pp. 157-170). London, UK: Taylor & Francis Group.

Hassenzahl, D. (n.d.). What do we Mean by Risk and Resilience? Retrieved from https://serc.carleton.edu/integrate/workshops/risk_resilience/what_is_rr.html

Henderson, D. R. K. (2013). *The Performance of House Foundations in the Canterbury Earthquakes.* (Master of Engineering in Civil Engineering), University of Canterbury, New Zealand. Retrieved from https://ir.canterbury.ac.nz/handle/10092/8741

Hijazi, I., Ehlers, M., Zlatanova, S., Becker, T., & van Berlo, L. (2011). Initial investigations for modeling interior Utilities within 3D Geo Context: Transforming IFC-interior utility to CityGML/UtilityNetworkADE. In T. H. Kolbe, G. König, & C. Nagel (Eds.), *Advances in 3D Geo-information sciences* (pp. 95-113): Springer.

Hughes, M. W., Quigley, M. C., Van Ballegooy, S., Deam, B. L., Bradley, B. A., & Hart, D. E. (2015). The sinking city: Earthquakes increase flood hazard in Christchurch, New Zealand. *GSA Today, 25*(3), 4-10.

Hurley, J. (2018). A Data-driven approach to asset management. Retrieved from https://www.raconteur.net/risk-management/data-driven-approach-asset-management

Institute of Public Works Engineering Australia [IPWEA], Association of Local Government Engineers of New Zealand, & NAMS. (2015). *International Infrastructure Management Manual* (5th ed.). Wellington, New Zealand: IPWEA ; NAMS Group.

InteliBuild (Producer). (2016, 21st March 2019). Laser Scanning & BIM or Scan-to-BIM. [Video file] Retrieved from https://www.youtube.com/watch?v=fqoNXUymGko

IRDR. (2013). What we do - Overview. Retrieved from http://www.irdrinternational.org/what-we-do/overview/

Irizarry, J., Karan, E. P., & Jalaei, F. (2013). Integrating BIM and GIS to improve the visual monitoring of construction supply chain management. *Automation in Construction, 31*, 241-254.

Ishida, T. (1999). Understanding digital cities. In T. Ishida & K. Isbister (Eds.), *Digital Cities: Technologies, Experiences, and Future Perspectives* (pp. 7-17): Springer.

Ishida, T., Akahani, J., Hiramatsu, K., Isbister, K., Lisowski, S., Nakanishi, H., Okamoto, M., Miyazaki, Y., & Tsutsuguchi, K. (1999). *Digital City Kyoto: Towards a social information infrastructure*. Paper presented at the 3rd International Workshop on Cooperative Information Agents, Uppsala, Sweden.

Isikdag, U., Underwood, J., & Aouad, G. F. (2008). An investigation into the applicability of building information models in geospatial environment in support of site selection and fire response management processes. *Advanced engineering informatics, 22*(4), 504-519.

Isikdag, U., & Zlatanova, S. (2009). Towards defining a framework for automatic generation of buildings in CityGML using building Information Models. In J. Lee & S. Zlatanova (Eds.), *3D geo-information sciences* (pp. 79-96): Springer.

Jiao, Y., Wang, Y., Zhang, S., Li, Y., Yang, B., & Yuan, L. (2013). A cloud approach to unified lifecycle data management in architecture, engineering, construction and facilities management: Integrating BIMs and SNS. *Advanced engineering informatics, 27*(2), 173-188.

Johnson, R. (2000). *GIS technology for disasters and emergency management*. Retrieved from https://www.esri.com/~/media/Files/Pdfs/library/whitepapers/pdfs/disastermgmt.pdf

Johnston, E. W., & Hansen, D. L. (2011). Design lessons for smart governance infrastructures. In A. P. Balutis, T. F. Buss, & D. Ink (Eds.), *Transforming American Governance: Rebooting the Public Square* (pp. 197-212): National Academy of Public Administration.

Kam, W. Y., Pampanin, S., Dhakal, R. P., Gavin, H., & Roeder, C. W. (2010). Seismic performance of reinforced concrete buildings in the September 2010 Darfield (Canterbury) earthquakes. *Bulletin of the New Zealand Society for Earthquake Engineering, 43*(4), 340-350.

Kam, W. Y., Pampanin, S., & Elwood, K. (2011). Seismic performance of reinforced concrete buildings in the 22 February Christchurch (Lyttleton) earthquake. *Bulletin of the New Zealand Society for Earthquake Engineering, 44*(4), 239-278.

Kang, T. W., & Hong, C. H. (2013). *The architecture development for the interoperability between BIM and GIS*. Paper presented at the 13th International Conference on Construction Applications of Virtual Reality, London, UK.

Kang, T. W., & Hong, C. H. (2015). A study on software architecture for effective BIM/GIS-based facility management data integration. *Automation in Construction, 54*, 25-38.

Karan, E. P., & Irizarry, J. (2014). *Developing a spatial data framework for facility management supply chains*. Paper presented at the Construction Research Congress.

Kassem, M., Kelly, G., Dawood, N., Serginson, M., & Lockley, S. (2015). BIM in facilities management applications: a case study of a large university complex. *Built Environment Project and Asset Management, 5*(3), 261-277.

Kemec, S., Zlatanova, S., & Duzgun, S. (2012). *A new LoD definition hierarchy for 3D city models used for natural disaster risk communication tool*. Paper presented at the 4th International Conference on Cartography & GIS, Albena, Bulgaria.

Kenley, R., & Harfield, T. (2018). *Scoping study for a location referencing model to support the BIM environment* (1925671550). Retrieved from https://austroads.com.au/publications/asset-management/ap-r568-18

King, A., & Bell, R. (2009). RiskScape Project: 2004-2008. *GNS Science consultancy report, 247*, 162.

Kivits, R. A., & Furneaux, C. (2013). BIM: enabling sustainability and asset management through knowledge management. *The Scientific World Journal, 2013*, 1-14.

Ko, C.-H. (2009). RFID-based building maintenance system. *Automation in Construction, 18*(3), 275-284.

Kongar, I., Giovinazzi, S., & Rossetto, T. (2017). Seismic performance of buried electrical cables: evidence-based repair rates and fragility functions. *Bulletin of Earthquake Engineering, 15*(7), 3151-3181. doi:10.1007/s10518-016-0077-3

Kurwi, S., Demian, P., & Hassan, T. M. (2017). *Integrating BIM and GIS in railway projects: A critical review*. Paper presented at the 33rd Annual ARCOM Conference, Cambridge, UK.

Kwasinski, A., Eidinger, J. M., Tang, A. K., & Tudo-Bornarel, C. (2014). Performance of Electric Power Systems in the 2010–2011 Christchurch, New Zealand, Earthquake Sequence. *Earthquake Spectra, 30*(1), 205-230. doi:10.1193/022813eqs056m

Landis, P. (n.d.). 28 Uses of GIS Technology. Retrieved from https://360hr.com.au/28-uses-of-gis-technology/

Lapierre, A., & Cote, P. (2007). *Using Open Web Services for urban data management: A testbed resulting from an OGC initiative for offering standard CAD/GIS/BIM services*. Paper presented at the Urban and Regional Data Management. Annual Symposium of the Urban Data Management Society, Stuttgart, Germany.

Layfield, F. H. B., & Great Britain. Dept. of Energy. (1987). *Sizewell B public inquiry: report*: Her Majesty's Stationary Office.

Li, G., Zhao, J., Murray, V., Song, C., & Zhang, L. (2019). Gap analysis on open data interconnectivity for disaster risk research. *Geo-spatial Information Science*, 1-14.

Linkov, I. (Producer). (2015, 25 March 2019). Risk vs. Resilience: Similarities and Differences. [Presentation slides] Retrieved from https://www.agci.org/sites/default/files/pdfs/lib/main/RiskResiliencAspenDec15Distr.pdf

Linkov, I., Bridges, T., Creutzig, F., Decker, J., Fox-Lent, C., Kröger, W., Lambert, J. H., Levermann, A., Montreuil, B., & Nathwani, J. (2014). Changing the resilience paradigm. *Nature Climate Change, 4*(6), 407-409.

Linturi, R., Koivunen, M., & Sulkanen, J. (2000). Helsinki Arena 2000-Augmenting a Real City to a Virtual One. In T. Ishida & K. isbister (Eds.), *Digital Cities* (pp. 83-96): Springer.

Linturi, R., & Simula, T. (2003). Virtual Helsinki: Enabling the Citizen, Linking the Physical and Virtual. In P. Van den Besselaar & S. Koizumi (Eds.), *Digital Cities III. Information Technologies for Social Capital: Cross-cultural Perspectives* (pp. 113-140): Springer.

LINZ. (2016). *Smart Cities Strategic Assessment*. Retrieved from https://www.linz.govt.nz/system/files_force/media/doc/sdp_smart-cities_strategic-assessment_20161214.pdf?download=1

LINZ. (2017). Smart Cities. Retrieved from https://www.linz.govt.nz/about-linz/what-were-doing/projects/smart-cities

Liu, M. (2016). *Decision Support Framework for Post-earthquake Restoration of Sewerage Pipelines and Systems.* (Doctor of Philosophy in Civil Engineering), University of Canterbury, New Zealand. Retrieved from https://ir.canterbury.ac.nz/handle/10092/12802

Liu, R., & Issa, R. R. A. (2012). 3D visualization of sub-surface pipelines in connection with the building utilities: Integrating GIS and BIM for facility management. In R. R. A. Issa & I. Flood (Eds.), *Computing in Civil Engineering* (pp. 341-348).

Liu, X., Wang, X., Wright, G., Cheng, J. C. P., Li, X., & Liu, R. (2017). A state-of-the-art review on the integration of Building Information Modeling (BIM) and Geographic Information System (GIS). *ISPRS International Journal of Geo-Information, 6*(2), 21.

Ma, Z., & Ren, Y. (2017). Integrated Application of BIM and GIS: An Overview. *Procedia Engineering, 196*, 1072-1079.

Massie, A. (2011). Weeks 4-7: The February 22nd 2011 M6.3 earthquake and the start of the repair of the Christchurch distribution network. Retrieved from http://thunderboltnz.blogspot.co.nz/2011/03/weeks-4-7.html

Massie, A., & Watson, N. R. (2011). Impact of the Christchurch earthquakes on the electrical power system infrastructure. *Bulletin of the New Zealand Society for Earthquake Engineering, 44*(4), 425-430.

MBIE. (2012). *Repairing and rebuilding houses affected by the Canterbury earthquakes*. Retrieved from Wellington, New Zealand: https://www.building.govt.nz/building-code-compliance/canterbury-rebuild/repairing-and-rebuilding-houses-affected-by-the-canterbury-earthquakes/

MCDEM. (2016). *Civil Defence Emergency Management Amendment Act*. New Zealand.

MCDEM. (2019). Project AF8. Retrieved from https://projectaf8.co.nz/

Mignard, C., & Nicolle, C. (2014). Merging BIM and GIS using ontologies application to urban facility management in ACTIVe3D. *Computers in Industry, 65*(9), 1276-1290. doi:https://doi.org/10.1016/j.compind.2014.07.008

Ministry of Civil Defence and Emergency Management [MCDEM]. (2018). *National Disaster Resilience Strategy - Draft for Consultation*. New Zealand.

Mooij, J. E. (2003). Smart Governance?: Politics in the Policy Process in Andhra Pradesh, India. *Overseas Development Institute Working Papers, 228*, 28p. Retrieved from https://www.odi.org/sites/odi.org.uk/files/odi-assets/publications-opinion-files/2464.pdf

Nam, T., & Pardo, T. A. (2011). *Conceptualizing smart city with dimensions of technology, people, and institutions*. Paper presented at the Proceedings of the 12th annual international digital government research conference: digital government innovation in challenging times.

Nath, S. K. (2005). An initial model of seismic microzonation of Sikkim Himalaya through thematic mapping and GIS integration of geological and strong motion features☆. *Journal of Asian Earth Sciences, 25*(2), 329-343.

New Zealand Government. (2018). Smart Wellington. Retrieved from https://www.digital.govt.nz/showcase/smart-wellington

New Zealand Lifelines Council [NZLC]. (2017). *New Zealand Lifelines Infrastructure Vulnerability Assessment: Stage 1*. Retrieved from https://www.civildefence.govt.nz/assets/Uploads/lifelines/National-Vulnerability-Assessment-Stage-1-September-2017.pdf

New Zealand Standards. (2009). AS/NZS ISO 31000:2009. In *risk management*. Wellington, New Zealand: MBIE.

New Zealand Standards. (2011). NZS 3604:2011 In *Timber Framed Buildings* (pp. 447). Wellington, New Zealand.

Nextspace Limited (2018, 11 October). [personal communication]. Smart City Data Management.

Niu, S., Pan, W., & Zhao, Y. (2015). A BIM-GIS integrated web-based visualization system for low energy building design. *Procedia Engineering, 121*, 2184-2192.

NZGD. (2016). New Zealand Geotechnical Database. Retrieved from https://www.nzgd.org.nz/HelpSupport/AboutNZGD.pdf.

O'Rourke, T. D., Jeon, S. S., Toprak, S., Cubrinovski, M., Hughes, M. W., Van Ballegooy, S., & Bouziou, D. (2014). Earthquake Response of Underground Pipeline Networks in Christchurch, NZ. *Earthquake Spectra, 30*(1), 183-204. doi:10.1193/030413eqs062m

O'Rourke, T. D., Jeon, S. S., Toprak, S., Cubrinovski, M., & Jung, J. K. (2012). *Underground lifeline system performance during the Canterbury earthquake sequence*. Paper presented at the 15th World Conference on Earthquake Engineering, Lisbon, Portugal.

Orense, R., Kiyota, T., Yamada, S., Cubrinovski, M., Hosono, Y., Okamura, M., & Yasuda, S. (2011). Comparison of liquefaction Features observed during the 2010 and 2011 Canterbury earthquakes. *Seismological Research Letters, 82*(6), 905-918. doi:10.1785/gssrl.82.6.905

Orion. (2010). *Asset Management Plan: a 10-year management plan for Orion's electricity network from 1 April 2010 to 31 March 2020*. Retrieved from http://www.oriongroup.co.nz/assets/Company/Corporate-publications/AMP-apr10-mar20.pdf

Parker, M., & Steenkamp, D. (2012). The economic impact of the Canterbury earthquakes. *Reserve Bank of New Zealand Bulletin, 75*(3), 13-25.

Patacas, J., Dawood, N., Vukovic, V., & Kassem, M. (2015). BIM for facilities management: evaluating BIM standards in asset register creation and service life planning. *Journal of Information Technology in Construction, 20*(10), 313-318.

Pocock, D., Shetty, N., Hayes, A., & Watts, J. (2014). Leveraging the relationship between BIM and asset management. *Infrastructure Asset Management, 1*(1), 5-7.

Quigley, M. C., Hughes, M. W., Bradley, B. A., van Ballegooy, S., Reid, C., Morgenroth, J., Horton, T., Duffy, B., & Pettinga, J. R. (2016). The 2010–2011 Canterbury earthquake sequence: Environmental effects, seismic triggering thresholds and geologic legacy. *Tectonophysics, 672*, 228-274.

Rafiee, A., Dias, E., Fruijtier, S., & Scholten, H. (2014). From BIM to geo-analysis: view coverage and shadow analysis by BIM/GIS integration. *Procedia Environmental Sciences, 22*, 397-402.

Renehan, B. (2016). Model Progression Specifications – Resources. Blog post Retrieved from http://bimfix.blogspot.com/2016/03/model-progression-specification.html

Rich, S., & Davis, K. H. (2010). *Geographic information systems (GIS) for facility management*. Retrieved from https://foundation.ifma.org/docs/default-source/Whitepapers/foundation-geographic-information-systems-(gis)-technology.pdf?sfvrsn=2

Ring, U., & Hampton, S. (2012). Faulting in Banks Peninsula: tectonic setting and structural controls for late Miocene intraplate volcanism, New Zealand. *Journal of the Geological Society, 169*(6), 773-785.

SanJosé-Alonso, J. I., Finat, J., Pérez-Moneo, J. D., Fernández-Martín, J., & Martínez-Rubio, J. (2009). *Information and knowledge systems for integrated models in Cultural Heritage*. Paper presented at the Proceedings of the 3rd ISPRS International Workshop 3D-ARCH 2009, Trento, Italy.

Scally-Irvine, K., & Louisson, O. (2016). *Evaluation of the Smart Cities Programme 2015-2016 Land Information New Zealand*. Retrieved from https://www.linz.govt.nz/system/files_force/media/doc/sdp_smart-cities_report_20170322.pdf?download=1

Scholl, H. J., Barzilai-Nahon, K., Ann, J., Popova, O. H., & Re, B. (2009). *E-Commerce and e-Government: How do they Compare? what can they Learn from each Other?* Paper presented at the 42nd Hawaii International Conference on System Sciences, Koloa, Hawaii.

Schuler, D. (2002). Digital Cities and Digital Citizens. In M. Tanabe, P. Van den Besselaar, & T. Ishida (Eds.), *Digital Cities II: Computational and Sociological Approaches* (pp. 567-576): Springer.

Schulte, C., & Coors, V. (2009). *Development of a CityGML ADE for dynamic 3D flood information*. Paper presented at the Taking the Benefits of Geographic Information Technologies, Stuttgart, Germany.

Schultz, A. J. (2012). *The Role of GIS in Asset Management: Integration at the Otay Water Distict.* (Master of Science (Geographic Information Science and Technology)), University of Southern California, California.

Selçuk, A. S., & Yücemen, M. S. (2000). Reliability of lifeline networks with multiple sources under seismic hazard. *Natural hazards, 21*(1), 1-18.

Sharpened Productions. (2018). .GLB File Extension. Retrieved from https://fileinfo.com/extension/glb

Shayeganfar, F., Anjomshoaa, A., & Tjoa, A. M. (2008). *A smart indoor navigation solution based on building information model and google android*. Paper presented at the 11th International Conference on Computers for Handicapped Persons, Linz, Austria.

Shen, W., Hao, Q., & Xue, Y. (2012). A loosely coupled system integration approach for decision support in facility management and maintenance. *Automation in Construction, 25*, 41-48.

Shiffer, M. J. (1999). Planning support systems for low-income communities. In D. A. Schön, B. Sanyal, & W. J. Mitchell (Eds.), *High technology and low-income communities: Prospects for the positive use of advanced information technology* (pp. 193-211). Cambridge, MA: MIT Press.

Song, C., & Li, G. (2017). *Gap Analysis on Open Data Interconnectivity for Disaster Risk Research (Penultimate Version) : A study report of the CODATA Tast Group on Linked Open Data for Global Disaster Risk Research*. Retrieved from Integrated Research on Disaster Risk [IRDR], Beijing, China: http://www.irdrinternational.org/download/12621/

Statistics New Zealand. (2006). Canterbury Region Territorial authorities resident populations and dwellings. *2006 Census.* Retrieved from http://archive.stats.govt.nz/Census/about-2006-census/final-counts-tables/canterbury-region.aspx

Stevenson, J. R., Kachali, H., Whitman, Z., Seville, E., Vargo, J., & Wilson, T. (2011). Preliminary observations of the impacts the 22 February Christchurch Earthquake had on organisations and the economy: A report from the field (22 February-22 March 2011). *Bulletin of the New Zealand Society for Earthquake Engineering, 44*(2), 65-76.

Suter, M. (2011). *Focal Report 7: CIP resilience and risk management in critical infrastructure protection policy: exploring the relationship and comparing its use*. Retrieved from Centre for Security Studies, ETH Zurich: https://www.research-collection.ethz.ch/bitstream/handle/20.500.11850/153674/1/eth-6129-01.pdf

Tarolli, P., & Cavalli, M. (2013). Geographic Information Systems (GIS) and Natural Hazards. In P. T. Bobrowsky (Ed.), *Encyclopedia of Natural Hazards* (pp. 378-385). Dordrecht: Springer Netherlands.

Tashakkori, H., Rajabifard, A., & Kalantari, M. (2015). A new 3D indoor/outdoor spatial model for indoor emergency response facilitation. *Building and Environment, 89*, 170-182.

Tegtmeier, W., Zlatanova, S., Van Oosterom, P. J. M., & Hack, H. R. G. K. (2014). 3D-GEM: Geo-technical extension towards an integrated 3D information model for infrastructural development. *Computers & geosciences, 64*, 126-135.

Uma, S. R., Dhakal, R. P., & Nayyerloo, M. (2013). *Vulnerability assessment of Christchurch buildings in Canterbury earthquakes* (1972192558). Retrieved from https://www.gns.cri.nz/static/pubs/2013/SR%202013-020.pdf

UNISDR. (2005). *Hyogo framework for action 2005–2015: Building the resilience of nations and communities to disasters*. Paper presented at the World Conference on Disaster Reduction (A/CONF. 206/6), Kobe, Hyogo, Japan.

United Nations Office for Disaster Risk Reduction [UNISDR]. (2015). *Sendai framework for disaster risk reduction 2015–2030.* Paper presented at the 3rd United Nations World Conference on Disaster Risk Reduction, Sendai, Japan.

United States Geological Survey [USGS]. (2018, August 5). M 6.9 - 3km SSE of Loloan, Indonesia. Retrieved from https://earthquake.usgs.gov/earthquakes/eventpage/us1000g3ub#executive

Van Westen, C. J. (2013). Remote sensing and GIS for natural hazards assessment and disaster risk management. *Treatise on geomorphology, 3*, 259-298.

Van Westen, C. J., Montoya, L., Boerboom, L., & Badilla Coto, E. (2002). *Multi-hazard risk assessment using GIS in urban areas: a case study for the city of Turrialba, Costa Rica*. Paper presented at the Proc. Regional workshop on Best Practise in Disaster Mitigation, Bali.

Vanlande, R., Nicolle, C., & Cruz, C. (2008). IFC and building lifecycle management. *Automation in Construction, 18*(1), 70-78.

Vatseva, R., Solakov, D., Tcherkezova, E., Simeonova, S., & Trifonova, P. (2013). Applying GIS in seismic hazard assessment and data integration for disaster management. In S. Zlatanova, S. R. Peters, A. Dilo, & H. Scholten (Eds.), *Intelligent Systems for Crisis Management* (pp. 171-183): Springer.

Wang, S., & Xie, J. (2002). Integrating Building Management System and facilities management on the Internet. *Automation in Construction, 11*(6), 707-715.

Watson, N. R. (2010). Impact of the Darfield earthquake on the electrical power system infrastructure. *Bulletin of the New Zealand Society for Earthquake Engineering, 43*(4), 421-424.

Welch, D. P., Sullivan, T. J., & Filiatrault, A. (2014). Potential of building information modelling for seismic risk mitigation in buildings. *Bulletin of the New Zealand Society for Earthquake Engineering, 47*(4), 253-263.

Wildfire, C. (2018). How can we spearhead city-scale digital twins? Retrieved from http://www.infrastructure-intelligence.com/article/may-2018/how-can-we-spearhead-city-scale-digital-twins

Xiong, C., Lu, X., Hori, M., Guan, H., & Xu, Z. (2015). Building seismic response and visualization using 3D urban polygonal modeling. *Automation in Construction, 55*, 25-34.

Xu, Z., Lu, X., Guan, H., Han, B., & Ren, A. (2014). Seismic damage simulation in urban areas based on a high-fidelity structural model and a physics engine. *Natural hazards, 71*(3), 1679-1693.

Yalcinkaya, M., & Singh, V. (2014). *Building information modeling (BIM) for facilities management–literature review and future needs*. Paper presented at the IFIP International Conference on Product Lifecycle Management.

Yang, W. B., Yen, Y. N., & Cheng, H. M. (2012). *An integrated management system for historical buildings: The case study of dihua historical street districts in Taiwan*. Paper presented at the Euro-Mediterranean Conference, Berlin.

Zerger, A. (2002). Examining GIS decision utility for natural hazard risk modelling. *Environmental modelling & software, 17*(3), 287-294.

Zhang, X., Arayici, Y., Wu, S., Abbott, C., & Aouad, G. F. (2009). *Integrating BIM and GIS for large-scale facilities asset management: a critical review*. Paper presented at the Proceedings of the 12th International Conference on Civil, Structural and Environmental Engineering Computing, Funchal, Madeira, Portugal.

Zorn, C., Davies, A., Robinson, T., Pant, R., Wotherspoon, L. M., & Thacker, S. (2018). *Infrastructure failure propagations and recovery strategies from an Alpine Fault earthquake scenario*. Paper presented at the 16th European Conference on Earthquake Engineering, Thessaloniki, Greece.

Zou, Y., Kiviniemi, A., & Jones, S. W. (2017). A review of risk management through BIM and BIM-related technologies. *Safety science, 97*, 88-98.

Appendices

Appendix A —Christchurch Infrastructure at the Time of the CES

A.1. Horizontal Infrastructure Network

Within Christchurch, ownership of the horizontal infrastructure networks varies. The 3 Waters facilities (potable water, wastewater, and storm water) are owned and operated by CCC. National electricity is distributed by the state-owned entity Transpower New Zealand Ltd., whilst Orion New Zealand Ltd., joint-owned by CCC and Selwyn District Council, operates the electricity network in Christchurch. Telecommunications infrastructure includes the networks operated by companies such as Enable Networks Limited and Spark (formerly Telecom) (CCC, 2018).

The National Engineering Lifelines Committee (NELC), Local Lifelines groups, the Earthquake Commission, and the Ministry of Civil Defence and Emergency Management (MCDEM), promote the importance of lifeline resilience, which is further enforced with the Civil Defence and Emergency Management (CDEM) Amendment Act 2016 (CDEM, 2016). The Act amended the previous CDEM Act of 2002 which required lifeline utilities "to be able to function to the fullest possible extent," even to a reduced level, during and after an emergency. The NELC focuses on collaboration with lifeline utility representatives, engineers, scientists and emergency managers to provide a framework for the integration of asset, risk, and emergency management across utilities.

Prior to the CES, significant assessment of the Christchurch metropolitan area lifelines was undertaken (Christchurch Engineering Lifelines Group, 1997). Following the report, all sectors including transportation, 3 Waters, electrical, and communications underwent enhancing the resiliency of lifelines. The following sections present an overview of the horizontal infrastructure in Christchurch, focussing on the 3 Waters and electricity networks.

A.1.1. Electrical Distribution Network

Transpower is the national supplier of electrical power in New Zealand, transmitting high voltages from generating sites to demand centres. Orion, the third largest power distribution company in New Zealand, conveys power from Transpower demand centres to end-user customers across Christchurch City and the surrounding Canterbury area. Transpower's five Christchurch transmission grid exit points (GXPs) transform power from 200 kV to 66 kV, 33 kV, and 11 kV, distributed through the network operated by Orion. Orion (2010) provided the best source of data for the value and composition of their network prior to the CES as summarised below.

The 66 kV network made up approximately 1% of Orion's network within Christchurch and had an estimated Optimised Depreciation Replacement Cost (ODRC) of NZ$33m. The cables spanned 63 km and were generally made up of either: radial pairs of 3-core aluminium, oil filled, aluminium sheathed cables (87% or 55km); or 3X1 core copper, cross-laminated polyethylene (XLPE) cables.

There was approximately 25 km of 33 kV cable (0.5% of the network), predominantly in the western part of Christchurch City. The ODRC of the 33 kV network was roughly NZ$5.6m and comprised the following three types:

- km oil filled (installed 1967-1977),
- km Paper Insulated Lead-Covered, Armoured (PILCA) (installed 1978-1988),
- 19 km XLPE (installed 1992-2007).

The 11 kV network formed the second largest underground asset type in Orion's network, with an ODRC of NZ$212.6m, comprised approximately 2,200-2,300 km of cable (45% of the total network), 99.6% of which was in urban Christchurch. Like the 33 kV network, the 11 kV cables were either PILCA or XLPE, with copper or aluminium cores, and high-density polyethylene (HDPE) or PVC outer protective jackets. The approximate breakdown of the cable type and length are summarised below (Kongar *et al.*, 2017):

- 1,491 km of PILCA,
- 380 km of XLPE,
- 59 km of PILCA HDPE,
- 370 km unknown type.

The Orion network fed into 15 district/zone substations in and around Christchurch City as shown in Figure A-1.

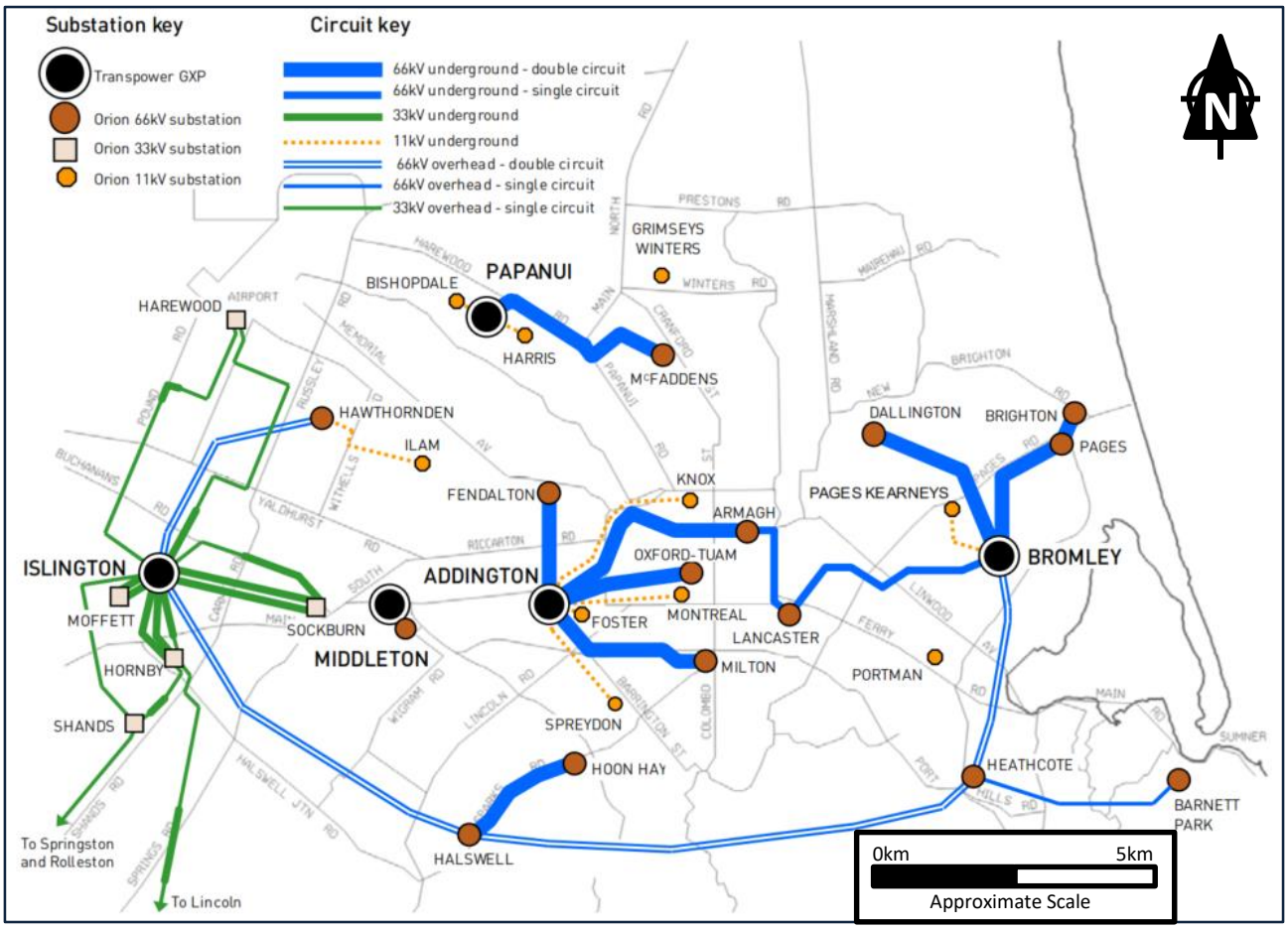

Figure A-1: Christchurch substation and medium voltage cable layout (Orion, 2010)

District/zone substations transform 66 kV (or 33 kV) power to 11 kV as well as linking the sub-transmission system and distribution substations (Figure A-2). 11 kV power is taken from either a district/zone, network, or alternative distribution substation, to supply the consumer's 400 V voltage distribution system.

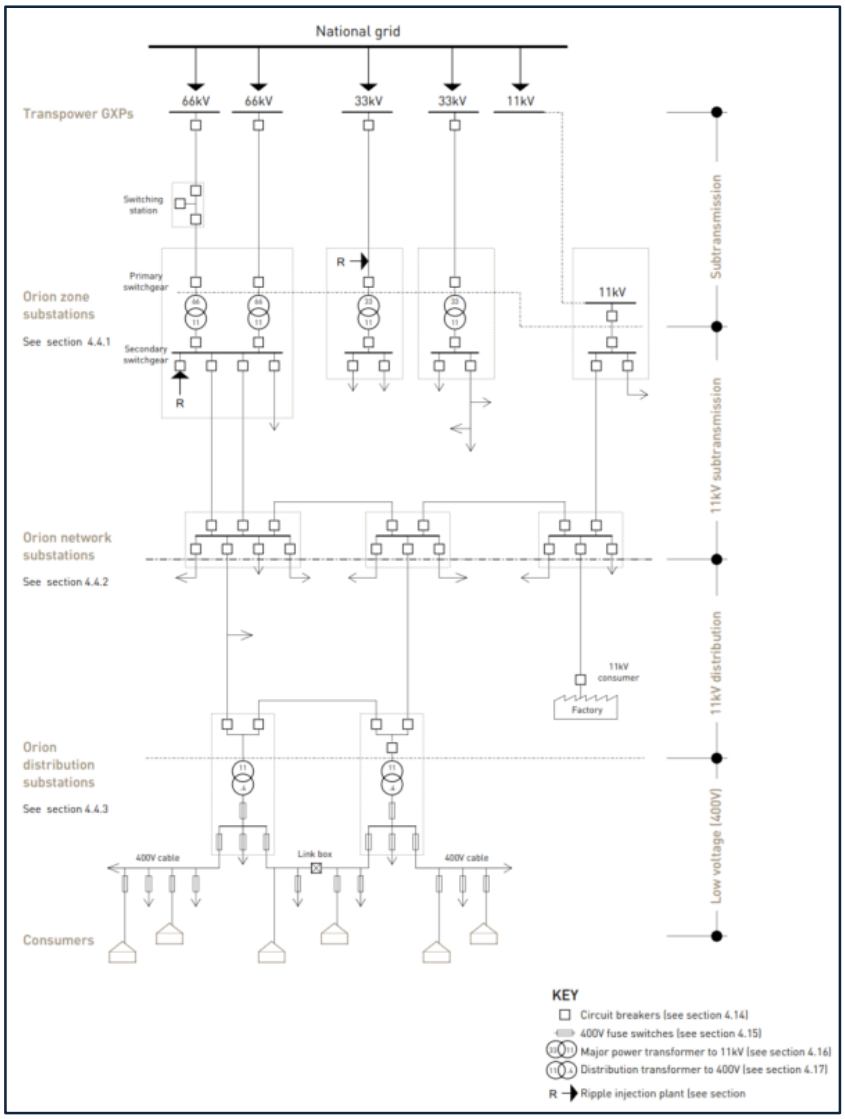

Figure A-2: Orion network voltage level/asset relationships (Orion, 2010)

Making up 52% of Orion's network (2,522 km of distribution cable) with an ODRC of NZ$232.7m, the 400 V network is the main source of power distribution to its customers. Pre-1966, most of the cables were paper lead/PILCA-based after which, the introduction of PVC insulation replaced some of these older cables. From 1974 onwards, the 400 V network was built using XLPE cables. Also included as part of the 400 V network were approximately 5,500 above ground link boxes and 26,000 above ground boundary boxes, which sent the electricity supply to customers.

A.1.2. The Water Network

For the land drainage network, CCC maintained approximately 500 km of pipeline ranging from 0.1- 2.1 m in diameter. These pipes were predominantly reinforced concrete rubber ring jointed (RCRRJ) as well as perforated subsoil pipes, ceramic, asbestos cement, and single and double skin "brick barrel" pipes (Christchurch Engineering Lifelines Group, 1997). Figure A-3 shows the known layout of the open tributary, brick barrel, and >0.45 m diameter piped waterway networks at the time of the Risks and Realities report (Christchurch Engineering Lifelines Group, 1997).

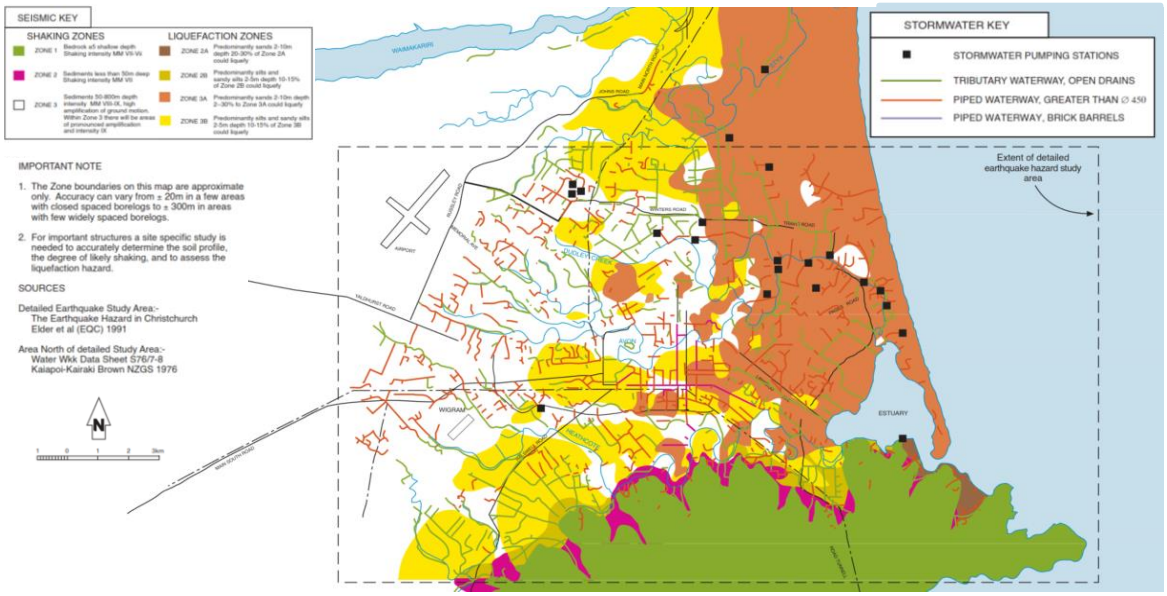

Figure A-3: Storm water system extract (Christchurch Engineering Lifelines Group, 1997)

Cubrinovski *et al.* (2014) summarised the dataset of geocoded files for 1,900 km of wastewater distribution pipelines collected through reconnaissance and assessment undertaken by SCIRT, the results of which are reproduced in Table 10.

Table 10: Christchurch City sewer infrastructure (Cubrinovski et al., 2014)

Material type	Gravity main	Pressure main	Other	Total length (km)
AC	138	34	1	**173**
BB	6	–	–	**6**
CI	15	5	1	**21**
CONC	768	24	4	**796**
EW	381	0	0	**381**
HDPE	15	3	3	**21**
MDPE80	1	5	0	**6**
MPVC	3	19	0	**22**
OTHER	43	4	15	**62**
PVC	45	5	1	**51**
UPVC	310	49	1	**360**
Total	1,725	148	26	1,899

Christchurch Engineering Lifelines Group (1997) discussed a potable water network of 1,300 km of pipes, fed by 84 pumping stations and 37 service reservoirs. Pumping stations draw water from five underground aquifers at depths between 22 m and 190 m below ground level (bgl). They also noted that the city is predominantly split into five supply zones, each with differing pressures however; in an emergency, the valves at zone boundaries can be opened to connect all zones.

Cubrinovski *et al.* (2014) also presented the topology of the submain and crossover network of the potable water network, which presents a 400 km difference in the mains network from the values reported in Christchurch Engineering Lifelines Group (1997). The discrepancies between both are likely due to the installation of new networks in the time between the two sources. Table 11 presents the breakdown of material and pipe type for the mains water from Cubrinovski *et al.* (2014).

Table 11: Christchurch water mains infrastructure (Cubrinovski et al., 2014)

Material type	Trunk mains	Mains	Submain	Crossovers	Total length (km)
AC	5	850	15	1	**871**
CI	0	189	0	0	**189**
CLS	14	38	0	–	**52**
DI	0	52	0	–	**52**
GI	–	2	154	30	**186**
HDPE	–	0	845	69	**914**
MDPE80	–	5	413	40	**458**
MPVC	–	148	1	0	**149**
Other	0	27	14	0	**41**
PVC	0	315	68	4	**387**
SRS	10	24	0	0	**34**
Total	29	1,650	1,510	144	3,333

A.2. Vertical Infrastructure

Prior to the CES, the reported residential dwelling stock of Christchurch City in the 2006 Census was approximately 9,500 of unoccupied and 135,000 occupied properties (Statistics New Zealand, 2006). Most houses built in Christchurch comprised a timber-framed superstructure designed in accordance with the national building code, NZS 3604:2011 (New Zealand Standards, 2011) or earlier documents, with some examples of steel framing and structural masonry. Generally, residential foundations built within the last 30 years comprised a concrete slab-on-grade construction, whilst older dwellings were predominantly built using a suspended timber floor on a joist and bearer system, supported by timber, concrete or aggregate piles and a reinforced or unreinforced perimeter foundation wall providing lateral resistance (Buchanan and Newcombe, 2010).

Outside of residential development, CCC (2010) published a fact pack of Christchurch City which listed the following statistics around the city's-built environment:

- The Christchurch City Plan listed 582 heritage items, which included buildings, places, and objects.
- There were eight hospitals, 163 schools, three major tertiary institutions, 19 library facilities and 12 sports centres and swimming pools.
- Retail businesses in the central city and the 12 main suburban centres were approximately 1,100.

Whilst not directly relating to number of physical structures, there were an estimated 38,000 businesses in the city. ("business" for these statistics is defined as an enterprise with annual sales/expenses exceeding NZ$30,000).

Uma *et al.* (2013) produced an inventory of Christchurch using the asset model development for "Riskscape" (King and Bell, 2009), based on 160,000 buildings. Acknowledging that the data are post-CES, it provides an indicative view of construction type across Christchurch. Figure A-4 presents the number of buildings that fall into each of the construction material categories and whilst the report goes on to discuss sub-categorising this based on use/occupancy into residential, commercial, and industrial, the quantities of these sub-categories were not reported.

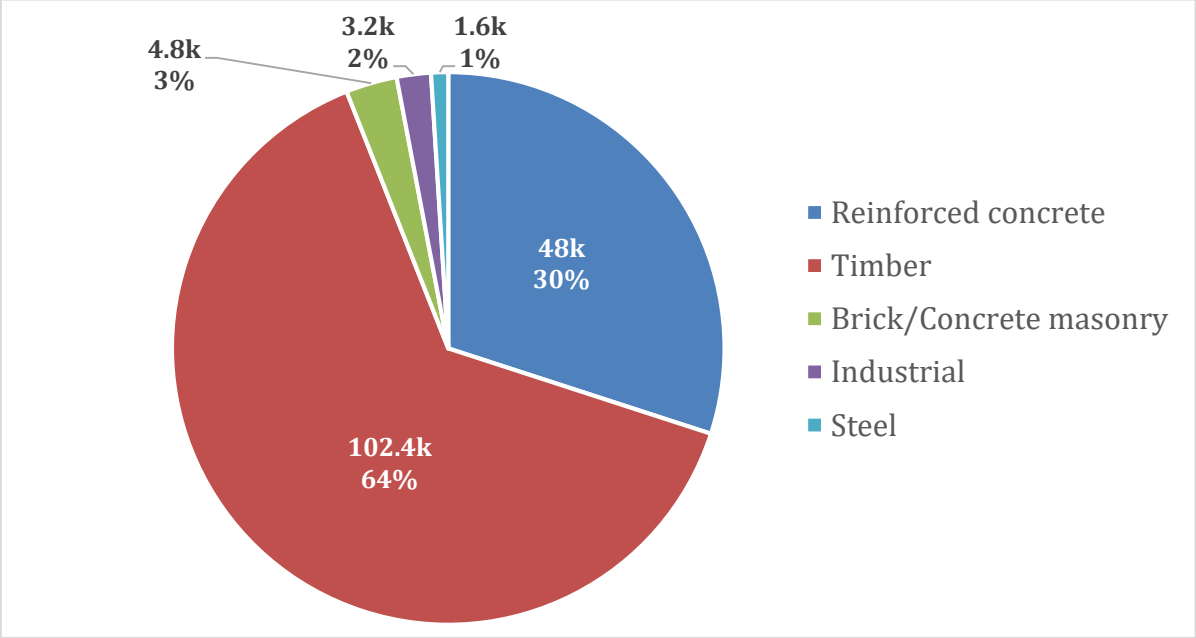

Figure A-4: Building stock classifications (Uma et al., 2013)

Appendix B —Performance of Infrastructure during the CES

B.1. Horizontal Infrastructure

B.1.1. Electrical Network

B.1.1.1. 4th September 2010 Darfield Earthquake

Despite the 4.0 m fault offset which intersected two of the single circuit 220 kV transmission lines in Darfield, no power outages occurred across these lines. Similarly, no damage was observed to the steel lattice towers that were near the fault rupture. However, the fault offset caused high-tension loads to the ground wires, resulting in bending of two tower extensions. The Islington to Papanui 66 kV overhead circuit broke at the terminal tower and cracking was observed on spill prevention containment walls around transformers at the Papanui 66 kV substation. At three of the substations (Addington-Middleton, Islington, and Hororata), circuits and transformers were tripped either by: fault protection measures; vibration of the mercury switches recording false over-temperature readings; or by sloshing of oil causing high oil pressure warnings, tripping the transformer. Transpower estimated repair costs through early October 2010 were in the order of NZ$150,000, indicating that only a small number of items were damaged at the Transpower substations.

The reported damage to the Orion network appears to be significantly less than to Transpower in its higher voltage assets. Of the 2,200 km buried cable network managed by Orion, around 24 cables (Eidinger and Tang, 2012) equivalent to approximately 88 km (4%), were damaged with 30 faults occurring along this cable length (Kwasinski *et al.*, 2014). There was also minor damage to overhead lines in rural areas due to whipping of poles and conductors, and leaning in areas of significant land movement and liquefaction. However, there was no disruption to supply in any of these circumstances. The information in the literature indicates that only two 33 kV poles were leaning (Eidinger and Tang, 2012) and the two oil-filled low pressure 66 kV circuits on the Dallington pedestrian bridge were partially crushed where the cables transitioned from a buried condition into the pile-supported bridge (Kwasinski *et al.*, 2014) as shown in Figure B-1.

Figure B-1: Crushed 66kV cables at Dallington bridge (Eidinger and Tang, 2012)

In the 400 v network, at the junctions between underground cables and the ring main unit switchgears, there were several cases where cables had been pulled, some by up to 0.5 m, causing some arching damage. The remaining recorded damage to the low voltage network comprised two ground mounted transformer pads undergoing significant movement, causing excessive stress on low voltage cables, and approximately 100 m of cable being damaged, all of which required replacing (Watson, 2010).

The rural 11 kV network managed by Mainpower sustained damage due to conductor clashes and severe leaning of poles. Within the buried network managed by Mainpower, 17 faults were identified in the 11 kV cables, caused by sideways forces and stretching, with damage observed over several metres around the immediate fault. This recorded damage resulted in Mainpower replacing approximately 3 km of cable, in 11 cable sections (Watson, 2010).

Generally, the majority (approximately 80%) of the issues caused to the network were a result of transformers tripping due to the oil surge protection measures (Kwasinski *et al.*, 2014; Watson, 2010). Estimates of fault restoration presented in Cubrinovski and Green (2010) indicated that 90% of the service was restored by the end of day one, and by day 10, nine of the 20 high voltage cable faults had been repaired. The estimated repair cost was in the order of NZ$4m (Giovinazzi *et al.*, 2011).

B.1.1.2. 22nd February 2011 Christchurch Earthquake

Significantly greater levels of damage were caused to the electrical network because of the 22nd February 2011 Christchurch Earthquake. As a result, there were considerably more reports in the literature which document the recorded damage. Of particular note are the observations by Massie (2011), which contain photographs of cable damage (Figure B-2) and were subsequently reported further in Massie and Watson (2011). Giovinazzi and Wilson (2012), and those who had previously documented damage caused by the 4th September 2010 Darfield Earthquake (Eidinger and Tang, 2012; Giovinazzi *et al.*, 2011; Kwasinski *et al.*, 2014) also reported damage sustained to the electrical network. These have also been summarised by asset type below.

Figure B-2: Typical 11kV cable damage following the 22nd February 2011 Christchurch Earthquake (Massie, 2011)

A large amount of the damage occurred to PILCA cables with the predominant fault resulting from existing joints pulling apart (Kwasinski *et al.*, 2014). Other faults were caused due to inflexibility of the cables, leading them to become "kinked" (Figure B-2). Massie and Watson (2011) reported that at the time of writing, 600 cables had been repaired comprising approximately 1,500 joint repairs with major cable damage shown in the schematic in Figure B-3. Generally, when compared to the 4th September 2010 Darfield Earthquake, it cost approximately ten times more(NZ$40-50m) and took a total of 10 days to restore 90% of the service (Giovinazzi *et al.*, 2011).

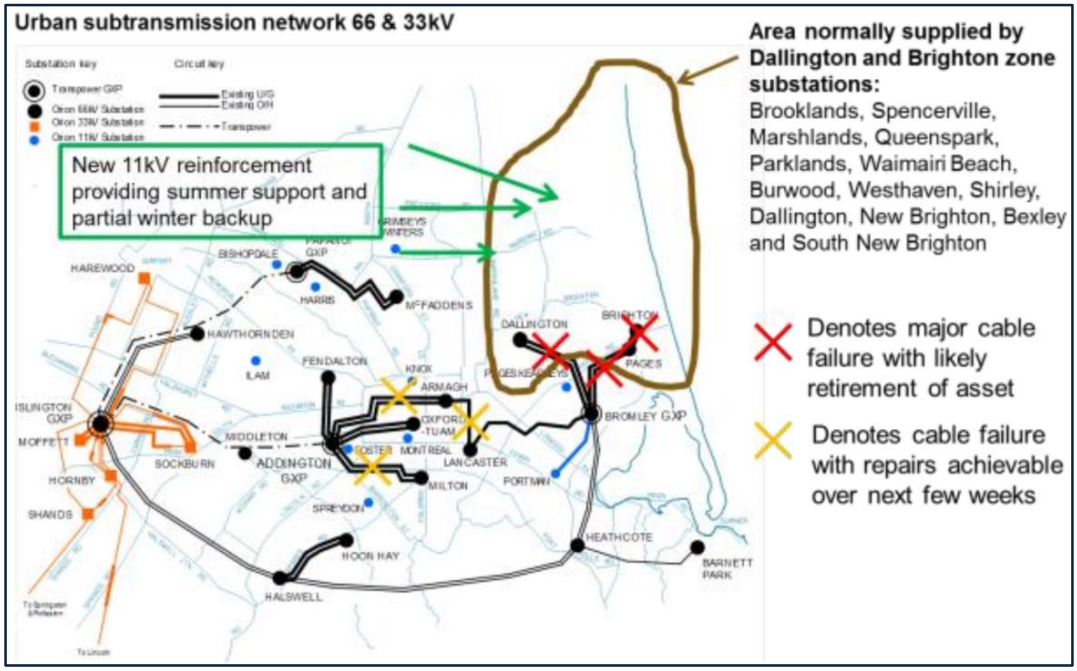

Figure B-3: Major cable damage following the 22nd February 2011 Christchurch Earthquake (Massie and Watson, 2011)

Within the 220 kV network managed by Transpower, the damage sustained to the system was modest. The Bromley substation experienced some liquefaction and component damage, and one 66 kV tower out in the Port Hills sustained damage from a rock falling through the tower, but remained standing. Many of the Transpower high-voltage systems tripped offline without sustaining damage (Kwasinski *et al.*, 2014).

Upon review of the available literature, there appears to be no damage sustained, or at least recorded, to the 33 kV network. However, across the 66kV network, the available literature (Eidinger and Tang, 2012; Giovinazzi *et al.*, 2011; Kwasinski *et al.*, 2014; Massie and Watson, 2011) indicates that approximately 30 out of 60 km sustained damage and occurred to all parallel cables over lengths of less than 10cm i.e. damage was concentrated at specific locations and not randomly along entire lengths of cable. The observed cable failures occurred in areas of readily observed liquefaction indicating that failures were not due to high levels of ground shaking alone. In eastern Christchurch, where Permanent Ground Deformations (PGDs) were prevalent (5- 50 cm), all four cables suppling the Dallington and Brighton zone substations were damaged beyond repair and had to be abandoned (including the two cables crossing Dallington pedestrian bridge, damaged from the 4th September 2010 Darfield Earthquake but repaired prior to the 22nd February 2011 Christchurch Earthquake). The remaining known faults manifesting along the pipe-type, oil-filled, thermal backfilled cables occurred in areas of Central Christchurch where PGDs were of a much smaller magnitude (1- 5 cm). Three of these failures occurred in areas of moderate liquefaction between Armagh and Addington substations, likely due to settlements and lateral spreading of the nearby Avon River. It is surmised that the observations in Kwasinski *et al*. (2014) relating to six failures occurring along a 3 km length of cable through central Christchurch, are these same sets of cables. In these observations, it was noted that at five of the six locations (assumed to be the locations highlighted in Figure B-3), all parallel phases faulted. Within the XPLE cable network, nine repairs were required to the 1,600 mm^2 XPLE cables, including the cable (installed in 2002) between Armagh and Lancaster substations where failures occurred in three locations in areas of moderate liquefaction.

Through field inspections and numerical modelling undertaken by Kwasinski *et al.* (2014), the following generalised cable failure methods were identified:

- In all cases, no large PGDs were evident on the roadway above the cable faults.
- Cracking in the roadways/adjacent curb sides were commonly less than 1 cm.
- PGDs manifested by small differential settlements and cracking which crossed the street, transverse to cable alignments. However, the damage condition of cables did not match PGDs at the ground surface.
- All cables showed evidence of stretching in tension (generally less than 5 cm), resulting in yielding and lengthening of cable.
- Cracking observed in thermal concrete was transverse to the cables.
- Cables underwent curvature of 2- 4 cm in the vertical direction with a bend radius of less than 1 m. The tight bend radius resulted in insulation layers of XPLE cables being squashed, and the pipe-type cables to lose its pressure boundary.

One of the key observations/conclusions from this work identified that cables that were dug up showed evidence of complete insulation failure. Once insulation is damaged, cable failures can occur within seconds but may take minutes, days or even months.

Kwasinski *et al.* (2014), noted that Orion reported a total of 140 cables in the 11 kV network, including all 80 cables in the Brighton-Dallington areas, as being damaged. Table 12 presents a percentage breakdown for each of the land damage categories as assessed by Cubrinovski and Taylor (2011) of the approximately 1000 faults identified in 330 out of 2,300 km of cable (roughly 14%) (Giovinazzi *et al.*, 2011).

Table 12: Percentage of 11 kV cable faults for each land damage category following the 22nd February 2011 Christchurch Earthquake (Giovinazzi *et al.*, 2011).

Land damage category	% 11 KV cable faults
Moderate to severe	86%
Minor to moderate	8%
Minor	6%

The rate of 11 kV cable failures was 2-4 times higher than normal, extending for months after the 22nd February 2011 Christchurch Earthquake suggesting that many operable 11 kV cables had sustained insulation damage, taking some time to lead to ultimate failure. By 2013, 433 repairs had been carried out (Eidinger and Tang, 2012). Repairs generally comprised replacing a length of old cable with multiple faults, with approximately 20 to 100 m of XLPE cable (in most cases).

Very few of the 400 v distribution cables failed (approximately 0.6% or 15 of the 2,500 km). Overall the low voltage cables performed better and suffered fewer faults when compared to the 11 kV networks. Of the non-cable electrical network assets damaged as a result of the 22nd February 2011 Christchurch Earthquake, Massie and Watson (2011) reported five of the 314 substations were severely damaged, identified as the following:

- New Brighton and Pages Road substations lost to liquefaction.
- St Andrews Hill substation severely damaged by shaking.
- Wakefield Avenue North damaged by rock fall.
- Port Hills Road infill wall failed.

Kwasinski *et al.* (2014) inferred a correlation between a higher number of faults occurring in higher voltage cables being due to the percentage of cable buried versus overhead. Though, based on the information documented above, the inverse is considered true. When considered as percentages, the perception is that the higher voltage cables experienced more faults (i.e. 50% of 66 kV cables experienced a fault). However, when considered as total cable length, because there is a significantly greater quantity of 11 kV cable compared to 66 kV, this results in 31 km of 66 kV cable experiencing faulting versus 126.5 km of 11 kV cable. This correlation is further questioned with respect to higher voltage cables having a higher ratio of buried cables compared to overhead. When assessing the 400 v network, the majority of this network is buried when compared to the higher voltages, and yet only 0.6% of cable (roughly 16 km) was recorded as having faulted due to the 22nd February 2011 Christchurch Earthquake. Whilst the exact number of individual repairs to the electricity network is unknown, approximately 375 km of cable had been damaged, taking 700 electricity sector workers more than 200,000 working hours to repair (Giovinazzi and Wilson, 2012).

B.1.2. Water Network

B.1.2.1. 4th September 2010 Darfield Earthquake

Both Cubrinovski and Green (2010) and Eidinger and Tang (2012) highlighted damage to two residential suburbs that were affected the greatest, that of Brooklands and Spencerville to the north of Christchurch CBD. Neither had a functioning wastewater collection system and the former was without potable water. Also in this region, significant ground subsidence caused 25 manholes to be lifted by approximately 28-46 cm above existing road surface.

Elsewhere in Christchurch, other damaged water infrastructure included sliding smaller water storage tanks (four out of six that were made from steel, three out of four made from wood), as well as damage to the concrete roof of a buried concrete tank. Eight wells were also reported as damaged, thought to be due to casing pipe failures in liquefaction zones.

Eidinger and Tang (2012) provided the most comprehensive source of information relating to the wastewater network. Two of CCC's wastewater dry well lift stations had tilted and floated due to liquefaction and lateral spreading-based movement. Other typical damage to pipe networks included cracking and rupturing of brittle pipes, influx of groundwater laden with sand and silt causing blockages, and discharge of untreated sewage into local rivers. Initial estimates predicted roughly 70 km of wastewater pipes would have to be replaced, the majority of which were in areas of significant settlement and lateral spreading.

B.1.2.2. 22nd February 2011 Christchurch Earthquake

For the wastewater network, between 96 km and 142 km were out of service and approximately 474 km- 542 km were at reduced capacity (Cubrinovski *et al.*, 2011; Eidinger and Tang, 2012). The wastewater system was heavily damaged to the point of failure in April 2011, predominantly caused by the Bromley wastewater treatment plant (WWTP) operating at 30% capacity. The reduced capacity was due to damage caused to seven of the eight reinforced concrete mains pipes which fed to the treatment plant (with the eighth leaking). During this time 25% or 60 million litres of raw sewage leaked out of damaged pipes into residences, rivers, and the sea, causing health and environmental issues. There were no reported building collapses in the sewer system assets. However, several were damaged due to liquefaction and shaking including the Pages Road sewage pumping station where differential settlement of the structure occurred and floating of suction wells by 100- 150 mm. Liquefaction-induced differential settlement impacted all facilities at the Bromley wastewater treatment plant including one of two pumping stations, which had leaked due to damage to a mechanical coupling.

Building damage to the potable water network was reported in Eidinger and Tang (2012) where the majority of damage was sustained to water tanks. 12 were reported as damaged at the roof or roof-to-wall connections, seven tanks were leaking due to wall damage, and five had cracked at the wall-to-foundation connections.

The key takeaways from the water network performance during the 22nd February 2011 Christchurch Earthquake are the following:

- Due to the wastewater system being at greater depths than the potable water network (3-4 m versus ~0.6 m), it is more vulnerable to liquefaction effects.
- Overall the most severe damage was inflicted by lateral spreading.
- As demonstrated by the successful performance of HDPE pipes in Horseshoe Lake, all new pressure mains made extensive use of HDPE pipe.
- Whilst as would be expected, priority was given to repairing the potable water network. The extensive damage to the wastewater network and the secondary impacts that were caused to health and the environment should be carefully considered and reviewed with respect to resilience and future performance.

B.2. Vertical Infrastructure

B.2.1. 4th September 2010 Darfield Earthquake

Kam *et al.* (2010) presented statistics for the distribution of the 717 CCC/MCDEM Building Safety Evaluation (BSE) building safety placards for reinforced concrete buildings in the CBD, following the 4th September 2010 Darfield Earthquake. Of those assessed as at 20th September 2010: 91% were deemed green, meaning that there was no restriction on use or occupancy; 8% yellow (restricted use); and 1% Red (unsafe). These statistics demonstrate that seismic-resistant designed buildings performed as expected, and generally those that didn't were those built prior to the seismic codes in place at the time of the report.

Bruneau *et al.* (2010) provided a preliminary assessment of steel building damage and surmises that these structures suffered little damage. The observations made concluded that damage manifested as either slight plastic yielding, damage to the concrete components of the steel and concrete lateral load resisting frames, isolated instances of connector failure, and collapse of steel tanks and storage tanks. Bruneau *et al.* (2010) also noted that as a whole, the general building stock in the Christchurch CBD contained a small proportion of medium to high-rise steel buildings, as there had always been a strong tradition of using seismically designed reinforced concrete, dating back from the 1970s.

B.2.2. 22nd February 2011 Christchurch Earthquake

Eidinger and Tang (2012) estimated building and infrastructure damage in the range of NZ$15bn- NZ$25bn with more than 500 commercial buildings damaged in the CBD. That estimation was relatively accurate when reviewing the work by Kam *et al.* (2011) who presented statistics of CBD building damage following the 22nd February 2011 Christchurch Earthquake, similar to that undertaken for the 4th September 2010 Darfield Earthquake described in Section B.2.1. Kam *et al.* (2011) noted a total number of assessed CBD buildings as 2,721, as a split of 58% and 42% for commercial and residential buildings, respectively. Whilst the categories of safety placards do not distinguish between residential and commercial buildings, it can be reasonably assumed that the 48% of yellow and red placards (Section 2.3.3.4.2) weren't all assigned to just one type. Even if it was an even distribution, this would result in somewhere between 420 and 835 commercial buildings with a yellow or red placard, which is within the estimation by Eidinger and Tang (2012) above. Whilst the percentages reported by Kam *et al.* (2011) almost match those in Stevenson *et al.* (2011), the number of buildings vastly differs where Stevenson *et al.* (2011) presented a total of 3,621. Contrary to this, Uma *et al.* (2013) and Cubrinovski *et al.* (2014) documented that the CBD of Christchurch was practically lost with the majority of its buildings significantly damaged. There is a discrepancy in number of buildings where the former reports 90% of the 2,036 buildings as either being categorised as red or yellow, and the latter notes the majority of the 3,000 buildings damaged beyond repair.

This contradiction in views on extent of damage and number of buildings is likely to be due to either the following:

- Between the initial assessment in 2011 and the time of the 2014 article, some initially assessed as safe for occupancy as part of a rapid assessment may have later been deemed unsafe.
- Due to the time lapse between the 22nd February 2011 Christchurch Earthquake and the works by Cubrinovski *et al.* (2014) and Uma *et al.* (2013), it is possible that buildings that were damaged by later events (such as the 13th June 2011 Christchurch Earthquake and the 23rd December 2011 Christchurch Earthquake) were incorrectly identified as being damaged by the 22nd February 2011 Christchurch Earthquake.
- The definition and assessment area of "Christchurch CBD" may differ between the articles.

When the residential building stock was assessed, generally lightweight timber framed structures performed very well and whilst there was evidence of soft-storey failure (Figure B-4) and superstructure damage caused by slab rupture or different foundation systems, overall, most of these buildings maintained their structural integrity.

Two key points that Buchanan *et al.* (2011) made with respect to residential design is the importance of wall bracing stiffness and arrangement. The extensive assessments undertaken highlighted where newer architecturally designed houses had chosen to favour available views over symmetrical bracing wall configurations; the resulting damage was excessive. The second point related to foundation-superstructure connections where there were several examples of houses that appeared to have no obvious connection between the timber bottom plate and the foundations. In these cases, superstructures were observed to have slid by up to 300 mm over the foundations (Figure B-5).

Figure B-4: Examples of soft-storey failure of timber framed houses (Buchanan et al., 2011)

Figure B-5: (left) reinforced slab damage; (right) house sliding on foundations (Buchanan et al., 2011)